LIFETIME ASSESSMENT OF HIGH TEMPERATURE PIPING

REPORT 2015:187





Lifetime assessment of high temperature piping

By stress analysis and testing

JAN STORESUND, KRISTIN STEINGRIMSDOTTIR, JUHANI RANTALA, ROBIN SOLLANDER, ZHOUWANG CHEN, TOBIAS BOLINDER

Förord

Denna rapport är slutrapportering av projekt M12-218 Livslängdsbedömning av ångledningssystem med hjälp av spänningsanalys och provning (Energimyndighetens projektnummer P 36987) samt kompletteringsprojektet M 39205 Livslängdsbedömning av ångledningssystem - kompletterande provning och analys (Energimyndighetens projektnummer P 39205) som faller under teknikområde Material- och kemiteknik.

Projektet har följts av en referensgrupp bestående av Rikard Norling (Swerea KIMAB), Ulrika Farnebäck (Siemens) och Tommy Larsson (E.ON).

Värmeforsk har bedrivit värmeteknisk forskning inom det så kallade Basprogrammet sedan starten 1968. SEBRA, samverkansprogrammet för bränslebaserad el- och värmeproduktion, är efterföljaren till Värmeforsks Basprogram och startade som ett samarbetsprogram mellan Värmeforsk och Energimyndigheten 2013. All forskningsverksamhet som bedrevs inom Värmeforsk ingår sedan den 1 januari 2015 i Energiforsk. Därför ges denna rapport ut som en Energiforskrapport. Programmets övergripande mål är att bidra till långsiktig utveckling av effektiva miljövänliga energisystemlösningar. Syftet är att medverka till framtagning av flexibla bränslebaserade anläggningar som kan anpassas till framtida behov och krav. Programmet är indelat i fyra teknikområden: anläggnings- och förbränningsteknik, processtyrning, material- och kemiteknik samt systemteknik.

Stockholm januari 2016 Helena Sellerholm Områdesansvarig Bränslebaserad el- och värmeproduktion, Energiforsk AB



Sammanfattning

Högtrycksångledningar hos kraftvärmeanläggningar har i regel drifttemperaturer som medför att livslängden begränsas av krypning. Erfarenheten har visat att det vid tidpunkten för traditionellt dimensionerad livslängd, 100 000 timmar, är vanligt att krypskador i form av krypkaviteter har börjat uppstå lokalt i rörsystemen. I vissa fall finns det redan krypsprickor medan det i andra anläggningar inte observeras skador. Genom replikprovning kan eventuella krypskador identifieras på ett tidigt stadium och genom återkommande provning kan man säkert och med framförhållning byta ut komponenter i systemet när skadorna börjar nå oacceptabla nivåer.

Vid replikprovning är det små ytor som undersöks och en strategi för att fånga upp de största krypskadorna i ett ångsystem är avgörande. En metod är att prova överallt där det erfarenhetsmässigt kan finnas krypskador. Det kan dock medföra mycket omfattande provning. Genom att göra spänningsanalyser av rörsystemet för att identifiera de högst påkända områdena i systemet kan antalet provpositioner reduceras.

Elastiska analyser av rörsystem görs rutinmässigt för att kontrollera att spänningsnivåerna är inom enligt normer acceptabla gränser. Resultaten har också använts för att identifiera provpositioner. Modelleringsarbetet går snabbt men analyserna kan inte beakta krypning. För att kunna göra det har det behövts mycket tidskrävande modellering och därför finns det mycket begränsade erfarenheter av det. I föreliggande projekt har effekterna av krypning studerats i detalj i syfte att kunna identifiera kritiska positioner för oförstörande provning och för att kunna beräkna återstående livslängd.

Ett skript har utvecklats och verifierats som kan översätta en modell för elastisk analys i programmet Caepipe, till programmet Abaqus för krypanalys. Med denna modell har det visats att starter och stopp påverkar fördelning och nivåer av kryptöjningar i systemet. De högsta töjningarna som utvecklas under drift blev med tiden både högre och vid andra positioner jämfört med vad den elastiska analysen visade.

Vidare har T-stycken modellerats så att randvillkoren blir riktiga för att kunna överlagra systemspänningar från systemanalysen till den spänningsfördelning som råder p.g.a. det inre övertrycket. Krypanalyser har genomförts som visar lokalt stora töjningar som överensstämmer med observerade krypskador. I ett sista steg har även en svets modellerats i ett T-stycke för att kunna ta hänsyn till att krypegenskaperna i svetsgods och HAZ skiljer sig från grundmaterialet.

Krypdata för simuleringarna har tagits fram genom intryckskrypprovning. Provningen kräver endast små materialvolymer och en ny metod för att prova HAZ har utvecklats där krypegenskaperna från grundmaterial, genom HAZ och in i svetsgods har kartlagts stegvis men 0,5 mm avstånd mellan varje provning. Kryphastigheterna i HAZ och svetsgods blev 2,6 högre respektive 2,0 gånger lägre än i grundmaterialet. Med dessa relativa skillnader simulerades krypförloppet i ett modellerat T-stycke som hade bytts ut från huvudångledningen i Heleneholmsverket. Analysresultaten visade töjningsfördelningar som hade godtagbar överensstämmelse med de krypskador som observerades vid metallografiska undersökningar av T-stycket.

Sammanfattningsvis har projektet, genom krypanalys och intryckskrypprovning, resulterat i ett genombrott för bedömning av kryplivslängd hos ångledningssystem.



Summary

Main steam pipe systems in conventional power plants as well as combined power and heating plants are typically operating at temperatures where the design criterion is creep. The criterion for creep design of steam piping is creep rupture. Creep rupture involves a considerable amount of creep deformation. However, a safety factor of 1.25 and 1.5 on the rupture stress is applied for 200 000 and 100 000 hours design, respectively. The stress dependence on creep life is strong with a power of 3-5 at conventional creep design data. This means that the life time for a straight pipe that is fully utilized and built of an average material would be much longer than the design life, typically 400 000 hours or longer. This applies for both 100 000 and 200 000 hours design because of the difference in safety factor.

The safety factor is primarily considered to take account for possible reduction in creep strength in comparison to the average material, which the design stresses are based on. The lower bound in the creep strength scatter for creep resistant steels is typically 20 % lower rupture stress than the average material. Then, there are other factors in a pipe system that may reduce the life time: system stresses, reduced creep strength in welds, stress concentrations in components with complex geometries that are not caught by the design rules, etc. Hence, it is not possible to know the status with respect to consumed creep life in any detail after long-term operation without inspection and monitor of the system. Established test methods are magnetic particle testing for crack detection and replica testing for monitor of the development of creep cavitation that micro-cracks and finally macro-cracks.

One issue with replica testing is to find out where the critical positions are. Creep damage and creep cracks typically appear locally where the stresses, and thereby the accumulated creep strains, are enhanced [1][2][3]. Up to date, test positions are often selected by experience. However, if not all possible critical components can be included in a testing program, it is often impossible to be sure of that the representative ones can be selected by experience only.

Elastic pipe stress analyses are performed on new pipe systems by routine within the design review to check that the stresses due to thermal expansion and dead weight in addition to the internal pressure do not exceed allowed values. After long term operation it is crucial to update the in-data to such analyses since hanger and support adjustments changes. It is also common that reconstructions of the pipe system are performed during its lifetime. Reconstructions will in most cases change the boundary conditions for the remaining part of the system, too. Therefore, updates of the analysis is needed in accordance with results of inspections (walk downs) of the system hangers and supports (which should be performed at least once a year) and any reconstructions.

Elastic stress analyses can be used to pinpoint areas with enhanced stresses at the start of the operation but the effect of creep relaxation is not considered. Stress redistribution due to creep relaxation changes the stress levels and may also change or introduce new positions that are critical with respect to creep damage development [1][4][5]. Thus, it is possible that the elastic analysis cannot fully determine critical positions for replica testing. The elastic analysis will over-estimate the stress levels at some positions and under-estimate them at others and can therefore not be used for estimations of creep life.



By introduction of creep deformation in the analysis it would not only be possible to identify critical position. It would also be possible to calculate the creep strain as a function of time at such positions. This would give at straight forward measure of the consumed life time. The remaining life can be estimated with a high precision and the analysis can be verified by replica testing. Creep analyses of complex pipe systems require powerful hard and soft ware. Therefore, it is not until recently such analyses can be expected to be performed acceptably readily.

The purpose of the present study is to develop *i*) analyses that can pinpoint critical positions for testing correctly and in detail, *ii*) analysis methods that can be used for creep life assessment in live steam pipe system components, *iii*) use creep data of weld constituents from results of miniature creep testing *iv*) make comparisons between analyses by use of tabled data and those where creep test data for the analysed component is used.

Pipe system modelling

The main steam pipe system in E.ON Heleneholmsverket was used for the modelling work. Elastic pipe stress analyses by use of Caepipe have been performed with regular updates since the middle of the 1990's. In an Energiforsk project in 1996 the system was partially modeled in Abaqus to make it possible to study creep effects in the system. More exactly, the influence of refurbishment of the system on the remaining creep life was studied [5].

Since modelling of pipe systems is very time consuming in Abaqus and very convenient in Caepipe one task in the present project was to produce a script that automatically can translate a Caepipe model to an equal one in Abaqus. During this work the existing model from [5] was used for studies of effects of starts and stops and also in the development of a method for superposition of system stresses from the pipe system to the internal pressure in a T-piece. Creep data for 10CrMo9-10 in EN10028-3:2009 was used for the evaluation of the Norton parameters that were used in the analysis. The system operates at 105 bars and 530°C.

Influence of creep relaxation and starts and stops

Figure 1a shows the stress distribution in the Heleneholmsverket pipe system directly after the first start in service. The result is the same both for elastic and creep analyses since creep relaxation not yet has started. In figure 1b the stress distribution at the end of the first service period, i.e. one year in this case, is seen. A remarkable creep relaxation can be seen. Figure 2 shows the strain distribution after 98 000 hours and one start/stop cycle each 7 000 hours. The highest strains are not in the same positions as the highest stresses in Figure 1a and 1b. Thus, the positions with the highest strains in the system after long term base load service could not be fully predicted by the elastic analysis and not by creep analysis after creep relaxation either.



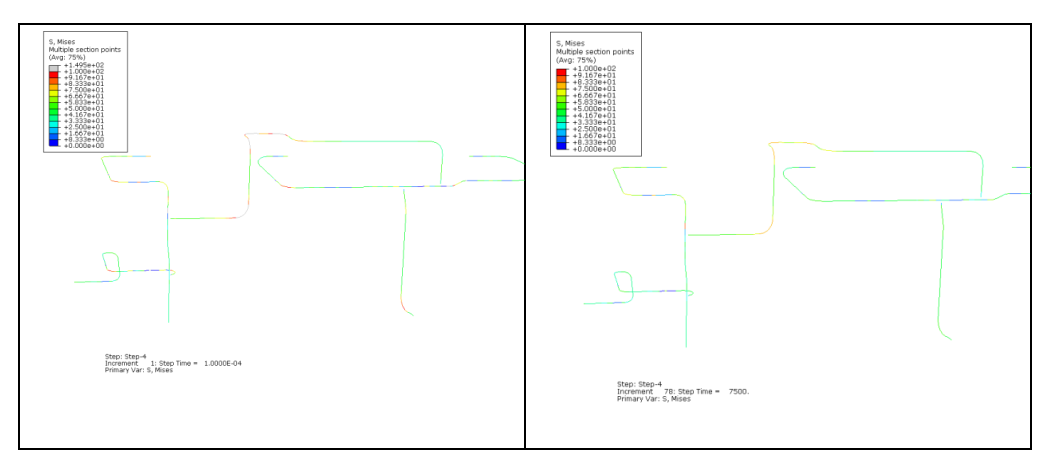


Figure 1. a) Elastic stress analysis,

b) Stress distribution after 1 year.

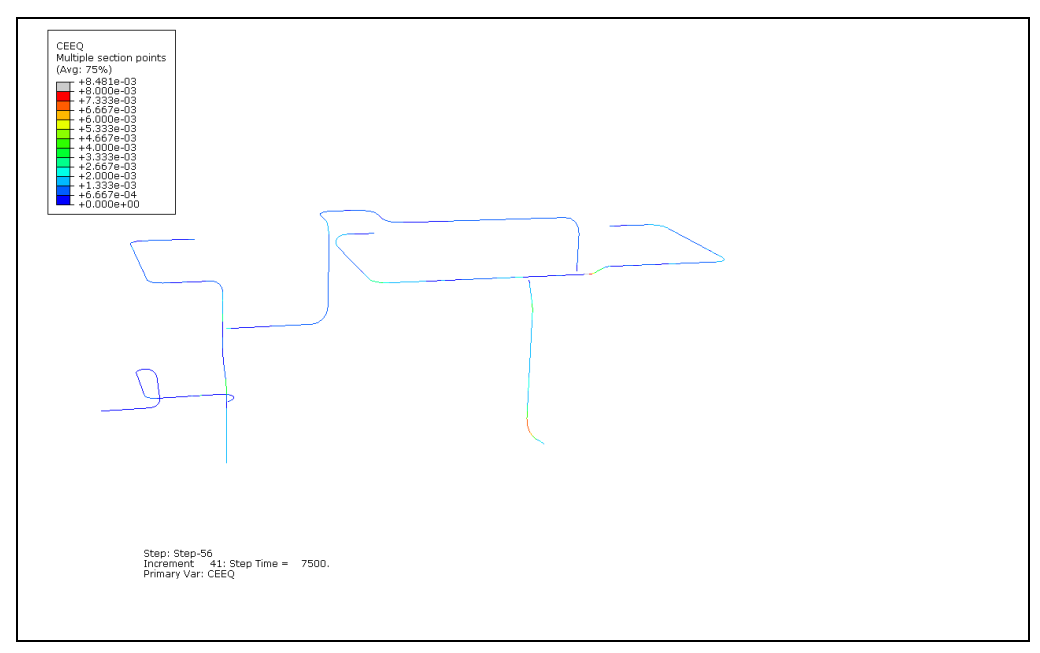


Figure 2. Strain distributions after 14 years in service and one stop each year.

A recent Caepipe model of the system was then transferred to Abaqus by use of the script that was developed. In this case the actual service time and number of start/stops, 178 000 hours and 130 cold starts, respectively, were used in the analysis. The results are shown in Figure 3 where it can be seen that the starts and stops give different strain distributions and higher strains compared to a simulated service period without starts and stops.



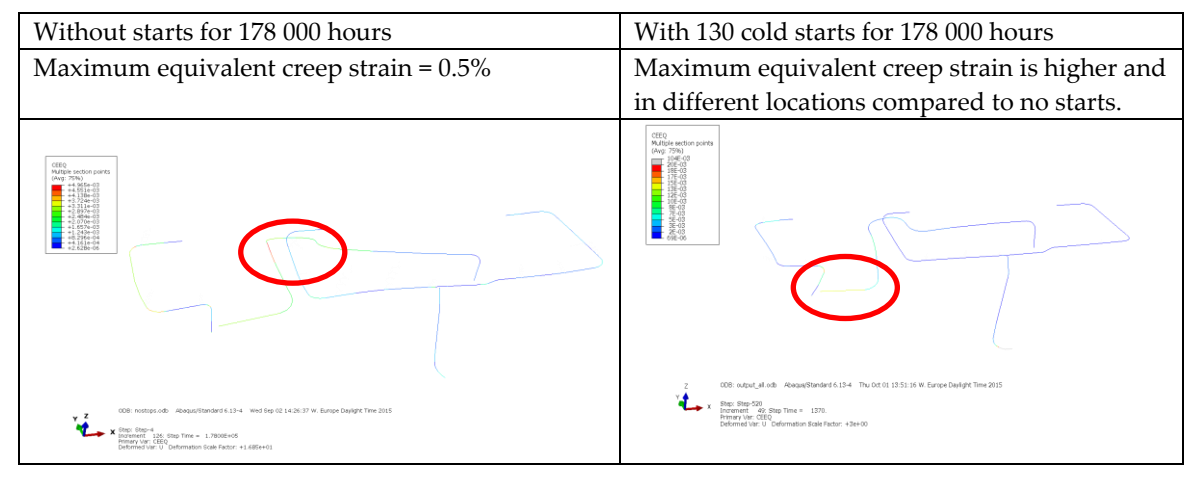


Figure 3. Demonstration of the effects of starts and stops where on the left hand side the model is run for 178 000 hours without stops, whereas the model on the right hand side has been stopped 130 times during 178 000 hours.

Superposition of system stresses on component analyses

Analyses with different extensions of a T-piece in a pipe system showed that it is clear that the stiffness of the T-joint in the piping system model is very important for the component analysis. A realistic stiffness in the piping system leads to less sensitivity for the component analysis. But as a thumb rule at least a pipe length of two diameters from each cone of the T-joint should be modelled in the component model. In cases were the stiffness in the piping system is thought to differ much from the actual stiffness a sensitivity analysis is suggested to determine the needed extent of the component model. Figure 4 shows the resulting equivalent strains in a T-piece that was chosen from the system after six years in service. The creep strains are due to internal pressure, dead weight and thermal expansion.

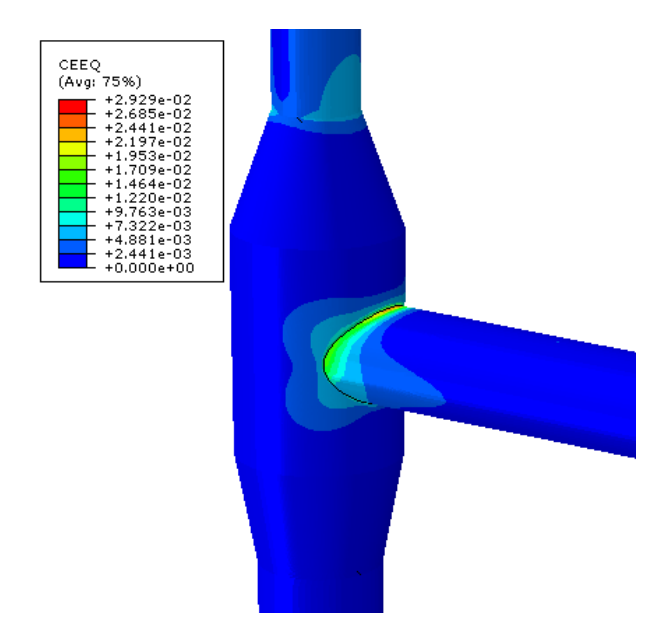


Figure 4. Equivalent creep strains after six years in service.



The highest strain accumulation is in a small area at the right angel position of the T-piece. This indicate that system stresses had a large influence on the strain level and strain distribution since internal pressure only would have given the highest strains at the saddle point position of the T-piece. Any effects of starts and stops were studied also in this analysis but there were no such effects in this position. The highest strain is 2.6 % which is quite a lot after only six years in operation. A significant part, approximately half the life time can be considered to have been consumed.

Creep damage in the studied main steam pipe

Three welds were cut from a part of the steam piping that was exchanged in Heleneholmsverket in the summer 2014. Two of them, tagged MR15 and MR20, were butt welds from a straight part of the pipe with a service time of 178 000 hours. The third weld. MR05, was a T-piece branch weld that have had 73 000 hours in operation (it had been exchanged once before). They were exchanged because the calculated life time was expired on bases of elastic analyses and tabled creep data.

The condition of the welds was examined metallographically with respect to creep damage. Creep cavitation was found in all the three welds. In MR15 small amounts of isolated cavities were observed in two thirds of the examined positions of the weld metal and the HAZs as well as the parent metals. One weld metal position revealed a 2.3 mm long creep crack but no creep damage in the remaining positions. In MR20 creep cavitation was observed in all examined positions and in higher amounts than in MR15 in many of them. In MR05 there were even higher amounts of creep damage in the HAZs with oriented cavitation at the saddle point positions. In the weld and parent metals creep damage was found just in quite a few positions. However, the total amount of creep damage in MR05 was higher than might be expected after 73 000 hours in service.

Impression creep testing

So far, tabled creep data has been used for the analyses. The influence of the specific creep properties of a component was studied by impression creep testing. This is a miniature creep testing method where an indenter with constant load is pushed into the material at elevated temperatures. The creep deformation during such a test is converted to a corresponding strain for a uniaxial test. Advantages with the impression creep are that only small quantities of material is required for the test, allowing for semi-destructive testing and testing of weld constituents such as HAZs. A restriction is that only primary and secondary parts of the creep curve are obtained by the testing. However, in creep analyses based on Norton's creep law, as in the present case, only secondary creep is utilized.

A new butt weld was produced from a pipe that was a spare part in Heleneholms-verket. It was also possible to use a retired T-piece from Heleneholmsverket for the testing. Before the testing the T-piece was investigated with respect to creep damage. Significant creep cavitation was found in the HAZs at both the right angle and the saddle point positions. In the latter position cavities were found also in adjacent parent and weld metals.

A new approach for impression creep testing of a weldment was conducted. A standard specimen is 10x10x2.5 mm but was in this case made thicker and covered



parent metal in the top layer, HAZ in the middle and weld metal at the bottom. Testing was performed on the parent metal, and then the specimen was ground to the intercritical part of the HAZ and tested there. This procedure continued with 0.5 mm grinding between each test. The specimen was turned 90° between each test to minimize any effects of deformation from the indenter in the test area. The results are shown in Figure 5, where the creep rate at 500 hours testing and the creep strain after 300 hours testing are shown versus the test position in the weldment. It can be seen that the creep rate is 2.6 times higher at the HAZ/parent metal borderline than in the parent metal. The weld metal strain rate is about half of that in the parent metal. In addition the parent metal was creep tested by use of conventional uniaxial specimens for comparison and verification of the impression creep testing. The uniaxial and the impression creep test results agreed very well.

The test results of the retired weld are also shown in Figure 5. This weld was tested in weld metal and in the parent metal adjacent to and remote from the HAZ (BM1 and BM2, respectively). It can be seen that the weld and the parent metal creep rate is 6-8 and 2-5 times higher than in the new weld, respectively.

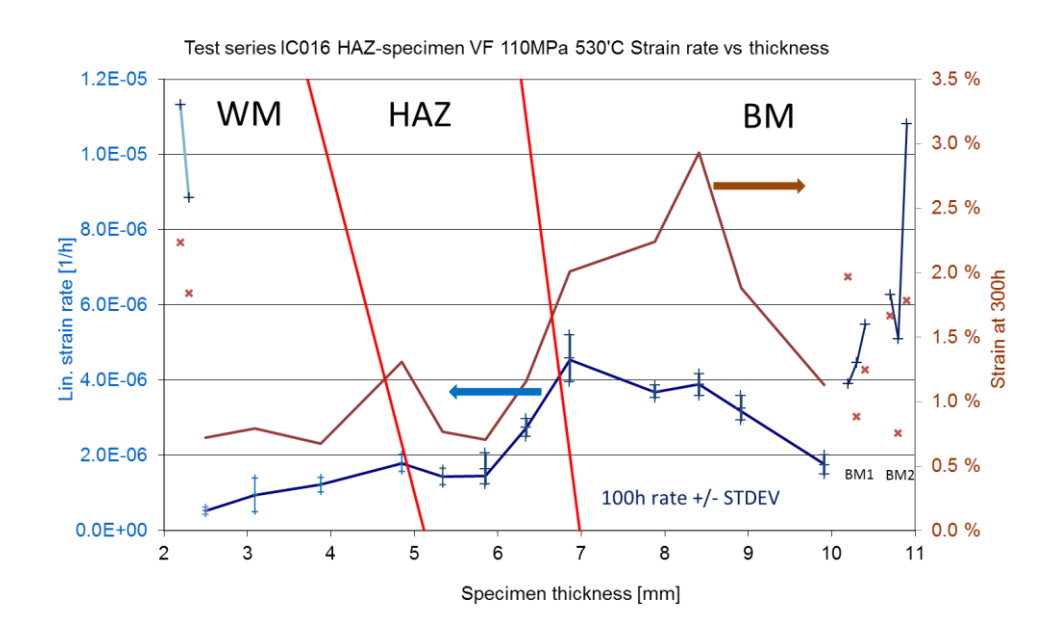


Figure 5. Linear creep rate and strain at 300 h vs. impression creep specimen thickness.

Evaluation of remaining lifetime of the main steam pipe system in Heleneholmsverket

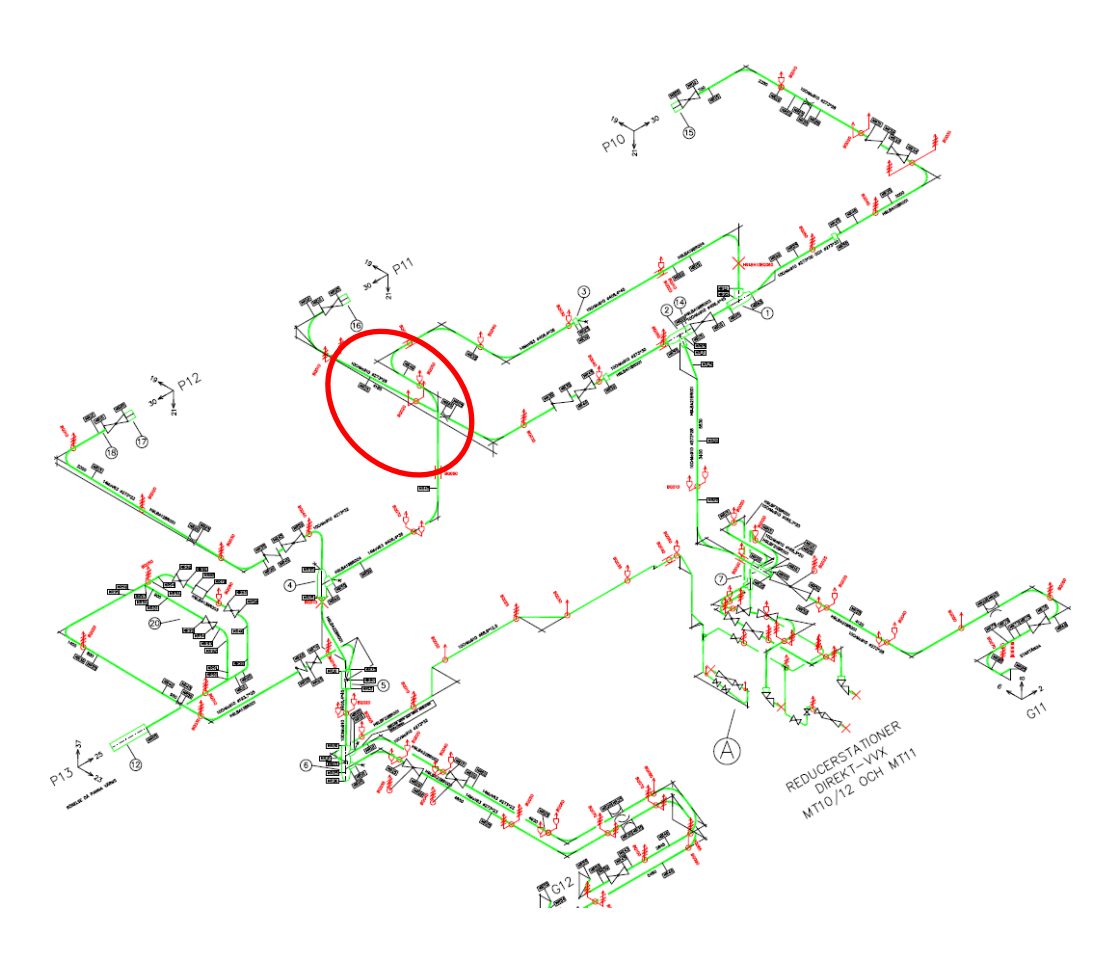
System analysis

The piping system that was translated with the script has been used for analyses with actual operational data from Heleneholmsverket. In addition, the effects of starts and stops according to the service data were studied. Five different parameter combination of the Norton creep material models have been tested for the piping system and will be evaluated against observed creep damages found in welds MR15 and MR20 in a straight part of the piping shown in the red circle in Figure 6. The five models have



different material parameters according to Norton's law, presented previously, see Eq. 1 below and the representing parameters *B* and *n* that vary between the models are shown in Table 1. A graphical presentation of the material models is shown in Figure 7, where all material models are shown with minimum linear strain rate vs. stresses amongst with the results of uniaxial creep of new material and data points for base material BM1 and BM2 for the testing of the T-joint base metal.

$$\frac{d\varepsilon}{dt} = B\sigma^n \tag{1}$$



Figur 6. Heleneholmsverket steam pipe system. The red circle marks the location of welds MR15 and MR20.



Table 1. Parameters for Norton's creep material model used for the piping analysis.

| Model No. | Description | В | n |
|--------------|--|----------|------|
| 1 | EN 10028-2 | 4.92E-17 | 5.08 |
| 2 | EN 10028-2 – lower bound, 20 % lower rupture stresses at same creep strain rate. | 1.53E-16 | 5.08 |
| 3 | LSCP data (logistic creep strain prediction [18]. | 2.16E-17 | 5 |
| 4 | IC testing- new unused material, base material data. Modell is assumed to have the same <i>n</i> value as evaluated from EN 10028-2. | 7.46E-17 | 5.08 |
| 5 | IC testing for a base material that has been in operation in Heleneholmsverket for 73 000 hours of operation. | 1.64E-16 | 5.08 |

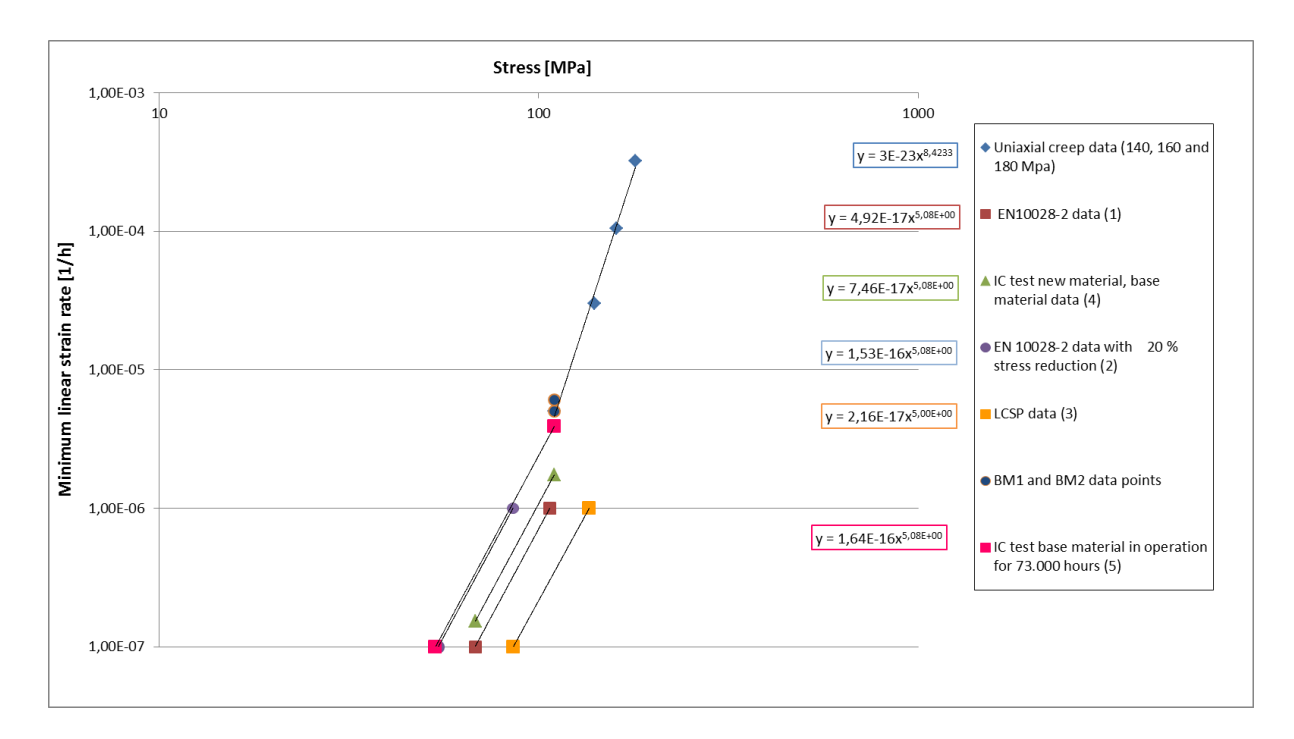


Figure 7. Minimum linear creep rates versus stress of parent metal for several Norton material models (numbered 1-5) as well as for produced data of uniaxial creep on new material and of impression creep on service exposed material (BM1 and BM2).

At the end of operation after 178 000 hours the creep strain in element 5 (MR15) and 6/7(MR20) is compared for different material models and is shown in Table 2. In a large part of the welds there were creep damages with index around 2a and 2b, respectively. Locally both higher and lower values were observes, but an average of 2a is estimated for the welds, with MR 20 having slightly higher creep damage on the average than MR15. Creep damage index 2a is estimated to correspond to a creep strain in the range 0.5-1 %.



Table 2. Equivalent creep strain results from the model.

| Model No. Part in system | 1 | 2 | 3 | 4 | 5 |
|--------------------------|---------|--------|---------|--------|--------|
| Element 5 (MR15) | 0.085 % | 0.26 % | 0.029 % | 0.13 % | 0.27 % |
| Element 6/7 (MR20) | 0.1 % | 0.29 % | 0.042 % | 0.15 % | 0.31 % |

Table 3. Correlation between the Norton B factor and the amount of equivalent creep strain.

| Norton B factor | 2,16E-17 | 4,92E-17 | 7,46E-17 | 1,53E-16 | 1,64E-16 |
|--|----------|----------|----------|----------|----------|
| Model | 3 | 1 | 4 | 2 | 5 |
| Equivalent creep strain from table 10 for MR20 | 0.042 % | 0.1 % | 0.15 % | 0.29 % | 0.31 % |

Component analysis

The T-piece that was cut out for examination and impression creep testing was modelled by FEM. The geometries were taken from the drawing of the T-piece. Also the T-piece branch weld geometry was included in the drawing. The HAZ was measured and modelled to 3.0 mm (Table 4) at the saddle point side of the weld, which is of particular interest since significant creep damage was observed there. Creep rates in weld metal and HAZ with the factors 0.5 and 3 times the parent metal creep rate, respectively, were used in the analysis. These factors are rounded numbers of the relative creep rates of the impression creep results of the new weld.

The analysis was first performed with materials data that correspond to tabled creep data. The creep properties in the weld metal and the heat affected zone were in analogy with the present test results of the new material, where the weld metal and the HAZ had approximately 2 and 3 times higher creep rate than the parent metal, respectively. The same factors were then used in relation to the parent metal properties evaluated from tabled creep data.

Since there was a significant effect of starts and stops on strain distributions in the system analysis, starts and stops were evaluated in the same way also for the T-piece, i.e. each start/stop sequence is 1370 hours.

Figure 8 shows the creep strain distribution at the T-piece weld after the first 1370 hours in operation of the system (the average service period between two start/stop cycles at Heleneholmsverket). Although the T-joint that was received for creep testing and metallographical examination was the third T-joint at the same place it is interesting to study the first period where the effect of creep relaxation is largest.

The highest strains present in the branch weld. The highest strains (red areas) started at the right angle positions at the T-connection and expanded along the HAZs and at 1370 hours the relatively high strains have spread half way to the saddle point, as can be seen in the figure. The maximum strain is 0,14 % already after 1370 hours.



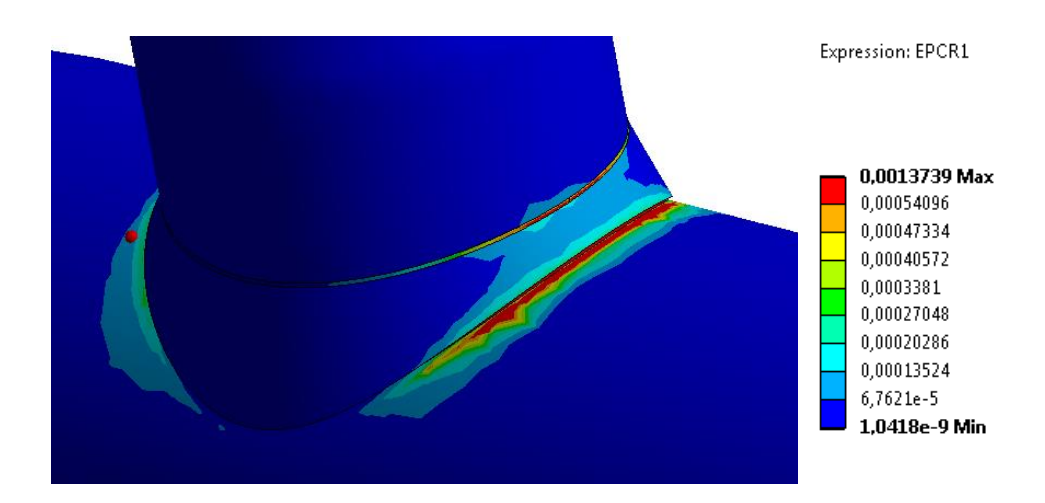


Figure 8. Detail of the T-piece showing the creep strain distribution after 1370 hours.

Finally, simulations that cover the actual life of the studied T-joint were performed. This is in 1990 when the system has an accumulated service time of about 105 000 hours. Thus, the analysis starts with actual system stresses at that time and continues for another 73 000 hours when it is taken out from operation. The resulting strain distribution in the T-piece is shown in Figure 9. Creep strains up to 1.5 % appear in the HAZs at one of the right angel positions. Enhanced strains also appear close to the cone at the vertical pipe. Strains in compression appears at the opposite right angel position. This is consistent with observed creep damage in the real T-joint. However, significant amounts of creep cavitation also appeared at the saddle point positions which did not have corresponding amounts of creep strain according to the analysis. This can be explained by simplifications of the system model that was needed for the verification of the translation script.

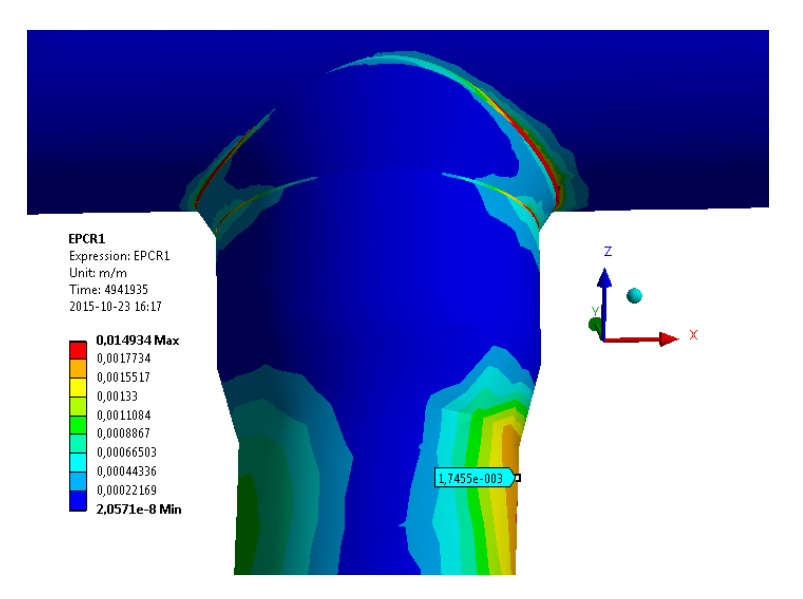


Figure 9. Detail of the T-piece showing the creep strain distribution after 73 000 hours.



Conclusions

The following conclusions can be drawn from the present study:

- Significant creep cavitation was observed in two butt welds and in a T-piece from the main steam pipe from a power plant that had been in operation for 170 000 hours and 73 000 hours, respectively. The damage in the T-piece can be considered as pre-mature.
- Impression creep testing with an innovative approach was used by manufacturing a "sandwich" type of specimen of the new weld which allowed the creep rates to be scanned from the base material across the HAZ to the weld metal by steps of 0.5 mm. The maximum creep rate in the HAZ was in the intercritical part and was 2.6 times higher than in the parent metal. The weld metal of the new weld was overmatching by a factor of two.
- Impression creep testing of parent and weld metals with 73 000 hours service exposure showed 3 and 6 times higher creep rates, respectively, than for corresponding materials in a virgin weld.
- The impression creep test results of virgin parent metal were consistent with uniaxial creep testing of the same material.
- Creep analysis of a main steam pipe system showed significant stress relaxation occurs after a relatively short service period. These effects cannot be covered by an elastic analysis, such as a Caepipe analysis.
- Creep analyses of a main steam pipe system including starts and stops resulted in
 higher levels of creep strain than without the starts and stops. In addition, the
 positions where the highest strains occurred were not the same. Thus, it is shown
 that a creep analysis that includes the effects of starts and stops can be needed to
 show actual creep strains as well as critical positions for non-destructive testing.
 Identification of critical positions with critical positions by elastic pipe system
 analysis, which is quite common today, should therefore be carried out with
 caution.
- Creep analysis of the main steam piping was carried out with creep data from standards and from the impression creep test results. Creep test results of new material and standard data gives similar creep strains in the system, approximately 0.1 % after 178 000 hours. The same analysis but with use of creep tests results of service exposed material and with lower bound standard data resulted in 0.3 % creep strain.
- A component model of a T-piece where system stress can be superimposed to internal pressure was developed successfully.
- A branch weld was then included in the model of the T-piece. The relative
 differences of creep rates between parent metal, HAZ and weld metal that was
 obtained by the impression creep testing was used in the model for simulations of
 service exposure.
- There is a quite good agreement between simulated creep strain distribution after 73 000 hours in service and observed creep damage in the real T-piece after the same time in service.



List of content

| 1 | Intro | oduction | 18 | | | | | | |
|---|-------|---|----|--|--|--|--|--|--|
| | 1.1 | Background | 18 | | | | | | |
| | 1.2 | Description of the research area | 19 | | | | | | |
| | 1.3 | The research task and its role within the research area | 19 | | | | | | |
| | 1.4 | Goal and target group | 20 | | | | | | |
| 2 | Reali | ization of the project | 21 | | | | | | |
| 3 | Cree | p damage in the studied main steam pipe | 23 | | | | | | |
| | 3.1 | Compilation of history with respect to service creep damage | 23 | | | | | | |
| | 3.2 | Selection of components/welds for verification of the analyses | 25 | | | | | | |
| | 3.3 | Characterization of creep damage in selected exchanged welds | 27 | | | | | | |
| | 3.4 | Characterization of creep damage in a cross-section of the MR05 weld | 30 | | | | | | |
| 4 | Deve | elopment of a script that enables fast modeling of pipe systems with | | | | | | | |
| | respe | ect to creep | 33 | | | | | | |
| | 4.1 | Models in Caepipe and abaqus | 33 | | | | | | |
| | 4.2 | Comparison of the script and the reference model | 36 | | | | | | |
| 5 | | bination of system and component analysis – determination of boundary ditions | 43 | | | | | | |
| | 5.1 | Sensitivity analyses | 43 | | | | | | |
| | 5.2 | Component models | 44 | | | | | | |
| | 5.3 | Geometries | 44 | | | | | | |
| | 5.4 | Material | 45 | | | | | | |
| | 5.5 | Boundary conditions and loading | 45 | | | | | | |
| | 5.6 | Results for the sensitivity analyses | 46 | | | | | | |
| | 5.7 | Discussion | 48 | | | | | | |
| 6 | Studi | lies of effects of starts and stops | 49 | | | | | | |
| | 6.1 | Model and anticipated operation | 49 | | | | | | |
| | 6.2 | Results | 49 | | | | | | |
| | 6.3 | Discussion | 57 | | | | | | |
| | 6.4 | Conclusions of the effect of starts and stops | 57 | | | | | | |
| 7 | Impr | ression creep testing | 58 | | | | | | |
| | 7.1 | Test method 5 | | | | | | | |
| | 7.2 | VTT design of the impression creep equipment | 61 | | | | | | |
| | 7.3 | Applications of impression creep technique | 63 | | | | | | |
| | 7.4 | Uniaxial and impression creep testing | 64 | | | | | | |
| | | 7.4.1 Uniaxial creep test results in new material | 64 | | | | | | |
| | | 7.4.2 Impression Creep test results of the new weld | 67 | | | | | | |
| | | 7.4.3 Impression Creep test results of the service exposed T-piece | 72 | | | | | | |
| | | 7.4.4 Conclusions | 75 | | | | | | |



| 8 | Evaluation of remaining lifetime of the main steam pipe system in Heleneholmsverket | | | | | | | | |
|----|---|----------|---|----|--|--|--|--|--|
| | 8.1 | Pipe Sy | ystem analysis | 76 | | | | | |
| | | 8.1.1 | The effects of start and stops with operational data, material model 1 | 78 | | | | | |
| | | 8.1.2 | Results of the evaluation of material parameters and comparson with creep damage in the service exposed main steam pipe system in Heleneholmsverket | 79 | | | | | |
| | | 8.1.3 | Discussion and conclusions of pipe system analysis | 80 | | | | | |
| | 8.2 | Compo | onent analysis | 80 | | | | | |
| | | 8.2.1 | Model of the chosen T-piece for the sensitivity analysis | 80 | | | | | |
| | | 8.2.2 | Results | 81 | | | | | |
| | | 8.2.3 | Model of the service exposed T-piece that was investigated in the present study | 83 | | | | | |
| | | 8.2.4 | Results of initial service | 85 | | | | | |
| | | 8.2.5 | Results of simulation of service that corresponds to the studied T-piece | 87 | | | | | |
| 9 | Result | analysi | s | 89 | | | | | |
| | 9.1 | Impres | ssion creep | 89 | | | | | |
| | 9.2 | System | n analysis | 89 | | | | | |
| | 9.3 | | | | | | | | |
| 10 | Discus | sion | | 91 | | | | | |
| 11 | Conclu | isions | | 92 | | | | | |
| 12 | Recommendations 9 | | | | | | | | |
| 13 | Propos | sals for | future research | 94 | | | | | |
| 14 | References 95 | | | | | | | | |

Appendices

- A Script for automatic translation of a Caepipe model to a Abaqus model for creep analysis
- B Welding data for the new pipe weld
- C Finite element analysis of impression creep



1 Introduction

1.1 BACKGROUND

Main steam pipe systems in conventional power plants as well as combined power and heating plants are typically operating at temperatures where the design criterion is creep. Creep is a time dependent deformation mechanism and therefore, design for creep involves a design life time. The design life is typically 100 000 hours for steam piping built before the 1980's and thereafter 200 000 hours.

The criterion for creep design of steam piping is creep rupture. Creep rupture involves a considerable amount of creep deformation. However, a safety factor of 1.25 and 1.5 on the rupture stress is applied for 200 000 and 100 000 hours design, respectively. The stress dependence on creep life is strong with a power of 3-5 at conventional creep design data. This means that the life time for a straight pipe that is fully utilized and built of an average material would be much longer than the design life, typically 400 000 hours or longer. This applies for both 100 000 and 200 000 hours design because of the difference in safety factor.

The safety factor is primarily considered to take account for possible reduction in creep strength in comparison to the average material, which the design stresses are based on. The lower bound in the creep strength scatter for creep resistant steels is typically 20 % lower in rupture stress compared to the average material. Then, there are other factors in a pipe system that may reduce the life time: system stresses, reduced creep strength in welds, stress concentrations in components with complex geometries that are not caught by the design rules, etc. Hence, it is not possible to know the status with respect to consumed creep life in any detail after long-term operation without inspection and monitor of the system.

Many plants operating in the creep range were built in 1960-90's and in most cases the design life started to be reached 15-20 years later. A long time before creep cracks appear there are changes in the material microstructure. For example, the formation of creep cavities, that can be used as a measure of on-going creep deformation. Over time more cavities are formed, they start to orient perpendicular to the principal stress direction, develop to micro-cracks and to finally macro-cracks. By taking replicas on metallographically prepared surfaces at critical positions this damage development can be monitored, proper re-inspection intervals can be set and components can be exchanged in a safe and controlled way at planned outages.

One problem with replica testing is to find out where the critical positions are. Creep damage and creep cracks typically appear locally where the stresses, and thereby the accumulated creep strains, are enhanced. Up to date, test positions are often selected by experience. However, if not all possible critical components can be included in a testing program, it is often impossible to be sure of that the representative ones are selected only by experience.

Elastic pipe stress analyses are performed on new pipe systems by routine within the design review to check that the stresses due to thermal expansion and dead weight in addition to the internal pres-sure do not exceed allowed values. After long term operation it is crucial to update the in-data to such analyses since hanger and support adjustments changes. It is also common that reconstructions of the pipe system are performed during its lifetime. Reconstructions will in most cases change the boundary



conditions for the remaining part of the system, too. Therefore, updates of the analysis is needed in accordance with results of inspections (walk downs) of the system hangers and supports (which should be performed at least once a year) and any reconstructions.

Elastic stress analyses can be used to pinpoint areas with enhanced stresses at the start of the operation but the effect of creep relaxation is not considered. Stress redistribution due to creep relaxation changes the stress levels and may also change or introduce new positions that are critical with respect to creep damage development. Thus, it is possible that the elastic analysis cannot fully determine critical positions for replica testing. The elastic analysis will over-estimate the stress levels at some positions and under-estimate them at others and can therefore not be used for estimations of creep life.

By introduction of creep deformation in the analysis it would not only be possible to identify critical position. It would also be possible to calculate the creep strain as a function of time at such positions. This would give at straight forward measure of the consumed life time. The remaining life can be estimated with a high precision and the analysis can be verified by replica testing. Creep analyses of complex pipe systems require powerful hard and soft ware. Therefore, it is not until recently such analyses can be expected to be performed acceptably readily.

The purpose of the present project is to develop *i*) analysis methods that can be used for creep life assessment in live steam pipe system components, *ii*) use newly developed methods for miniature creep testing of weld constituents and *iii*) use produced creep data in the analyses and compare with tabled data that are used regularly.

1.2 DESCRIPTION OF THE RESEARCH AREA

It has been recognized for a long time that creep cracks and creep damage usually appear locally in steam pipe components and that this is due to local stress enhancements over time. The geometry of components such as T-joints, branches and bends result in enhanced stresses at certain positions. These positions have been identified and creep analysis of such components, resulting in stress distribution and strain accumulation over time, has also been performed [1][2][3]. Effects of system stresses on individual components are on the other hand more difficult to predict in creep loaded systems. Work has been done previously on analyses of pipe systems with respect to creep [4][5] but there are still issues that remain to be studied. In addition to develop qualified tools for the analysis it is also crucial to use proper and updated input data from the settings of system hangers and supports [6][7].

1.3 THE RESEARCH TASK AND ITS ROLE WITHIN THE RESEARCH AREA

The present project is aimed to develop analysis methods of live steam pipe systems including its components and welds. The purposes of the analyses are to pin-point critical positions for non-destructive testing and to perform remaining life time assessments. The possibilities for this are, with the understanding that has been gained by the research on the area up to date, limited. The following tasks have been identified as important to make it possible to pin-point critical positions for non-destructive testing and to perform remaining life time assessments in creep loaded steam pipe systems:

• Effective modeling of creep exposed pipe systems – development and verification of script that can translate an elastic model to a creep model.



- Combination of system and component analysis determination of boundary conditions.
- Studies of effects of starts and stops by use of produced models.
- Miniature creep tests, impression creep (IC) testing, for determination of creep properties in welds, particularly in the heat affected zone.
- Finite element analysis of IC test.
- Modeling of welds in pipe components and component creep analyses including welds by use of produced creep data.
- Remaining life time analysis of pipe systems and pipe system components by use of design creep data and produced creep data.
- Verification of remaining life time analyses by comparison with a reference case (Heleneholmsverket). This includes reviews of hanger and support data as well as non-destructive testing results (magnetic particle and replica investigations).

The role of the tasks above is to develop the tools for remaining life assessments of high temperature steam pipe systems to a far higher level than up today. The understanding of creep behavior in such systems will at the same time be increased.

1.4 GOAL AND TARGET GROUP

- Advanced pipe system stress analyses that are capable to consider creep.
- Improve the modeling for system analyses with respect to cost-effectiveness to be comparable to elastic system analyses.
- Develop a method for superimposing pipe system stresses on analyses of stress/strain distributions of components such as T-joints.



2 Realization of the project

The starting point of the present project is a model of the greater part of the main steam pipe system at E.ON Heleneholmsverket that was produced in a Värmeforsk project entitled "Influence of refurbishment of steam piping systems on the remaining life time" by Segle et. al. [5].

This model was produced in Abaqus software which is well suited for creep analysis. However, Abaqus is suited for modelling of components rather than pipe systems, which would take much too long time in practice. Therefore, one task in the project is to produce a script, which in this case would be a program that is able to interpret a model of a pipe system that has been produced in software specialized for pipe systems, and translate it in to a model in Abaqus. Such software cannot handle creep but a pipe system can be modeled very fast compared to Abaqus.

Elastic pipe stress analyzes have been performed on the main steam piping at Heleneholmsverket by use of the Caepipe software by PA Ingenjörssupport. This model and updated analyzes since the last 20 years have been available to be used in the project. Thus, the script to be developed will be applied on this Caepipe model.

Re-occurring replica testing has been performed at the main steam pipe at Heleneholmsverket for 30 years. There is a lot of basic data and exchange of components as well as refurbishments that has been performed over the years. Thus, one task is to compile this to make it possible to choose parts of the system and components that can be used for verification of the resulting creep analyses.

Design creep data is frequently used for creep analyses. This was the case also in [5]. An option is to use data from creep tests of material from steam pipes. Since steam pipes likely consist of material from different batches it is then important to keep in mind that the creep properties may differ to some extent from one batch to another. Creep testing is also accelerated and involves significant extrapolation to service data whereas long term testing is behind design data. Thus, it is not obvious that creep test results always are a better choice than tabled creep data. Nevertheless, there are certain advantages to use actual creep data for the analysis: i) creep properties from welds and heat affected zones, which cannot be found in the design data and hardly not elsewhere as well and ii) the creep properties at the current stage of service exposure. However, with conventional creep testing there are difficulties with the welds and especially the HAZs since they are narrow. The width of the HAZ is typically around 3 mm in thickwalled multi-pass welds.

There are a few possibilities to test the creep properties in the HAZs. Impression creep (IC) and small punch (SP) testing are two methods that require small amounts of material and can therefore be considered as semi-destructive. In the present project, IC testing was chosen to produce HAZ and weld metal creep data. A full description of the method is given in section 5.

The test program covers two welds for the testing:

 A virgin weld of the same material as the main part of the pipe system, 10CrMo9-10. A pipe butt weld with the same dimensions as in the pipe system in Heleneholmsverket was produced by the welding company that is contracted for welding services in this plant.



• A component weld from a part of the system that was cut out in connection with a refurbishment of the system in 2014.

In this way, analyses by use of i) tabled data, ii) virgin material data and iii) service exposed data can be compared to each other and also compared to replica test results as a verification of the analyses. The test programme is described in detail below.



3 Creep damage in the studied main steam pipe

3.1 COMPILATION OF HISTORY WITH RESPECT TO SERVICE CREEP DAMAGE

Design and service data are given in Table 1.

Tabell 1. Konstruktions- och driftdata för huvudångledningen

Table 1. Design and service data for the main steam pipe

| Design pressure | 129 bar |
|---------------------|--|
| Service pressure | 105 bar |
| Design temperature | 530°C |
| Service temperature | 530°C (510°C for 8000 h between 1985 and 1987) |
| Service time | 75 000-200 000 hours for different parts of the system |

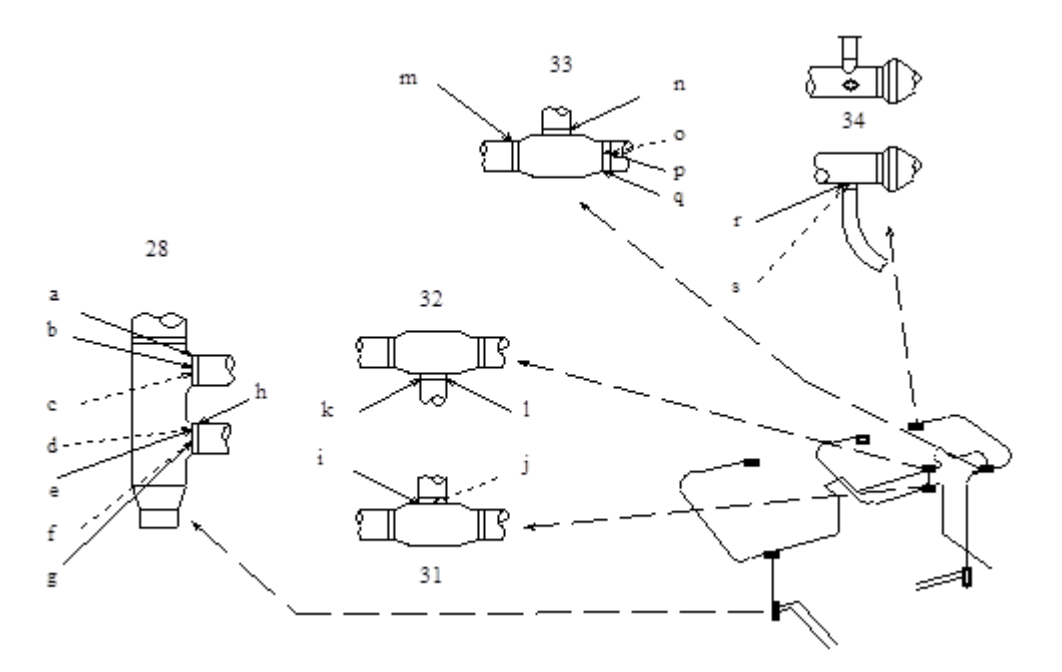
Replica testing of T-joints and valve housing started already in 1984. Already in the first years of replica testing creep cracks were found in some components and developed creep cavitation in a number of other ones. Smaller creep cracks were ground away without further actions whereas larger ones were weld repaired. The service temperature was decreased to 510°C for an 8 000 hours period to permit service in this condition. Then, some components were exchanged and the service temperature was increased to 530°C again in 1987.

Significant creep damage development was observed in five components at replica testing in 1990. However, the service time was limited to not more than 15 000 hours between 1985 and 1990, see Figure 1 and Table 2 [8]. This indicates that system stresses are involved in this damage development. The design may also play a significant role. The nominal pipe dimensions results in pipe hoop stresses of 63 and 77 MPa at service and design pressure, respectively. This can be compared to the highest allowable stress which is 60 MPa when a safety factor of 1.5 is applied. Thus, the usage factor at service pressure is over 1 (1.03).

In Figure 1 and Table 2 it can be seen that damage development often occurs at right angel positions of the T-joint branch welds. If only internal pressure controls the creep deformation damage would predominantly appear at the saddle positions instead. It is obvious that system stresses are involved. In Table 2 the creep damage is rated according to Nordtest NDT 010 [9] where the first number indicates the classical rating from 1 to 5. The second number after the dot is a sub-class where 1, 2 and 3 indicate small, medium and high amount of creep damage of the actual creep damage class, e.g. classes 2.1, 3.2 and 4.3 indicate separate cavities in a small amount, strings of cavities in a medium amount and micro-cracks in a large amount.

Damage class in intercritical and fine grained HAZ (HAZ-BM and HAZ in the table) is given in one column; damage class in coarse grained HAZ and weld metal adjacent to the fusion line (HAZ-WM and WM-HAZ in the table) is given in a second column. Creep cracks that are formed in the HAZ-WM and WM-HAZ areas are called type III cracks whereas those which are formed in the HAZ-BM and HAZ are called type IV cracks.





Figur 1. Komponenter från huvudångledningen med signifikant krypskadeutveckling i perioden 19851990. På respektive komponent finns också markerade vilka positioner som har haft
skadeutveckling, se tabell 2 för detaljerad information om skadenivåerna[8]. Drifttiden är ca
8 000 timmar mellan provningstillfällena för komponent 28 och 34 samt ca 15 000 timmar för
de övriga [8].

Figure 1. Components from the main steam pipe with significant creep damage development in the period 1985-1990. On each component it is marked at which position the damage development has occurred, see Table 2 for more detailed information. The service time is approximately 8000 h in the period for component 28 and 34. The other ones had a service time of 15 000 h in this period [8].

In Table 2 it is seen that a higher damage development than what may be expected is observed in a few positions. For example, component 28 at positions c and e (it was only 8 000 h between the investigations for this component), component 31 at position i and component 33 at position q where no or very little creep damage has developed to high damage classes including micro-cracks. It can also be seen that the damage development in most cases occurs in the HAZ-WM and WM-HAZ areas.

Up to date there have been a number of occasions where components and pipe sections have been exchanged because of creep exhaustion. More extensive exchanges were performed in 1993, 1995, 1996 and 2004. All components in Table 2 have, for instance, been exchanged. In recent years the strategy has been to replace part of the system that are old or exposed to enhanced stresses, indicated by Caepipe analyses of the system, before critical creep damage (cracks) is developed. Thus, there are components that have been changed twice.



Tabell 2. Positioner med skadeutveckling [8].

Table 2. Positions with damage development [8].

| Component | Pos. | Dama | ge rating 1985 | Damage r | ating 1990 |
|-----------|------|----------------|--------------------|-------------|-------------------|
| | | HAZ-BM, HAZ | HAZ-WM, WM- HAZ | HAZ-BM, HAZ | HAZ-WM, WM-HAZ |
| 28 | а | 2.1 | 3.2 | 2.3 | 4.2 |
| | b | 1 | 3.1/2.2 | 2.2 | 4.1/3.3 |
| | С | | 2.1 | | 4.1 |
| | d | | 3.1 | | 4.1 |
| | е | | 1 | | 3.1 |
| | f | | 3.2 | | 4.1 |
| 31 | i | | 2.3 | | 5.3 |
| | j | | 2.1 | | 2.3 |
| 32 | k | | 4.1 | | 4.3 |
| | - 1 | | 2.2 | | 4.1 |
| 33 | m | | 2.1 | | 3.1 |
| | n | | 2.1 | | 3.1 |
| | 0 | | 2.1 | | 2.3 |
| | р | | 1 | | 2.2 |
| | q | | 2.1 | | 4.2 |
| 34 | r | 1(5.3) | | 2.3 | |
| | S | | 2.1 (5.3) | | 3.1/2.2 |

^{*}Rating in brackets (5.3) indicates that creep cracks were ground away before replica testing at the bottom of the ground area.

3.2 SELECTION OF COMPONENTS/WELDS FOR VERIFICATION OF THE ANALYSES

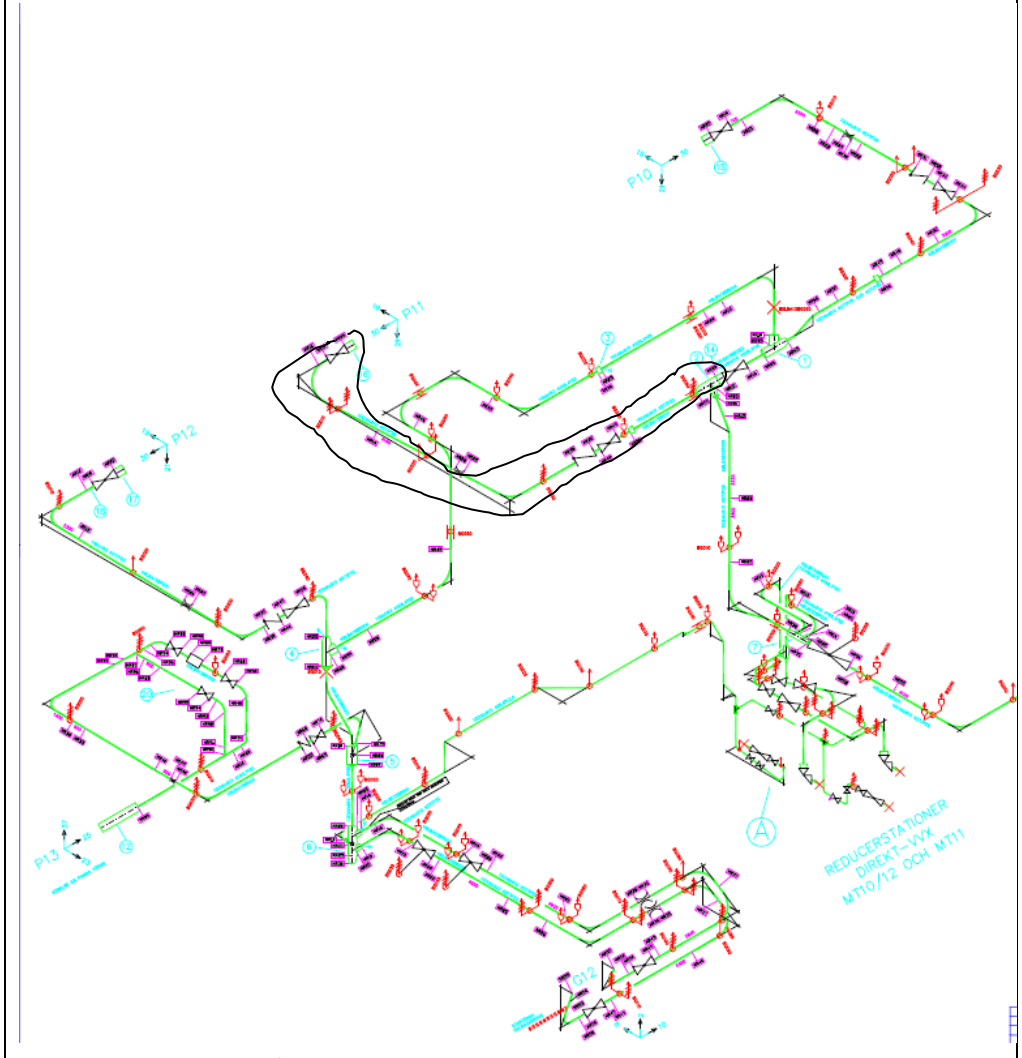
The verification of the analysis is, of course, dependent of the accuracy of the models themselves but it is equally crucial to have the accurate input data for the analysis. The steam pipe system of Heleneholmsverket has been refurbished once before and a number of T-joints have been replaced over the years as well.

Therefore, it is important to select a part of the system that has a fully documented history with respect to input data for the recurring elastic pipe stress analyses that have been performed over the years. In the same way the service exposed weld to be characterized with respect to creep damage and tested by IC should be selected from same part that the creep analyses are verified against. To do this properly, a complementary part or the project was applied for and approved. The findings from these investigations are presented below and in section 3.3.

An isometry of the pipe system is seen in Figure 2. The part of the system that is circumscribed was cut out in connection to the refurbishment 2014. This part can be seen in detail in Figure 3. There are two welds, marked MR15 and MR20, in the section that are original, i.e. they have been in operation since 1966. Thus, the service time is long, approximately 180 000 hours. According to files of replica testing 2011 microcracks were observed in MR15 whereas no creep damage was observed in MR20. The third marked weld, a T-piece branch weld, is marked MR05 in Figure 2. It would be



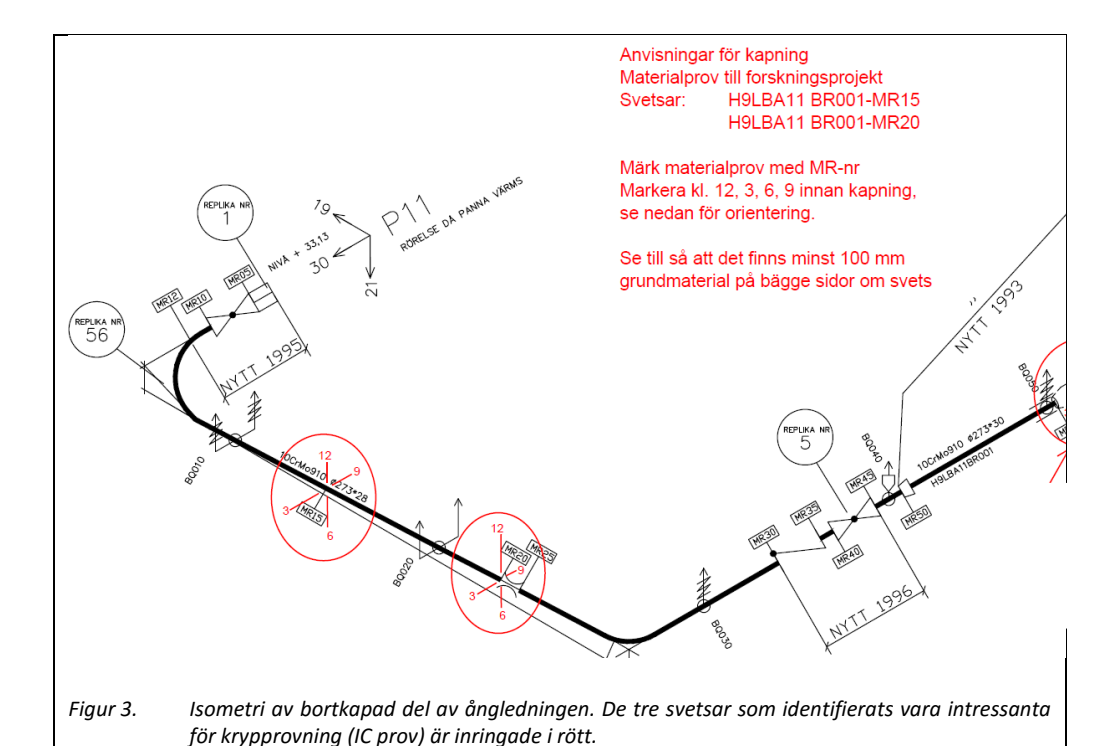
more interesting to verify the analysis with a T-piece since any influence of system stresses are more likely to appear there than at butt welds. However, this T-piece was installed in 1990 and had only been in service for 73 000 hours. It is not obvious that significant creep damage has developed during this limited service time. In the replica test files it can be seen that this weld was replica tested in 2001 where damage rating 2.1, separate cavities in a small amount was observed.



Figur 2. Isometri över ångsystemet innan ombyggnaden 2014. Inringad del skars ut i samband med ombyggnaden.

Figure 2. Isometry of the steam pipe system before the refurbishment 2014. The circumscribed part was cut out in connection with the refurbishment.





CHARACTERIZATION OF CREEP DAMAGE IN SELECTED EXCHANGED WELDS

for creep testing (IC tests) are circumscribed in red.

Figure 3.

3.3

Within the frame of the complementary study all the three welds M05, M15 and M20 were sent to laboratory for metallographical characterization of the creep damage. The first step was to perform replica testing on all welds to characterize amount and distribution of creep damage. This will make it possible to decide which weld that should be creep tested by IC and from which position of the weld the specimens should be extracted. The examined welds are shown in Figure 4.

Isometry of cut part of the steam line. The three welds that were identified to be interesting

The replica testing was carried out in the conventional way at 3, 6, 9 and 12 o'clock positions at each weld, se the markings in Figure 3. At each position an area across the weld was ground stepwise to a high fineness (400 mesh). The electropolishing was performed in adjacent base metals and HAZs on both sides of the weld as well as in the weld metal. After etching replicas were extracted and examined in light optical microscope. Observed creep damage was classified according to NT TR 302 [10]. It is basically the same as NT NDT 010 [9] but the definitions are stricter and the sub classes are denoted a (low) and b (high) instead 1 (low), 2 (medium), and 3 (high). The results of the evaluation are shown in Table 3. The examined areas are denoted with reference to the steam flow direction: 1 (base metal 1), 2 (HAZ 1), 3 (weld metal), 4 (HAZ 2) and 5 (base metal 2).





Figur 4. Komponenter a) H9LBA11BR001 M15, b) H9LBA11BR001 M20 and c) H0BA21BR001 M05. Figure 4. Components a) H9LBA11BR001 M15, b) H9LBA11BR001 M20 and c) H0BA21BR001 M05.

The table shows that a small, 2.3 mm long, creep crack was detected in the weld metal at the 6 o'clock position of MR15. This is a macro-crack according to Nordtest TR 302 [10] where the boundary between micro and macro-cracks is 2 mm. A number of micro-cracks were observed as well, se Figure 5a. At the other test positions very limited (separate cavities in a small extent, rating 2a) or no creep damage was detected. MR15 is a butt weld between two straight pipes. Therefore, it is not obvious that system stresses is responsible for the local damage. Local reduction in the weld metal creep strength may have contributed to this. There is a slight development from micro-cracks observed in 2011 to the small macro-crack 2014.

Tabell 3. Positioner med skadeutveckling.

Table 3. Positions with damage development.

| Pipe section/weld | Clock position | | Dam | age r | ating | | Comment |
|----------------------|-------------------|----|-------|-------|-------|------|--|
| H9LBA11BR001 | | 1 | 2 | 3 | 4 | 5 | |
| | | | | | | | |
| MR15 | 3 | 2a | 2a | 2a | 1 | 2a | |
| | 6 | 1 | 1 | 5 | 2a | 1 | Creep cavities and creep cracks up to 2.3 mm in wm |
| | 9 | 2a | 2a | 2a | 1-2a | 1-2a | |
| | 12 | 1 | 1-2a | 2a | 2a | 1 | |
| | | | | | | | |
| MR20 | 3 | 2a | 2b | 2b | 2a | 2a | Normalised microstructrure; >1000 cavities/mm² in wm |
| | 6 | 2a | 2b | 2b | 3bC | 2a | <1000 cavities/mm² in wm |
| | 9 | 2a | 2b | 2b | 2b | 2a | |
| | 12 | 2b | 2b | 2b | 2b | 2b | Normalised microstructrure |
| | | | | | | | |
| | | | | | | | |
| H9LBA21BR001 | | | | | | | |
| MR05 | 3 | 1 | 2b | 1 | 1 | 1 | Up to 2000 cavities/mm² in HAZ |
| | 6 | 2a | 3aC/K | 2b | 1 | 1 | Up to 2000 cavities/mm² in wm |
| | 9 | 1 | 1 | 1 | 1 | 1 | Possibly a few cavities but less than 100 cavities/mm ² |
| | 12 | 2b | 3bC/K | 2b | 1 | 1 | 3bC in cg haz; up to 3000 cavities/mm² in fg haz |

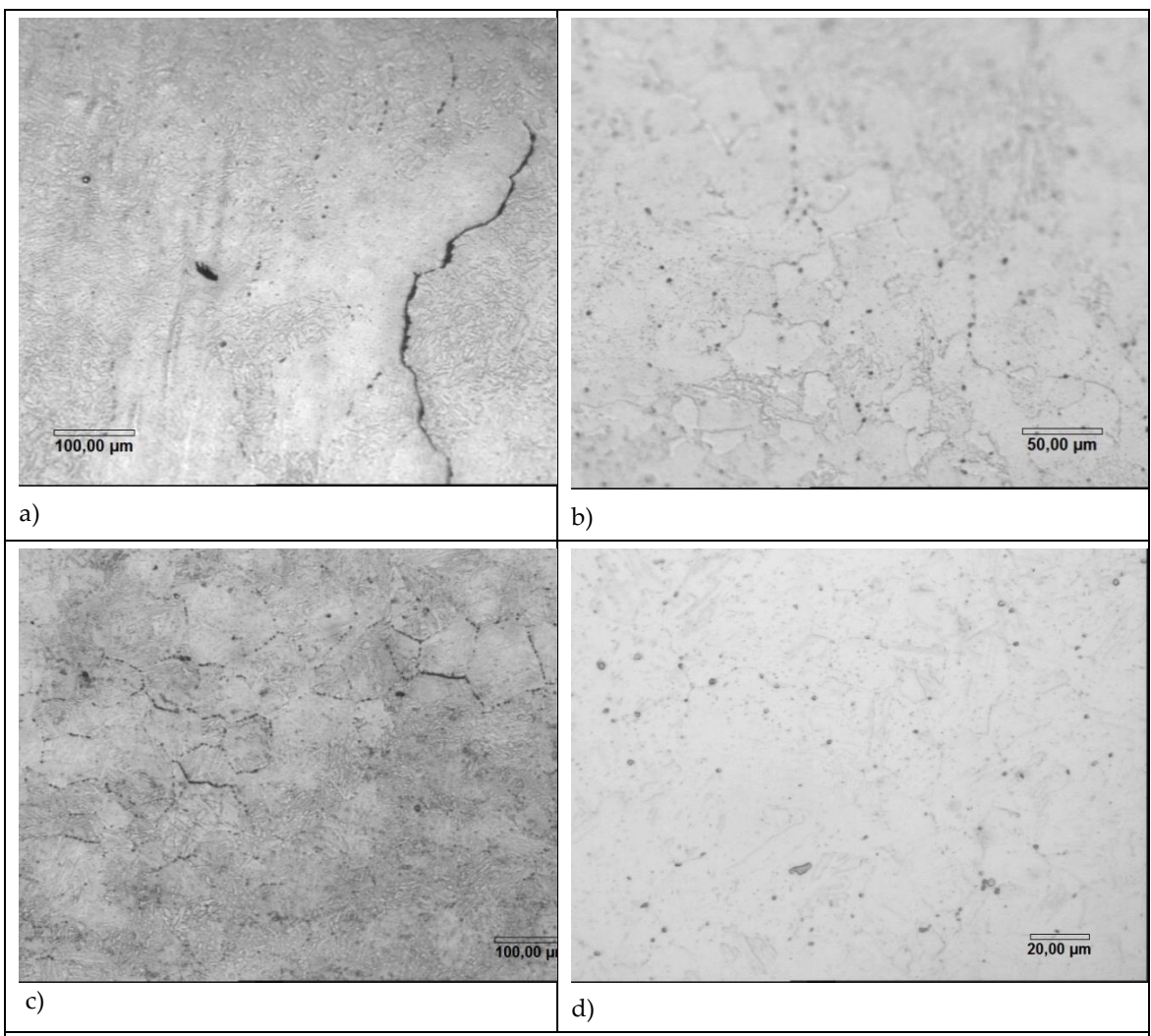
^{*} wm = weld metal, cg haz = coarse grained haz and fg haz = fine grained haz

A more even distribution of creep damage was observed in MR20 where damage rating 2b (separate cavities with more than 400 cavities/mm²) appeared in most weld metal and HAZ positions as well as in some parent metal positions. Oriented cavitation was observed in one HAZ position, see Figure 5b. Thus, there is a considerable damage development since 2011 where no creep damage at all was reported. The microstructure was normalized in two of the clock positions. This is likely due to the post heat treatment. In the 1960's this operation was often performed by use of ring burners which is associated with limited temperature control resulting in normalized or partially normalized welds.

MR05, the T-piece branch weld, showed significant creep damage in the HAZ and adjacent parent metal at the 6 and 12 o'clock positions that are placed towards the saddle points. The damage rating in the HAZ was 3bC and 3aC at respective clock positions, indicating diffuse oriented creep cavitation in large and small extent, see Figure 5c.

The T-piece fits very well for the analysis; i) there is groundwork for the creep analysis that consists of elastic pipe analyzes that cover the entire life-time of the T-piece, ii) there is significant creep damage and an expected creep damage distribution which can be used for verification of the analysis and the life time assessments. Thus, MR05 at the 6 o'clock position was chosen for excavation of material for IC testing.





Figur 5. Exempel på krypskador hos a) MR15, mikrosprickor i WM, b) MR 20, orienterade kaviteter i interkritisk HAZ, c) MR05, orienterade kaviteter i grovkornig HAZ vid pos. kl. 12 och d) rikligt med separerade kaviteter i interkritisk HAZ vid pos. kl. 3.

Figure 5. Examples of creep damage in a) MR15, micro-cracks in WM, b) MR20, oriented cavitation in intercritical HAZ, c) MR05, oriented cavitation in coarse grained HAZ at the 12 o'clock position and d) plenty of separate cavities in intercritical HAZ at the 3 o'clock position.

3.4 CHARACTERIZATION OF CREEP DAMAGE IN A CROSS-SECTION OF THE MR05 WELD

By replica testing it is possible to examine the microstructure at surfaces of selected positions of power plant components. Since the stress distribution due to internal pressure is quite equally distributed in a pipe wall it is thought that the creep damage that can be seen at the surface is representative for the creep damage within the whole thickness. This is true for many geometries but it is important to be aware of that there are exceptions. For example, headers with flat end caps the highest stresses are at the inside of the header wall close to the cap. In case of bending system stresses it is quite obvious that creep damage will start to from the outside of a component.

Welds consist of a laminate of different microstructures which in a creep process results in stress distributions and re-distributions that are dependent of the creep properties of the weld constituents and their interrelation to each other. Welds at positions with



geometrical stress enhancements as well as possible system stresses can then reveal distributions of creep damage in the through-thickness direction that are very difficult to predict. Therefore, a section of the T-piece branch weld at the 6 o'clock position was cut and prepared for metallographical investigation, see Figure 6.

In a first attempt the entire section was ground stepwise to a fine mesh (mesh 1200) and the polished mechanically with diamond suspension. However, no creep damage could be observed beneath the surface where significant creep cavitation appeared at replicas. The widths of the HAZs were measured. The results are shown in Table 4.

Tabell 4. Bredd av HAZ i tvärsnittet av svetsen.

Table 4. Width of the HAZs in the cross section.

| Side of weld | Average width of HAZ (mm) |
|---|---------------------------|
| Towards straight part of the T-piece (saddle point) | 3.0 |
| Towards branch part of the T-piece | 3.8 |

The author's experience is that electrolytic polishing, which typically is used in replica testing, can make creep cavitation much better visible than mechanical polishing. The cross section was then polished by use of a portable polishing machine that normally is used for replica testing. With this machine each polish is a spot with a diameter of approximately 8 mm. Since this area is relatively small a number of polishes were performed. This method revealed creep damage in parity with that observed at the replicas.

The characterization of the creep damage was done in the following way. The cross-section was polished and examined in light optical microscope. Areas of creep damage within different damage classes were contoured. Relatively much damage was found in the HAZ close to the outside. Polishes were taken and examined towards the inside as well as in to weld metal and out in the parent metal until creep damage no longer could be observed. The results are shown in Figure 7.

The figure shows that most damage is concentrated to the outer part of the wall at one of the HAZs. The parent metal in this area also reveals significant creep damage. At the other side of the weld small amounts of creep damage, damage rating 2a, was observed mid-wall.

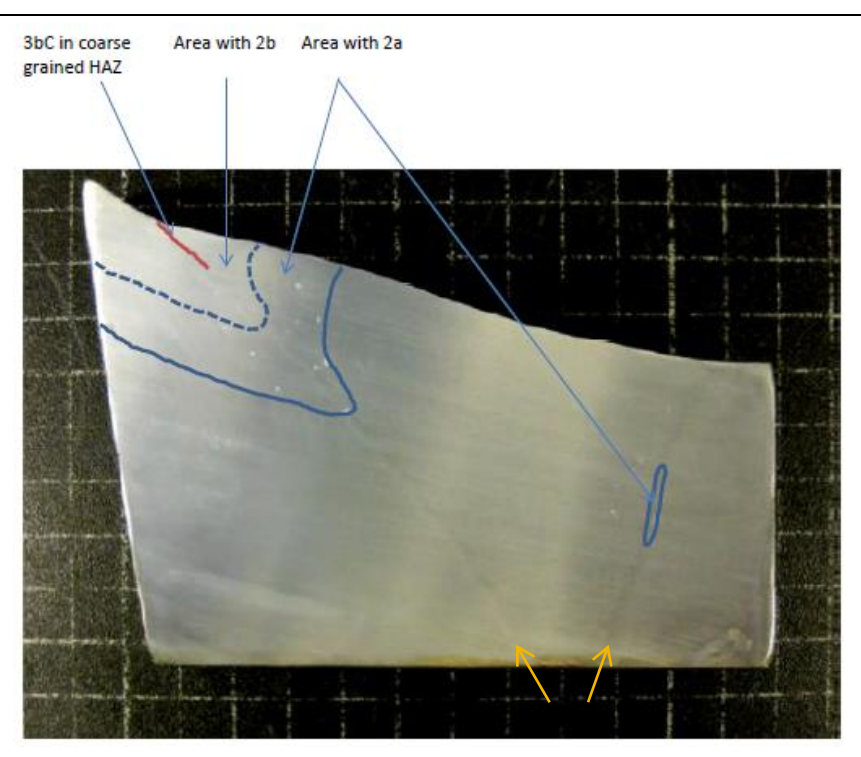
Creep damage is typically concentrated to the HAZs. Sometimes most damage is found in the weld metal. In the present case there is no wide spread cavitation in the weld metal. Most creep damage appears at the HAZ on the left hand side in Figure 7. It is obvious that the wall thickness is considerably thicker in the HAZ where most damage is than on the other side. Nevertheless, the stresses should be highest on the thicker side as stress controls the creep deformation. This is studied in detail in section 8 below.





Figur 6. Tvärsnitt av svets M05 vid position kl. 6. Provet är mekaniskt polerat och därefter elektrolytiskt polerat (runda områden) i områden med krypskador.

Figure 6. Cross-section of weld 05 at position 6 o'clock. The section mechanically polished. Then electrolytic polishing was performed in areas with creep damage.



Figur 7. Områden med olika krypskadeklasser enlig NT TR 302 hos tvärsnittet. Snittet är etsat och HAZ på båda sidor av svetsgodset syns svagt i de gula pilarnas riktning.

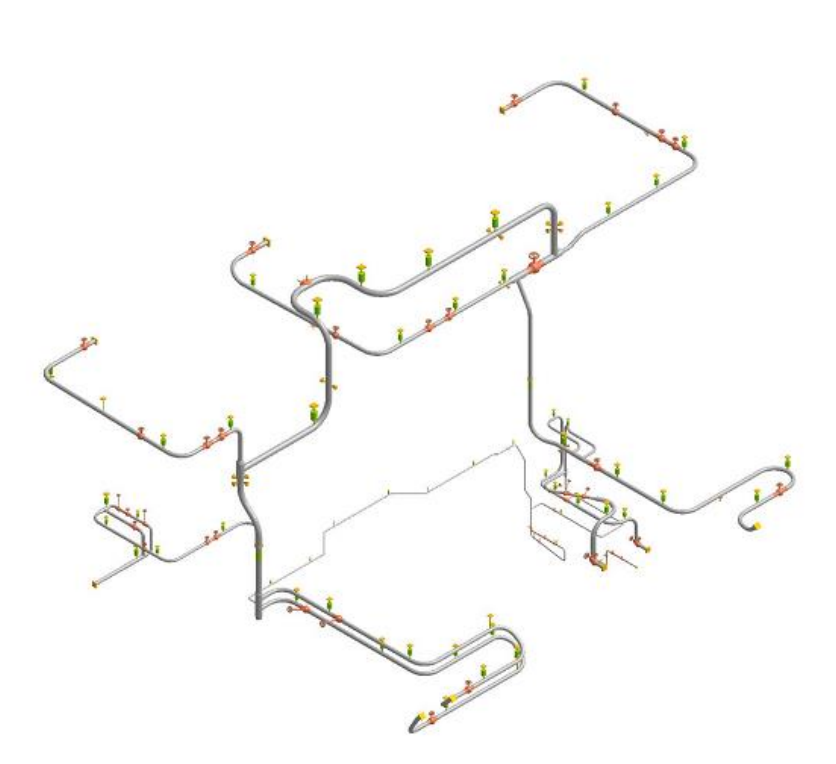
Figure 7. Areas with different creep damage classes according to NT TR 302. The section is etched and the HAZ is visible rather weakly in the directions of the yellow arrows on both sides of the weld metal.



4 Development of a script that enables fast modeling of pipe systems with respect to creep

4.1 MODELS IN CAEPIPE AND ABAQUS

Conventional piping programs like CaePipe and PipeStress that are widely used for evaluation of linear stress evaluation of piping systems are not capable of evaluating creep deformation. The Finite element program Abaqus is equipped for handling creep deformations according to [5]. A script that translates a Caepipe model to an Abaqus code for further evaluation with Abaqus has been developed in this project. The script translates the geometry of the piping model with loading and boundary conditions to a text file that can be used for evaluating creep deformations in the piping system. For complete evaluation of the Abaqus model a more detailed material model will have to be added with creep properties amongst with an expert knowledge of the program and conditions for creep evaluation. In Abaqus the piping is modelled with ELBOW31 elements that can handle stress- and creep strain rate gradients through the thickness of the pipes and is therefore suitable for detailed analysis for pipe systems exposed to creep. The script has been developed with Octave that is free online software available without any licensing. The complete script is available in Appendix 1.

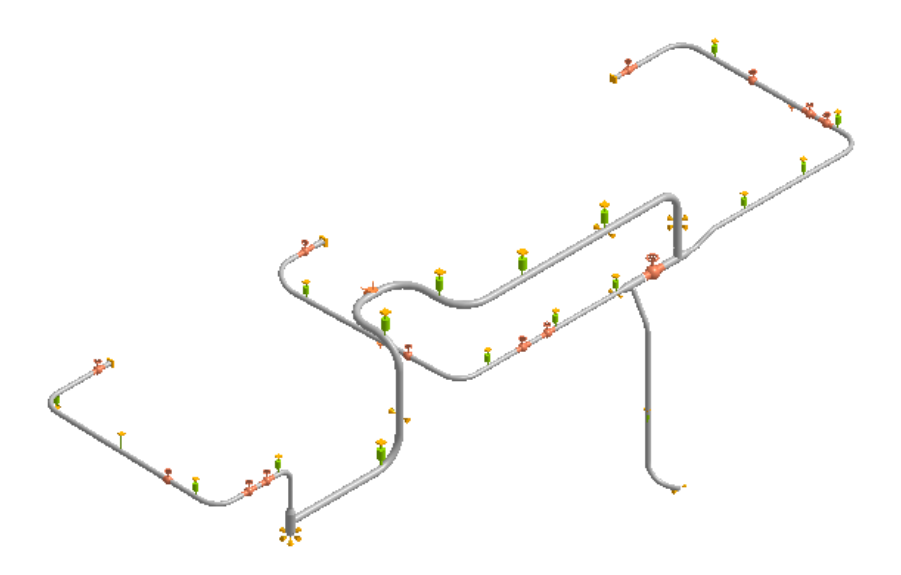


Figur 8. Komplett modell av Heleneholmsverkets ångsystem i Caepipe.

Figure 8. The complete piping model of Heleneholmsverket in Caepipe.



Z Y • X The complete piping model is simplified for translation with the script and evaluation of the model. Furthermore in the detailed analysis of the piping with creep analysis with comparison of creep material modelling it will simplify and shorten the analysis time. The piping model that is used for translation is shown in Figure 9 below.



Figur 9. Förenklad modell av Heleneholmsverket ångsystem för översättningsscript.

Figure 9. Simplified model of the Heleneholmsverket piping used for translating script.

To verify the script a comparison is done between the simplified Caepipe piping model and the model of Heleneholmsverket that has previously been modeled in ABAQUS [5], and will be named reference model in this evaluation. To confirm the validity of the script the von Mises stress levels are compared for the two models in four loading steps. They represent one start and stop of the system. In the simulation of the starts and stops the average service period between each stop has been assumed, i.e. 1370 hours. This is a simplification since there is a variation in service time from one year to another. First the dead weight is applied, and then internal pressure added to the system, followed by heating up the system where the system expands thermally and finally the system is in operation for 1370 hours until the system is then stopped. See the following steps below:

- 1. Dead weight of the piping system
- 2. Internal pressure
- 3. Thermal expansion
- 4. Creep step of 1370 hours of operation

The operational loading is used for the evaluation, where the internal pressure is 105 bar and the temperature is 530°C. For a creep analysis in pipe systems the Norton's creep law is used that includes both elastic and creep response. See equation (1) for the Norton's creep law. The equation only includes secondary creep.



$$\frac{d\varepsilon_{ij}}{dt} = \frac{(1+\nu)}{E} \left[\left(\frac{d\sigma_{ij}}{dt} \right) - \frac{\nu}{\nu+1} \left(\frac{d\sigma_{kk}}{dt} \right) \delta_{ij} \right] + \frac{3}{2} B \overline{\sigma}^{(n-1)} s_{ij}$$
 (1)

Where \mathcal{E}_{ij} , σ_{ij} , s_{ij} are the respective strain, stress and stress deviator tensor, $\overline{\sigma}$ is the von Mises effectives stress, E and v is the Young's modulus respective Poisson's number and B and n are the respective constant and exponent in Norton's creep law. The last term in equation (1) describes the creep response of the material.

The entire pipe system in the model has the material properties of 10CrMo9-10. In reality, the material 14MoV6 3 appears in leftmost part of the system. This part is far away from the components that were studied in detail and the analyses were verified against, see Figure 2 and 3. It is believed that using the properties of 10CrMo9-10 for the entire system in does not affect the results at the studied components.

To be able to define the parameters B and n in the creep law for the pipe system material, the creep law is considered in one dimension, see equation (2).

$$\frac{d\varepsilon}{dt} = B\sigma^n \tag{2}$$

The equation is integrated, see equation (3)

$$\int_{0}^{\varepsilon} d\varepsilon = \int_{0}^{t} B\sigma^{n} dt \to \varepsilon = B\sigma^{n} t \tag{3}$$

The parameters B and n can then be solved with an equation pair, equation (4) and (5). By use of tabled values [11] of the stresses that result in 1% creep strain at time 10 000 and 100 000 for 10CrMo9-10 at 530°C the equations will read:

$$0.01 = B \cdot 107^{n} \cdot 10000 \tag{4}$$

$$0.01 = B \cdot 68^n \cdot 100000 \tag{5}$$

The resulting values are $B=4.91*10^{-17}$ and n=5.08. Table 5 summaries the material constants used in the analysis.

Tabell 5. Materialkonstanter för 10CrMo9-10 vid 530°C som är använda i både skriptet och i referens modellen.

Table 5. Material constants for 10CrMo9-10 at 530°C used in both script and reference model.

| Constant | Value |
|-----------------------------|------------------------|
| В | 4.91*10 ⁻¹⁷ |
| N | 5.08 |
| E [GPa] | 162 |
| n | 0.3 |
| α [1/°C] | 13.4*10-6 |
| ρ [kg/m ³] | 7850 |

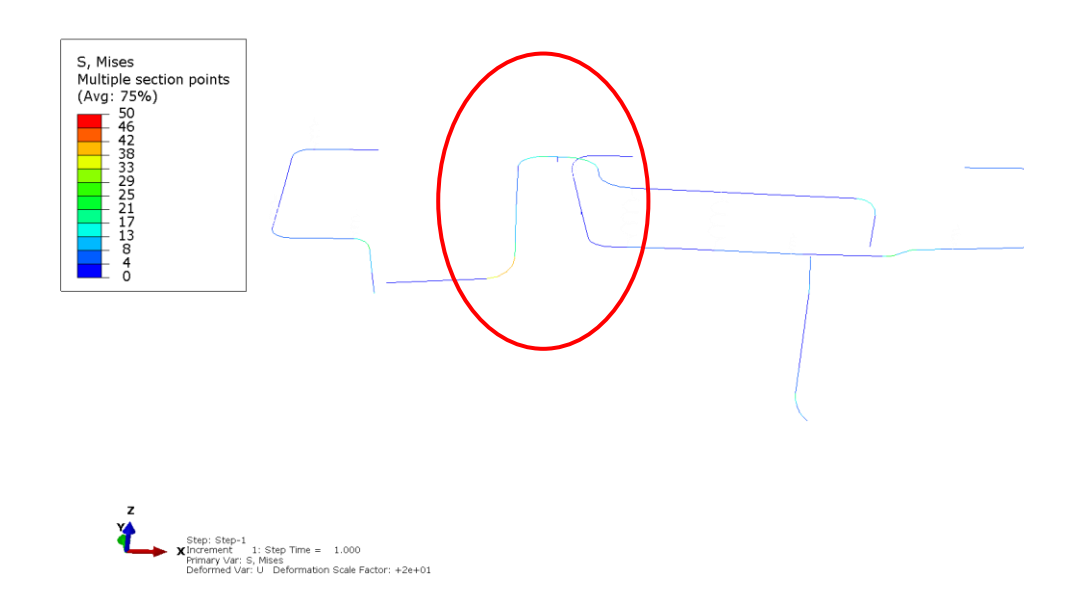


4.2 COMPARISON OF THE SCRIPT AND THE REFERENCE MODEL

Comparisons of the translated script model and creep analysis in [5] for the four loading steps are presented in figures 10-19 below. All stress levels in the figures are in units MPa.

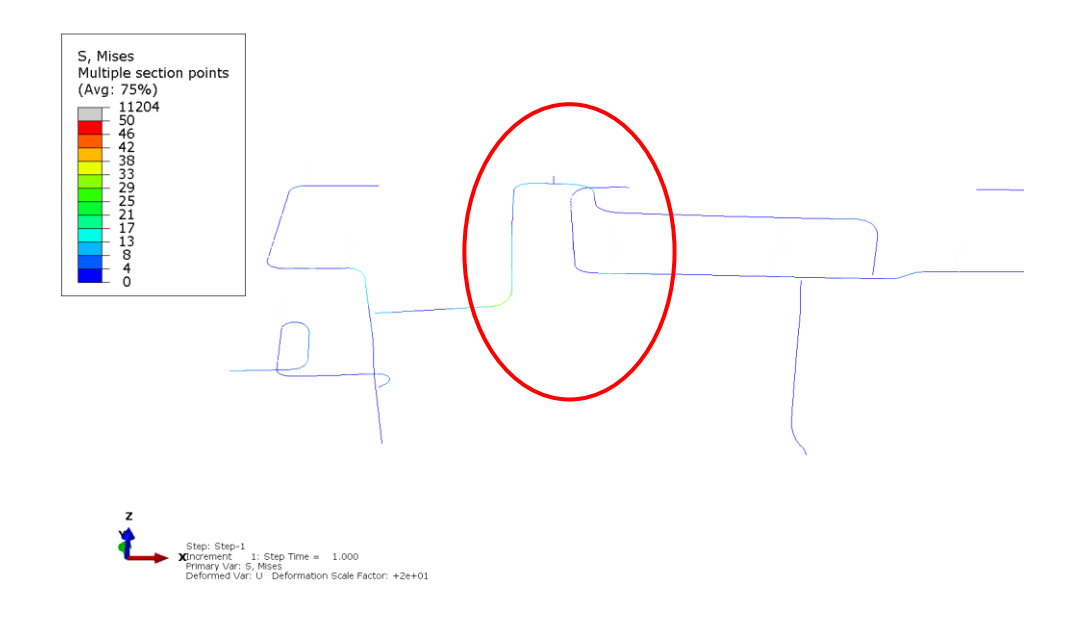
Step 1, dead weight comparison: The visual limit of the stresses for the dead weight is set to 50 MPa. A stress concentration is located in the multiple bend and the levels of von Mises stresses are very similar, the difference is about 20 % for this step. But since the stress levels are very low in this step small difference in stresses here show large percentage in difference. It is considered that the scripted model represents an acceptable translation of the piping system behavior in this loading step, see Figure 10 and 11.





Figur 10. Steg 1: Egenvikt hos den översatta scriptmodellen (enheten för spänningsnivåerna är MPA).

Figure 10. Step 1: Dead weight of the translated script model (units of MPa).



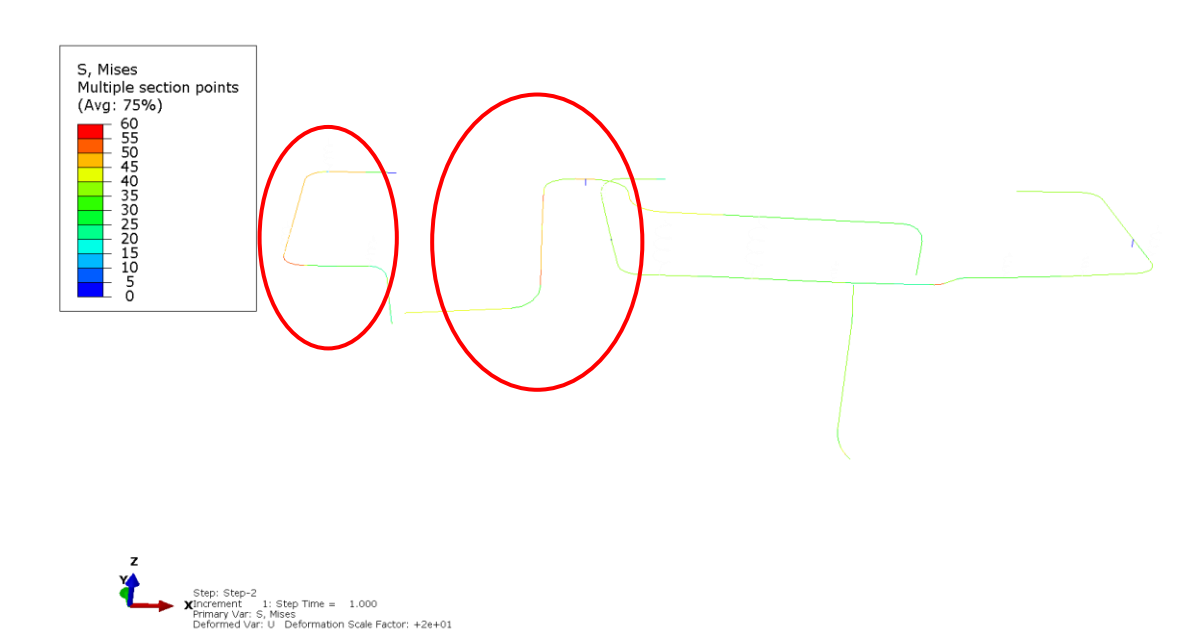
Figur 11. Steg 1: Egenvikt hos referensmodellen (enheten för spänningsnivåerna är MPA).

Figure 11. Step 1: Dead weight of the reference model (units of MPa).

Step 2, internal pressure comparison: The visual limit of the stresses for the internal pressure is set to 60 MPa. Two locations can be considered in this stress level for comparison, the same location as in step 1 where the stresses are lower in the bottom bend but are larger around the bend. And also there are similar stress levels in the upper corner of the piping system that is connected to Boiler12 (P12). The difference between stress levels in the models is about 4 %. It is considered that the scripted

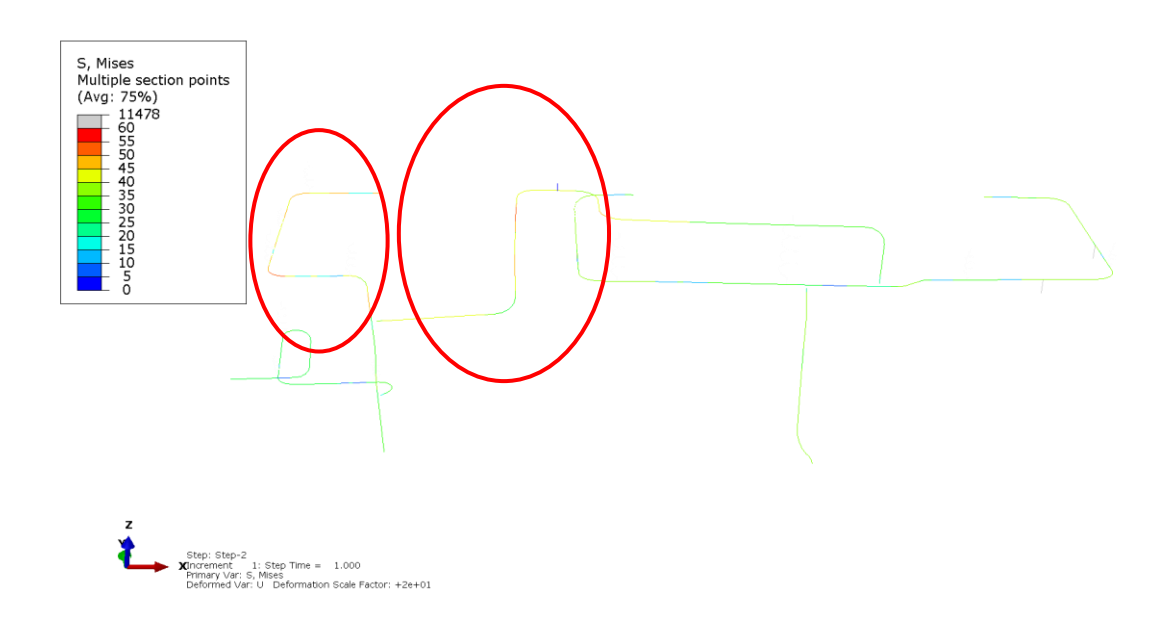


model represents a correct translation of the piping system behavior in this loading step, see Figure 12 and 13.



Figur 12. Steg 2: Inre övertryck hos modellen för scriptöversättning.

Figure 12. Step 2: Internal pressure of the translated script model.



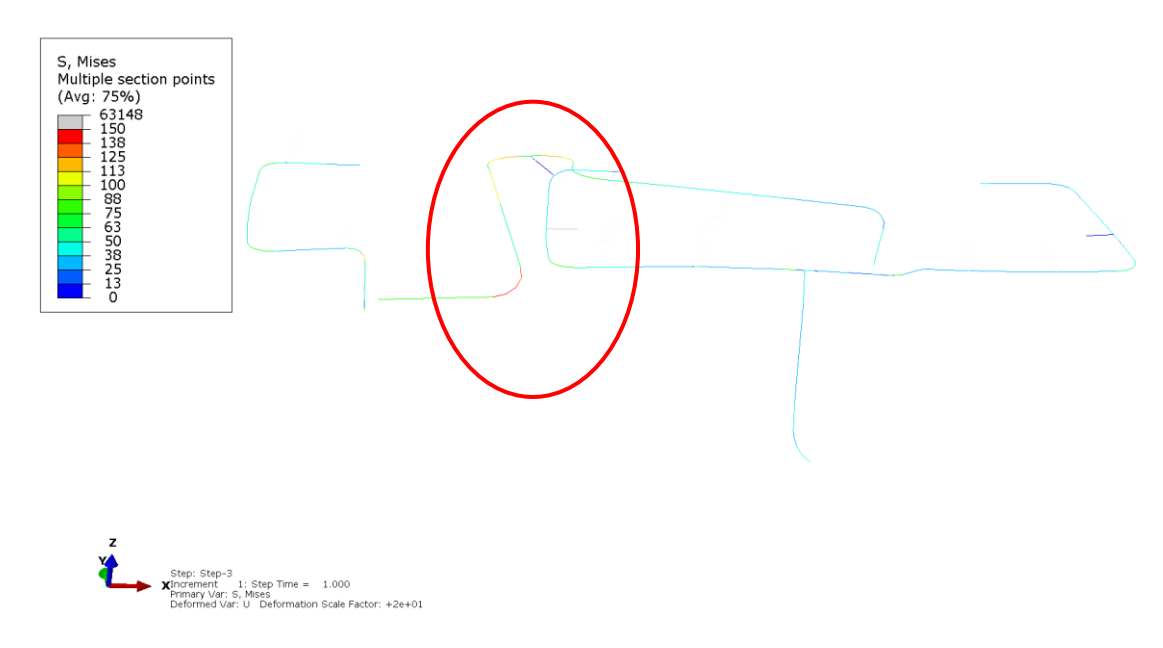
Figur 13. Steg 2: Inre övertryck hos referensmodellen.

Figure 13. Step 2: Internal pressure of the reference model.

Step 3, comparison: The visual limit of the stresses for the thermal expansion is set to 150 MPa. The same location as in step 1 is of interest in this step. The stresses are now

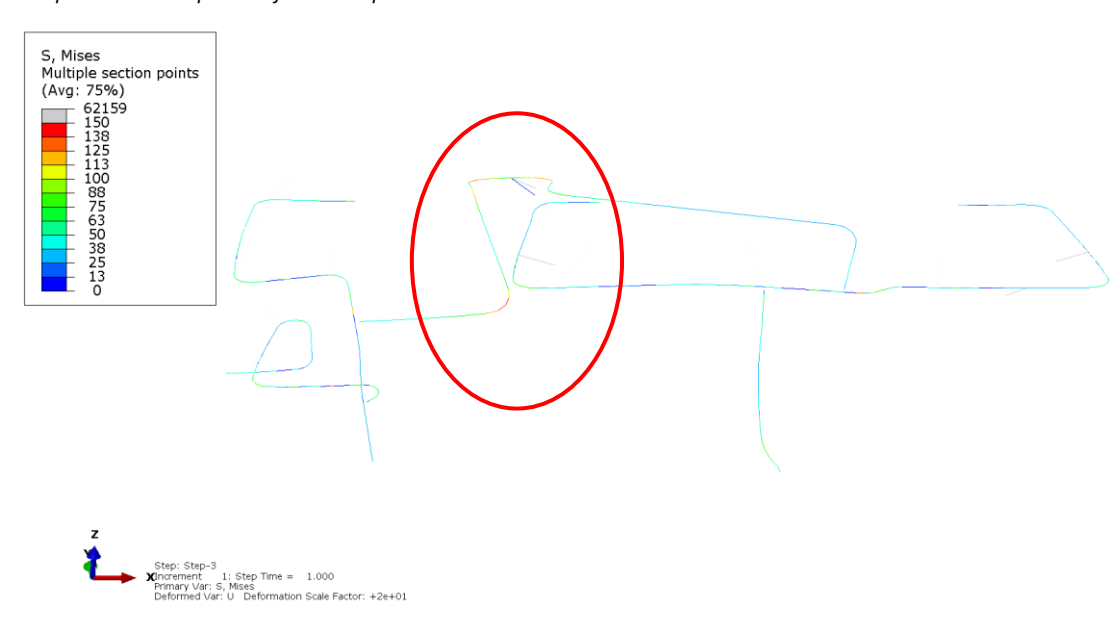


high in the bottom bend and in the multiple bend above. The difference in stress levels of the models are about 3 %. It is also noteworthy to see the deformation of the piping system that shows that the system deforms in a similar manner. It is considered that the scripted model represents a correct translation of the piping system behavior in this loading step, see Figure 14 and 15. It is the stresses that should be compared. The displacements are scaled differently and cannot be compared visually in the figures. The same applies for the comparisons of stresses in Figures 16-17 and strains in Figure 18-19 below.



Figur 14. Steg 3: Termisk expansion hos scriptmodellen.

Figure 14. Step 3: Thermal expansion for the script model.

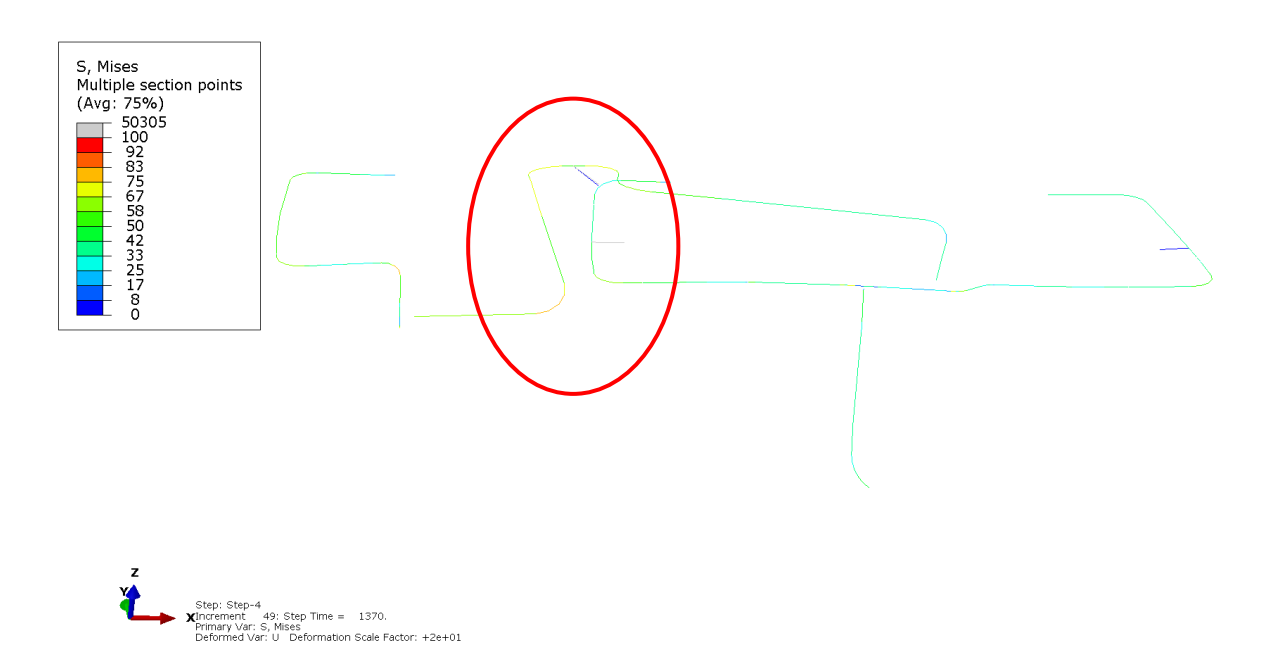


Figur 15. Steg 3: Termisk expansion hos referensmodellen.

Figure 15. Step 3: Thermal expansion for the reference model.



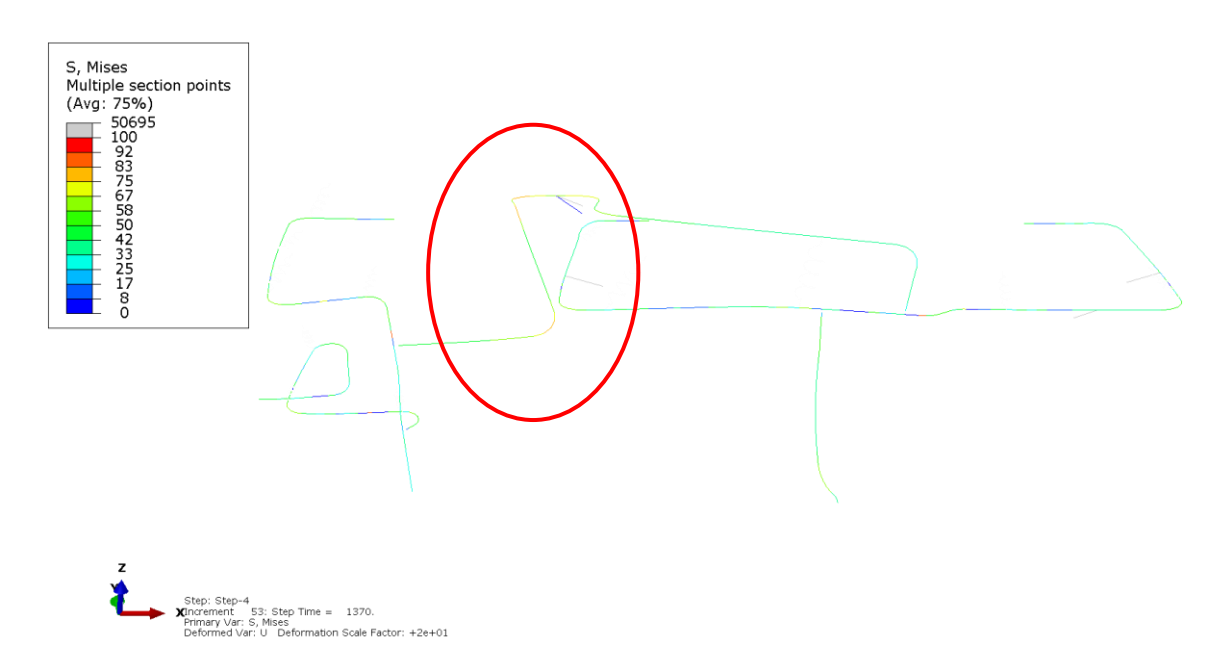
Step 4, comparison: The limit of the stresses for the creep simulation of 1 370 hours is set to 100 MPa. There is noteworthy creep relaxation in the system since the stresses have relaxed from within 150 MPa from the thermal expansion to less than 100 MPa after 1370 hours. The same location as in step 1 is of interest in this step where the stresses are now high in the bottom bend and also in the multiple bend above. The difference in stresses levels of the models are about 2 %. As expected there are some creep strains that are appearing in the bends where there have been high stresses in the end of the previous load step. It is considered that the scripted model represents a correct translation of the piping system behavior in this loading step as well; see Figure 16 and 17 for the stress distributions and Figure 18 and 19 for the strain distributions. For all loading steps the stress level show similar values with the same distribution in the piping system as the reference model and therefore it can be considered that the script translates a correct model description from Caepipe to Abaqus.



Figur 16. Steg 4: Efter krypsimulering i 1370 timmar hos scriptmodellen.

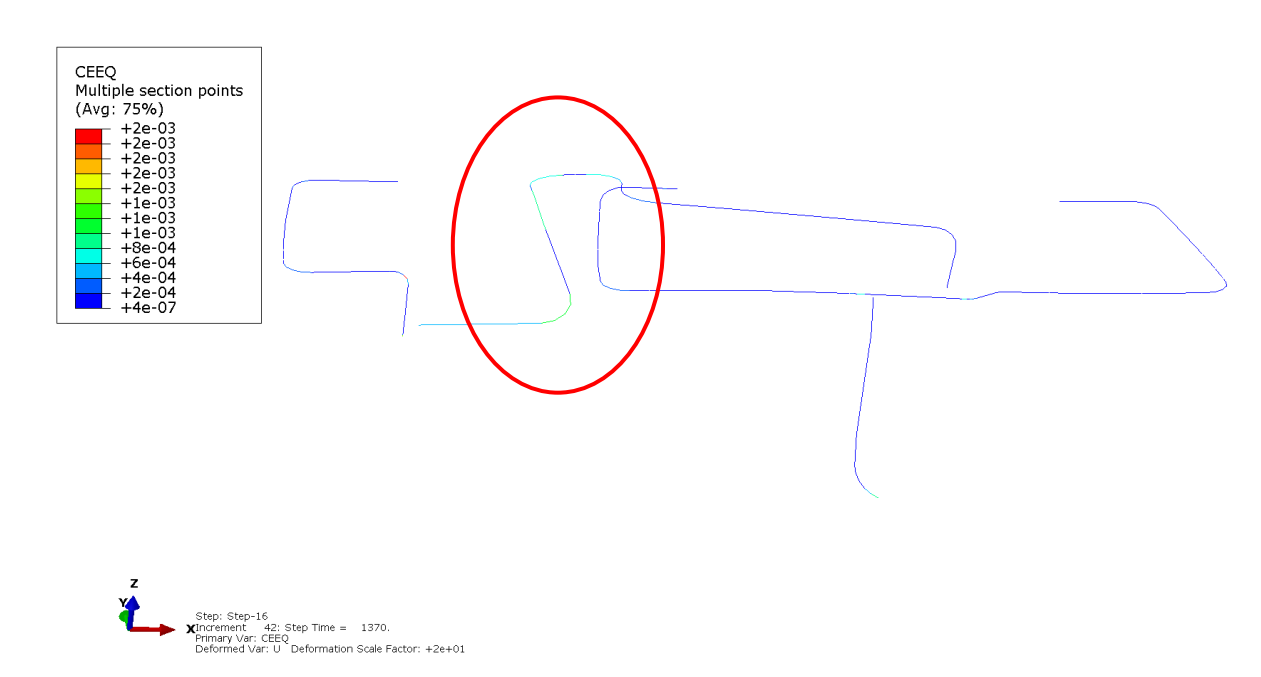
Figure 16. Step 4: After creep simulation for 1370 hours for the script model.





Figur 17. Steg 4: Efter krypsimulering i 1370 timmar hos referensmodellen.

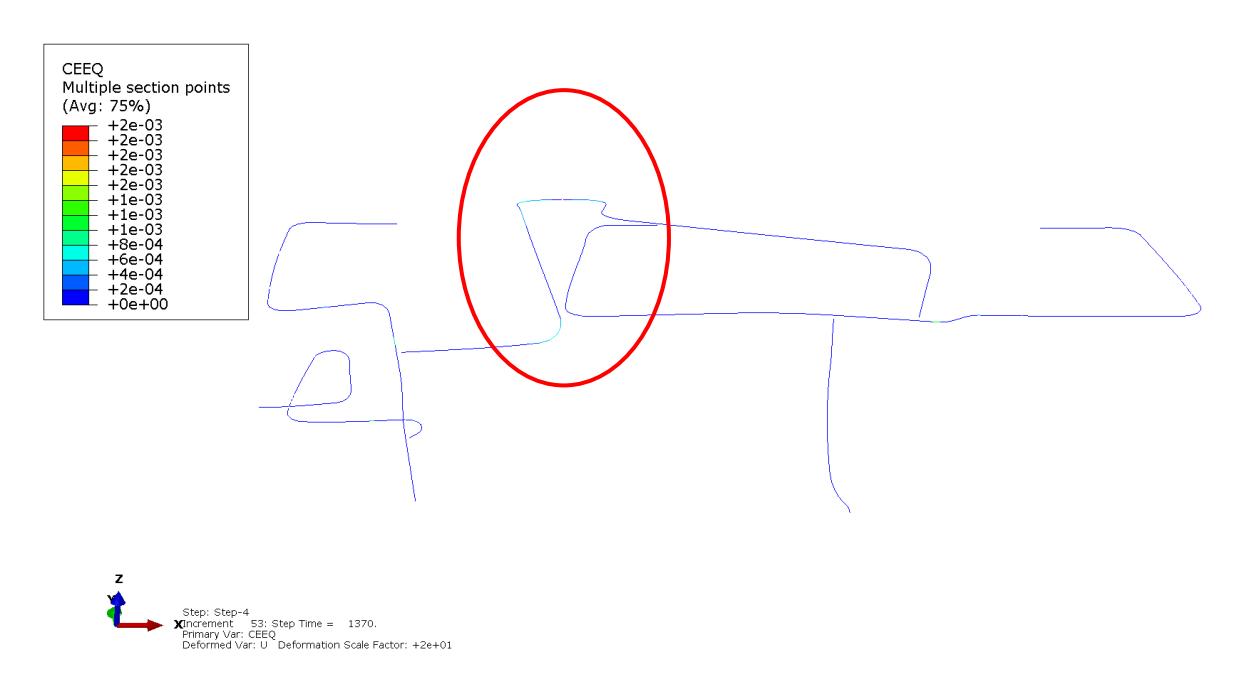
Figure 17. Step 4: After creep simulation for 1370 hours for the reference model.



Figur 18. Steg 4: Ekvivalenta töjningar hos scriptmodellen.

Figure 18. Step 4: Equivalent creep strains for the script model.





Figur 19. Steg 4: Ekvivalenta töjningar hos referensmodellen.

Figure 19. Step 4: Equivalent creep strains for the reference model.



5 Combination of system and component analysis – determination of boundary conditions

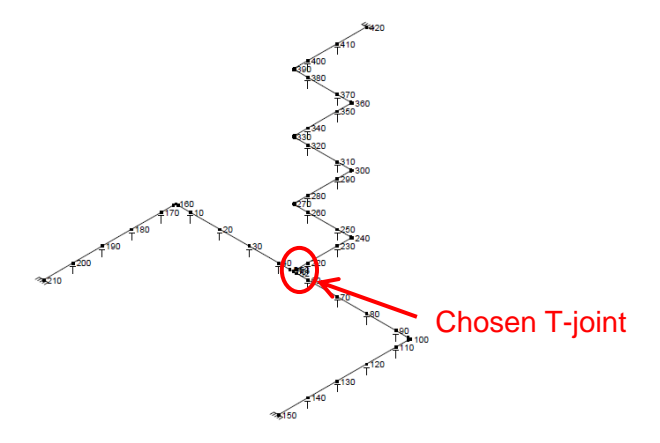
A 3D model of an arbitrary T-joint has been done in the project. The model is created in Abacus/Caepipe. The T-joint model is to be used together with a pipe system analysis, this to be able to get a correct and detailed picture of the stresses for the T-joint. Furthermore an Abaqus pipe system creep analysis cannot correctly simulate the creep behavior for a T-joint, but this can be done with a component model.

Displacements and rotations from the pipe system are extracted from the pipe system model and applied to the boundaries of the T-joint model. The stiffness of the T-joint in the piping system model is not necessarily the actual stiffness of the T-joint. Therefore the stresses in the T-joint model can be dependent on how much of the connecting pipes that are included in the T-joint model. The difference of stiffness between the system model and component model is less if more of the connecting pipes is included in the component model. This is because the relative error in stiffness between the pipe system and component model is less if more of the system is included in the component model.

To determine a general thumb rule of the necessary extension of the connecting pipes in the component model, two sensitivity analyses were performed. Below these sensitivity analyses are described in more detail. A creep behavior analysis was also conducted for the T-joint and is described below.

5.1 SENSITIVITY ANALYSES

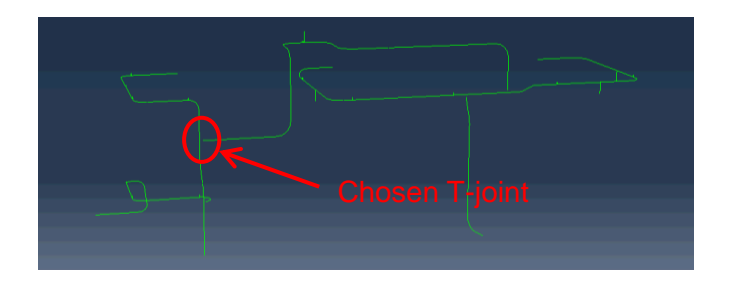
Two different pipe system models were used in the sensitivity analyses. One pipe system model is from Caepipe and one from Abaqus. The Abaqus model is the previous one from Heleneholmsverket [5] and the Caepipe model is from elsewhere. Figure 20 and Figure 21 the two pipe systems are shown and the modelled T-joint. The components were created using the parametric python script. Below the two created models are described.



Figur 20. Systemmodell med Caepipe.

Figure 20. Caepipe pipe system model.





Figur 21. Systemmodell med Abaqus.

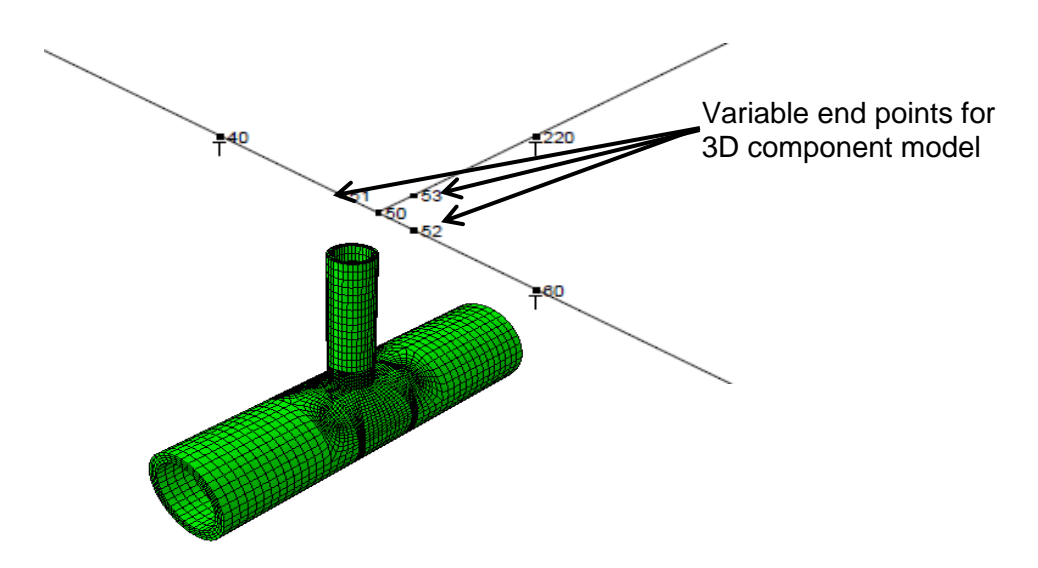
Figure 21. Abaqus pipe system model.

5.2 COMPONENT MODELS

A total of 5 different T-joint models were created, three models for the Abaqus pipe system model and two models for the Caepipe pipe system model. These models corresponded to different extensions of the connecting pipes. The different extensions were related to the pipe system model so that it was possible to extract displacements and rotations at the positions in the pipe system models corresponding to the boundaries of the T-joint models.

5.3 GEOMETRIES

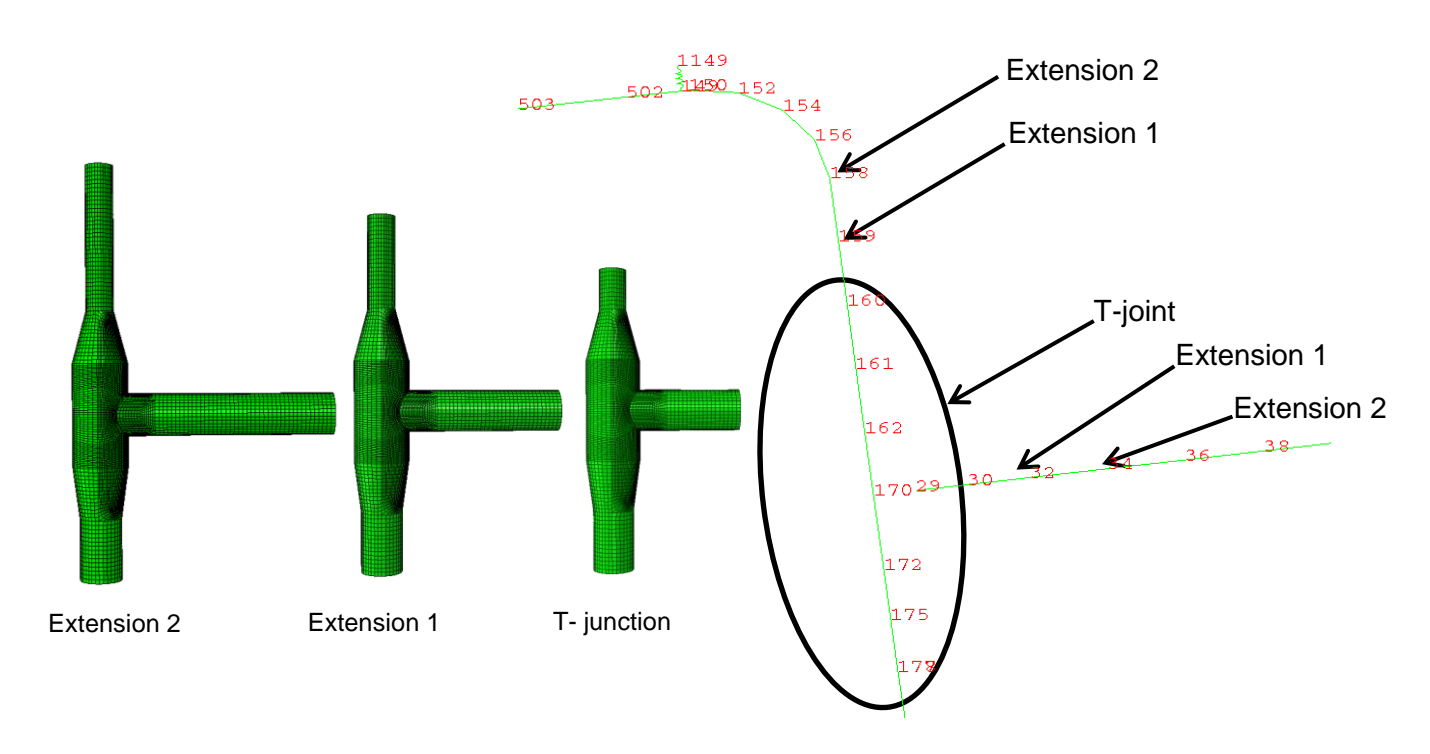
The different T-joints for the two different pipe systems are shown in Figur 22 and Figur 23.



Figur 22. Två modeller av T-stycken använda till Caepipe-rörmodellen.

Figure 22. Two T-joint models used for the Caepipe pipe system model.





Figur 23. Tre modeller av T-stycken använda till Abaqus-rörmodellen.

Figure 23. Three T-joint models used for the Abaqus pipe system model.

5.4 MATERIAL

The material used in the sensitivity analyses is a linear elastic material with the same material parameters as for the piping system models. In Table 6 the material parameters for the models are given.

Tabell 6. Materialparametrar för modellerna.

Table 6. Material parameters for the models.

| | E [GPa] | v | α [1/°C] |
|---------------------|-----------------------------|------|----------|
| Caepipe pipe system | 212 (20 °C) 161 (540 °C) | 0.30 | 14.1E-6 |
| Abaqus pipe system | 162 (530 °C) | 0.30 | 13.4E-6 |

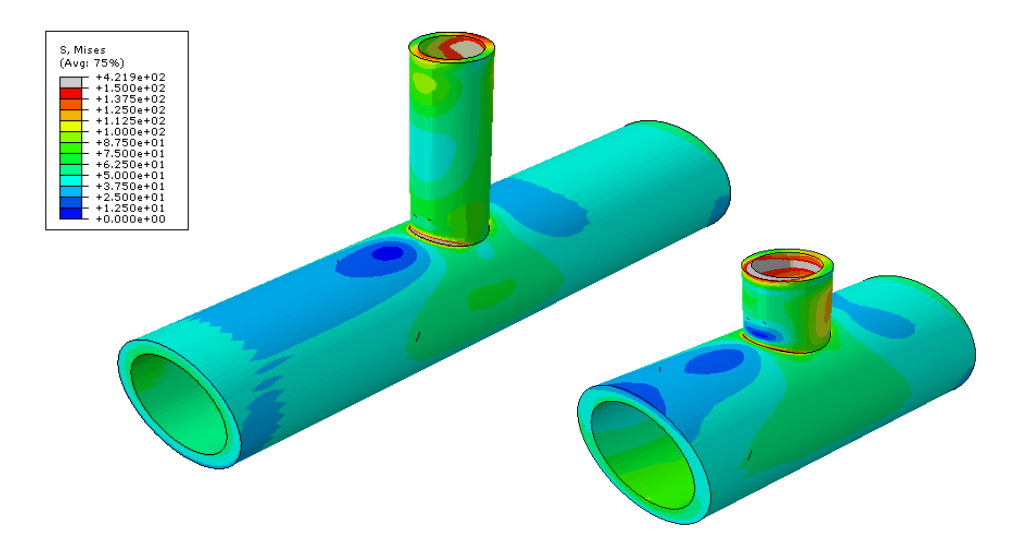
5.5 BOUNDARY CONDITIONS AND LOADING

Boundary conditions and loading for the component models consist of displacements on the boundary obtained from the pipe system models. These are extracted from the pipe system models and applied to the boundary of the component model. Internal pressure is also applied to the inner surface of the component models. The temperature is also applied on the entire model to get correct displacements due to thermal expansions.



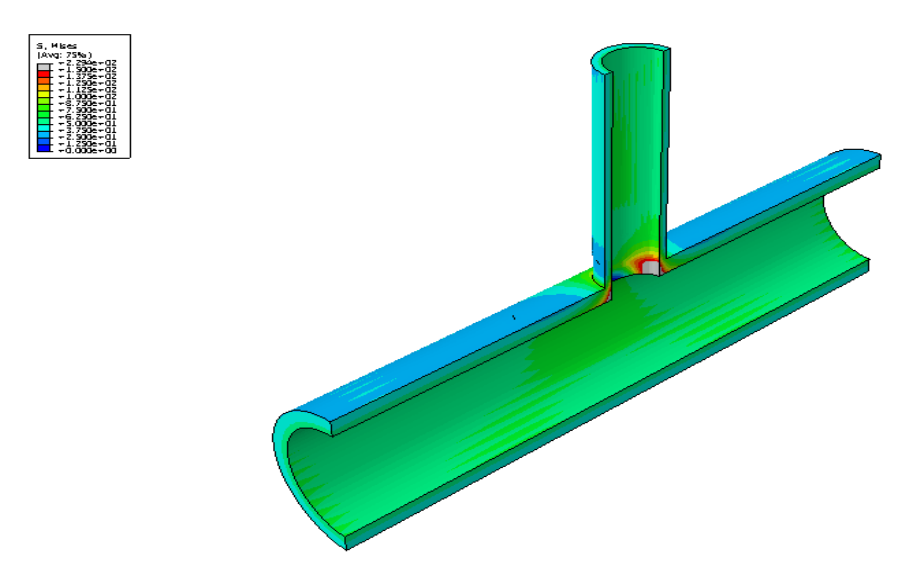
5.6 RESULTS FOR THE SENSITIVITY ANALYSES

In Figur 24 and Figur 25 the results for the T-joint in the Caepipe system are shown. As can be seen there are no big differences in the stress field between the two models, this is mainly because of the simplicity of the T-joint. The largest difference can be seen on the branching pipe. The difference in the stiffness for the T-joint between the component model and pipe system model is not very big as the component model does not show a large sensitivity to the extension of the modelled pipes. Furthermore it is clear that the two models both point at the same location for the highest stresses.



Figur 24. Jämförelse mellan von Mises-spänningar mellan de två T-styckena med laster från inre övertryck och termisk expansion.

Figure 24. Comparison of von Mises stress between the two T-joint models with loading internal pressure and thermal expansion.

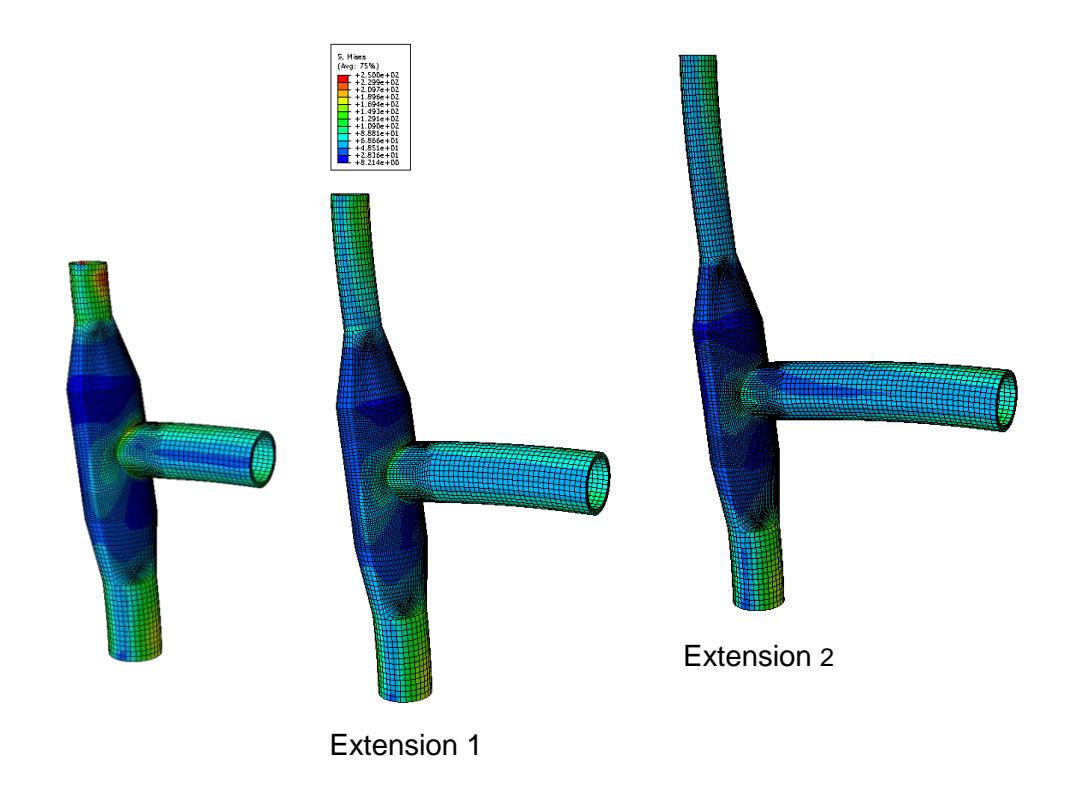


Figur 25. Jämförelse mellan von Mises-spänningar mellan de två T-styckena med laster från inre övertryck.

Figure 25. Comparison of von Mises stress between the two T-joint models with loading internal pressure.



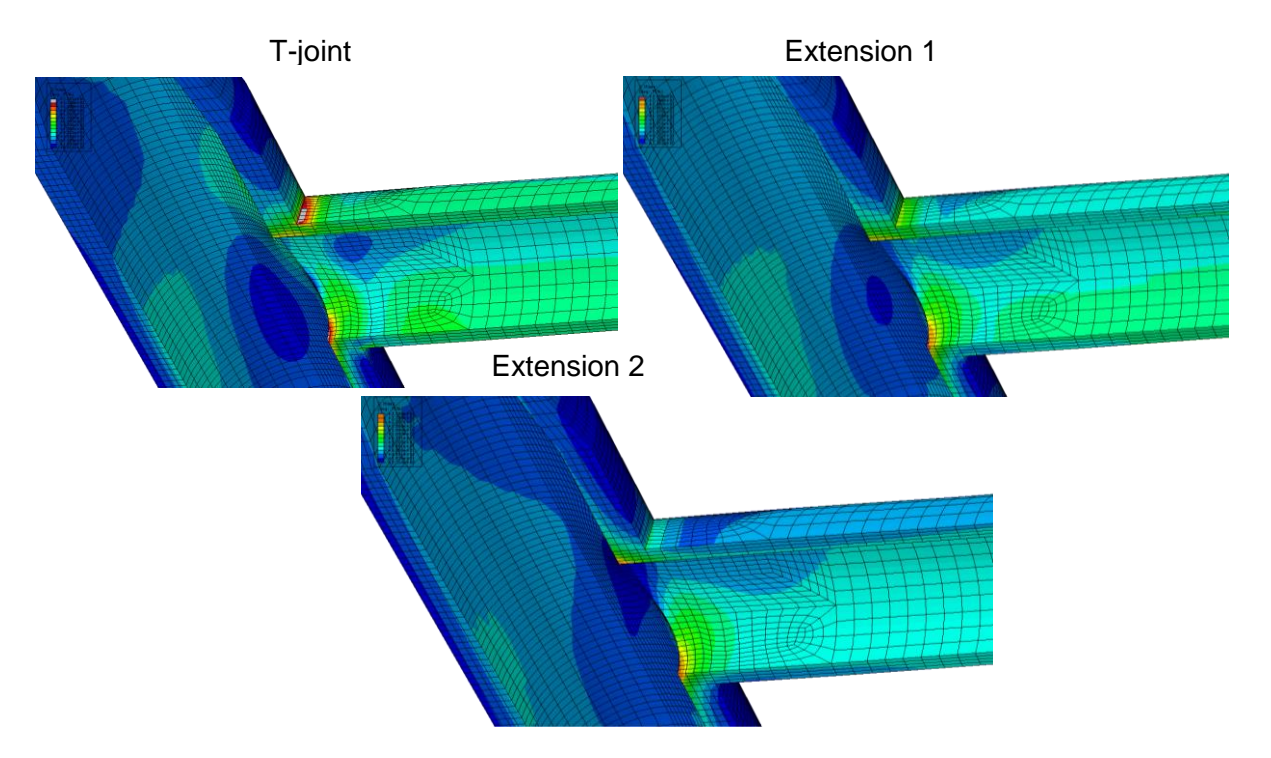
In Figures 26 and 27 the results for the sensitivity analysis for the Abaqus pipe system are shown. As can be seen, these results show a much larger sensitivity than the previous results. The reason for this is the difference in stiffness between the Abaqus piping system and the actual stiffness of the T-joint. But as the extensions of the pipes are increased the differences decrease as is expected.



T-joint

Figur 26. Jämförelse mellan von Mises-spänningar mellan de tre T-styckena med laster från inre övertryck och termisk expansion.

Figure 26. Comparison of von Mises stress between the three T-joint models with loading internal pressure and thermal expansion.



Figur 27. Jämförelse mellan von Mises-spänningar mellan de två T-styckena med laster från inre övertryck och termisk expansion.

Figure 27. Comparison of von Mises stress between the two T-joint models with loading internal pressure and thermal expansion.

5.7 DISCUSSION

From the results shown above it is clear that the stiffness of the T-joint in the piping system model is very important for the component analysis. A realistic stiffness in the piping system leads to less sensitivity for the component analysis. But as a thumb rule at least a pipe length of two diameters from each cone of the T-joint should be modelled in the component model. In cases were the stiffness in the piping system is thought to differ much from the actual stiffness a sensitivity analysis is suggested to determine the needed extent of the component model. The T-joint model itself is built up to be flexible and enable any all thicknesses and diameters to be modelled in a short time.



6 Studies of effects of starts and stops

6.1 MODEL AND ANTICIPATED OPERATION

The Heleneholmsverket piping model used in ref [5] has been used to study the effects of starts and stops. The piping system has the same material constants as stated in Table 5 in chapter 4.1. The piping system has been analyzed at design values, 530°C and 130 bar, and is evaluated for a total operational time of 100 000 hours. Each operational period between starts and stops that is estimated for each year is set to 7 500 hours that is a total operational time of 14 years.

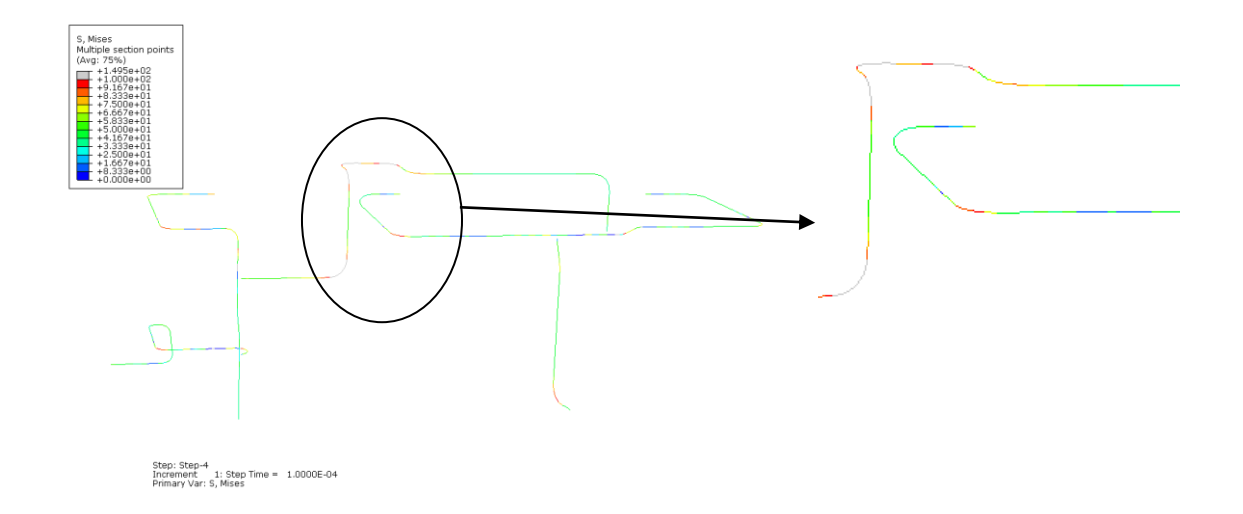
6.2 RESULTS

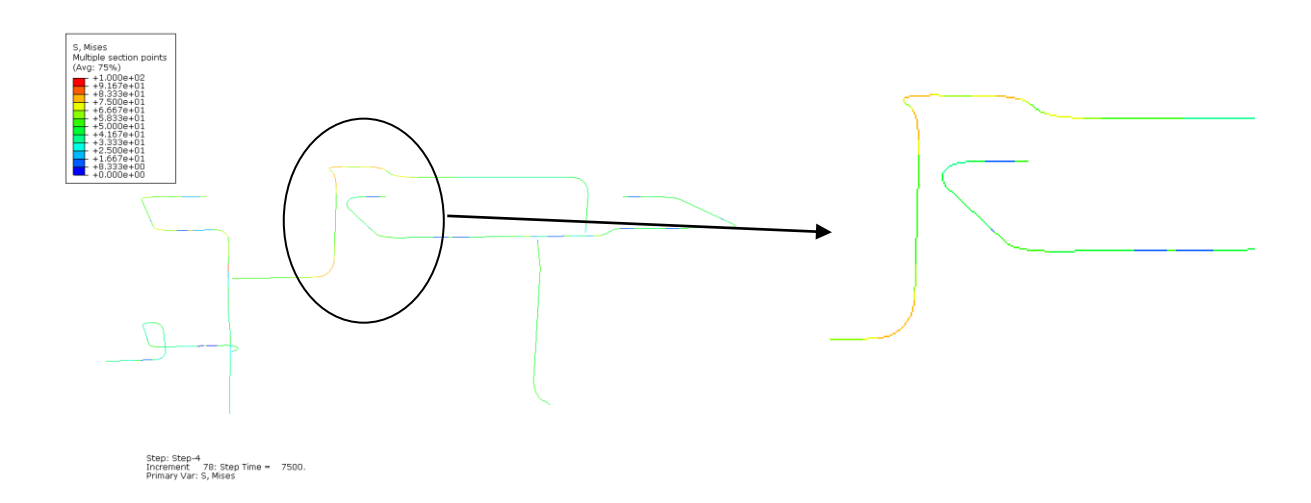
Figure 28 - Figur 35 below show how the system behaves within these 14 years of operation with respect to von Mises stresses (Figure 28 - Figur 31) and creep strain accumulation (Figur 32-Figur 35).

In the beginning there are high stresses at the bends in the middle of the pipe system, see the upper picture in Figure 28. A significant creep relaxation of these high stresses can be seen after one year, see the lower picture in Figure 28.

In Figur 29 above it can be seen that after start and some operation of the second year the stresses in the bends at the center of the system still are relaxed. However, one bend in the lower part of the system obtains relatively high stresses again; see the enlarged area in the upper part of Figur 29. This bend was creep relaxed as well during the first year and relaxes again during the second year, Figur 29, lower part.



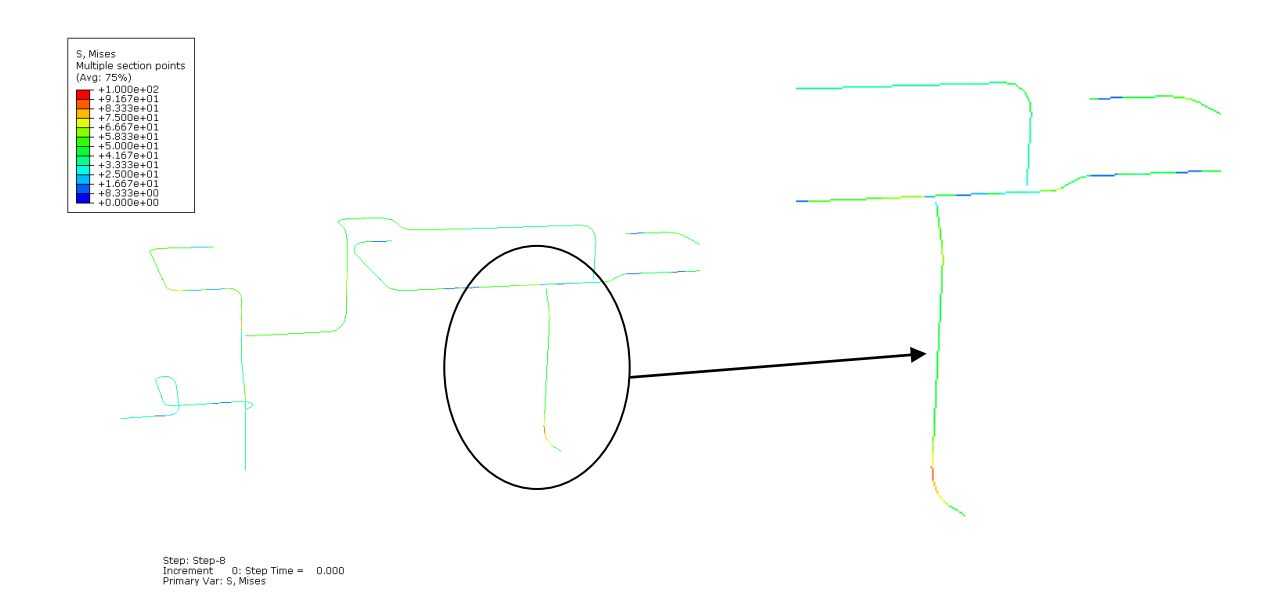


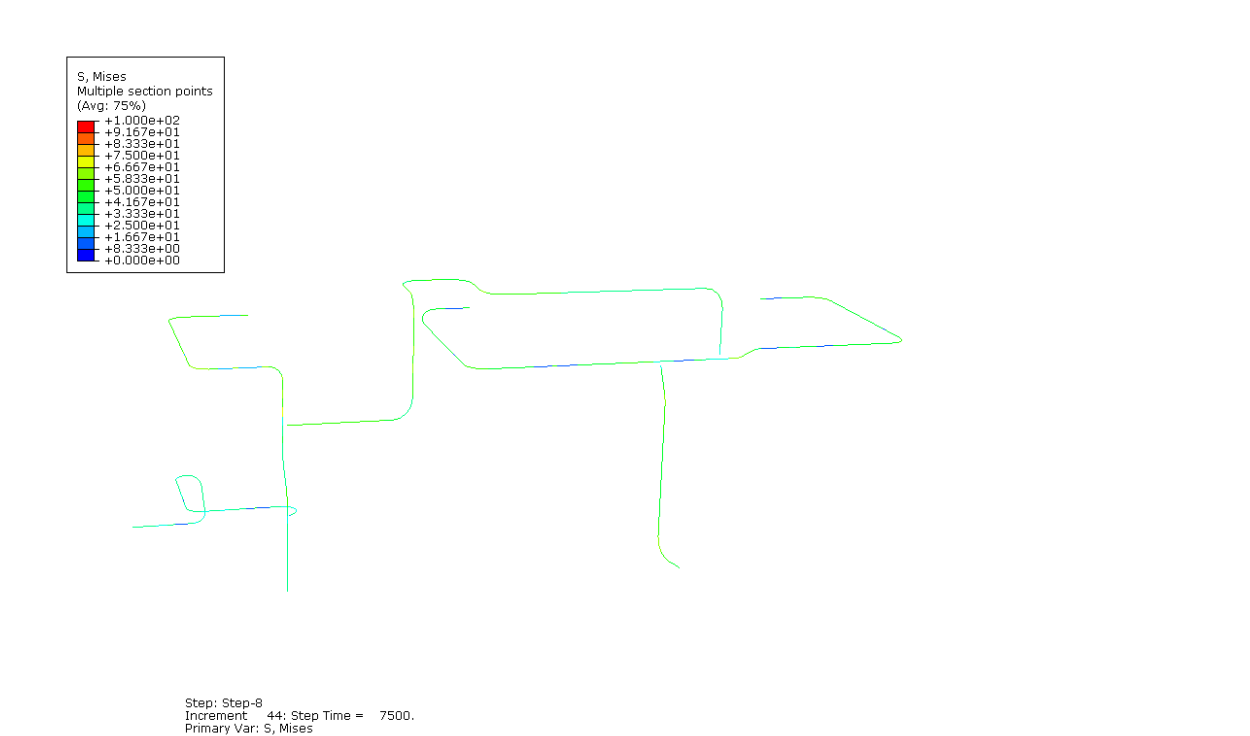


Figur 28. Övre bild: spänningsfördelning (von Mises) i början av det första året i drift, nedre bild: spänningsfördelning (von Mises) i slutet av första året. Systemet har relaxerat genom krypning.

Figure 28. Upper picture: Stress distribution (von Mises) in the beginning of the first year of operation, lower picture: Stress distribution (von Mises) at the end of the first year. The system has relaxed by creep.







Figur 29. Övre bild: spänningsfördelning (von Mises) i början av det andra året i drift, nedre bild: spänningsfördelning (von Mises) i slutet av andra året. Systemet är relaxerat.

Figure 29. Upper picture: Stress distribution (von Mises) in the beginning of the second year of operation, lower picture: Stress distribution (von Mises) at the end of the second year. The system is relaxed.



This behavior continues over the life time. Figur 30 shows repeated development of high stresses at the lower bends followed by relaxation at the end of year 5. Figur 31 shows a similar behavior also at year 14.

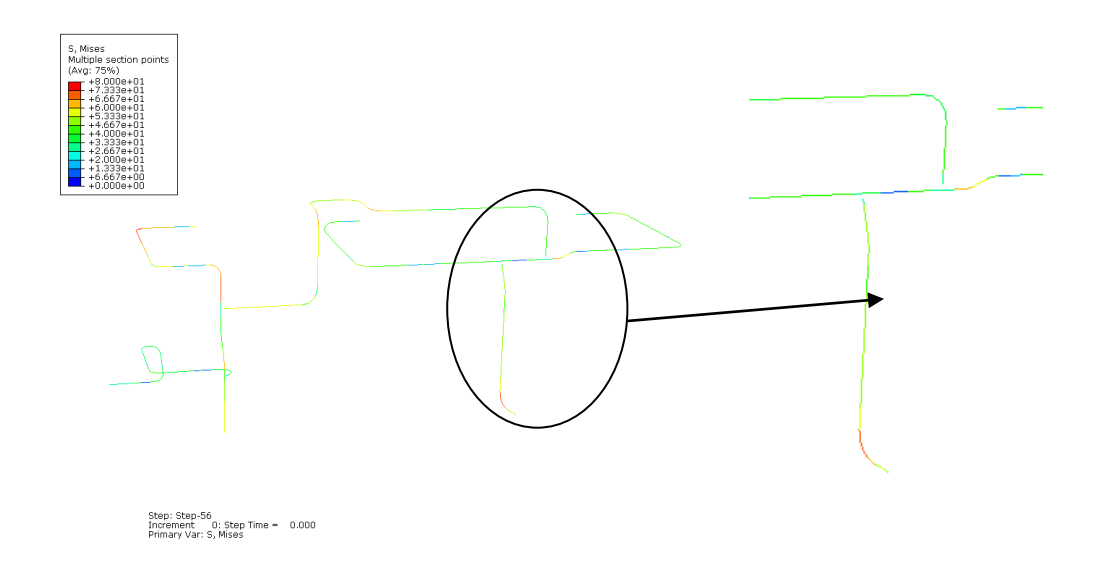
Note that the stress scale in these two figures (red areas correspond to 73-80 MPa) are somewhat different compared to the ones in Figures 30 and 31 (red areas correspond to 92 -100 MPa).

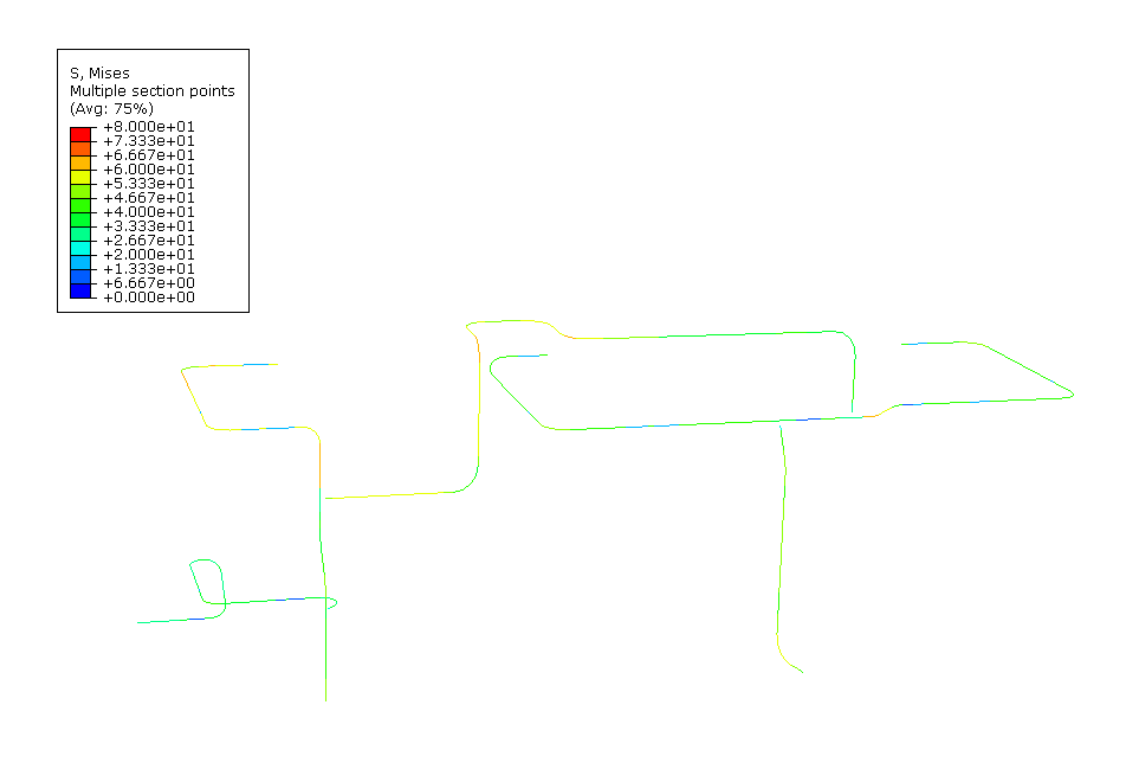


Figur 30. Övre bild: spänningsfördelning (von Mises) i början av det femte året i drift, nedre bild: spänningsfördelning (von Mises) i slutet av femte året. Systemet är relaxerat.

Figure 30. Upper picture: Stress distribution (von Mises) in the beginning of the fifth year of operation, lower picture: Stress distribution (von Mises) at the end of the fifth year. The system is relaxed.







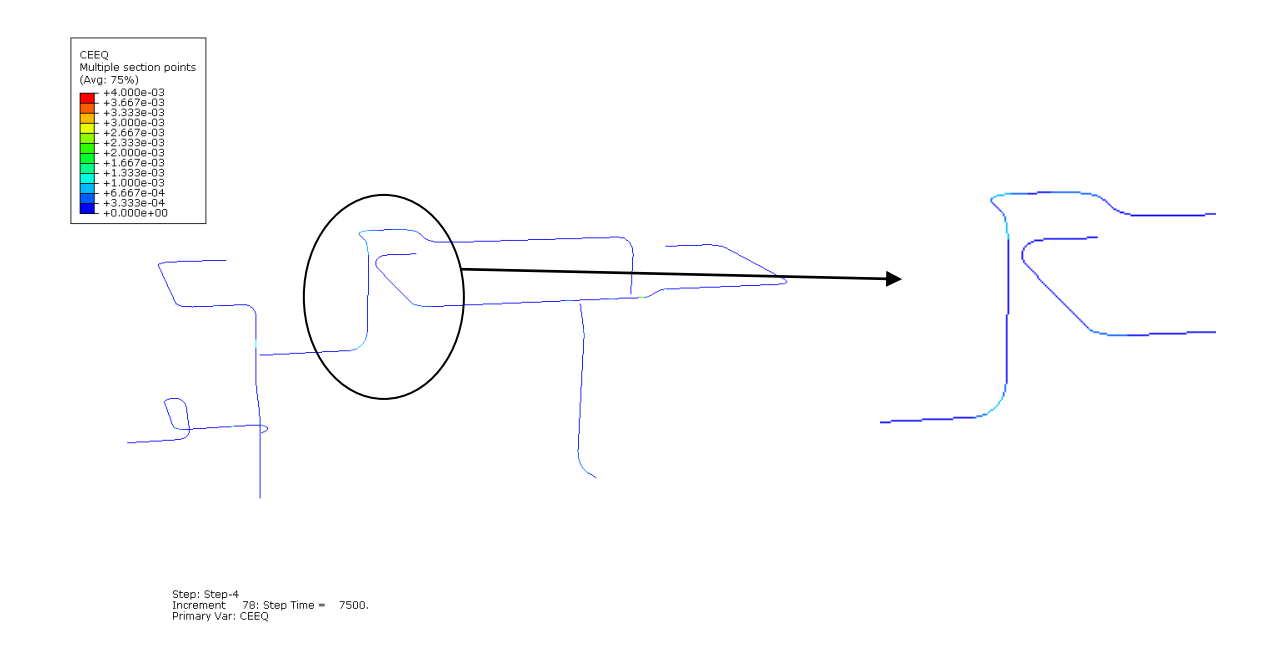
Step: Step-56 Increment 41: Step Time = 7500. Primary Var: S, Mises

Figur 31. Övre bild: spänningsfördelning (von Mises) i början av år 14 i drift, nedre bild: spänningsfördelning (von Mises) i slutet av år 14. Systemet är relaxerat.

Figure 31. Upper picture: Stress distribution (von Mises) in the beginning of year 14 of operation, lower picture: Stress distribution (von Mises) at the end year 14. The system is relaxed.



Figur 32 shows the accumulated creep strain after 1 year of operation. The highest strains have developed at the bends at the center of the system as a result of the initially highest stresses in this area followed by creep relaxation over the first year.

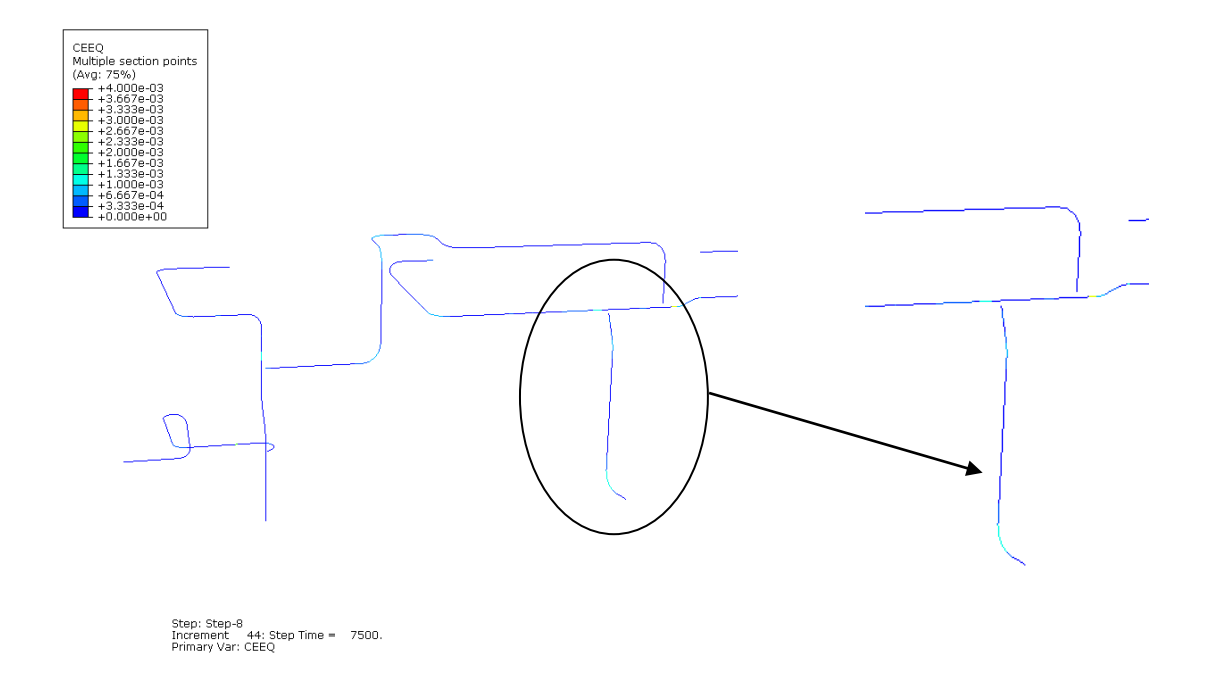


Figur 32. Ackumulerad kryptöjning i slutet av det första året i drift. De högsta kryptöjningarna är i böjarna i det inringade området.

Figure 32. Accumulated creep strain at the end of first year. The highest creep stains are in multiple bends.

At the end of the second year more creep strain has been developed at positions in the part in the system that is enlarged in Figur 33, particularly at the T-piece most to the right hand side and the lower bend where high stresses and relaxation reappeared as well as on the right hand side of the T-joint to the right stress concentrations to appear as well.





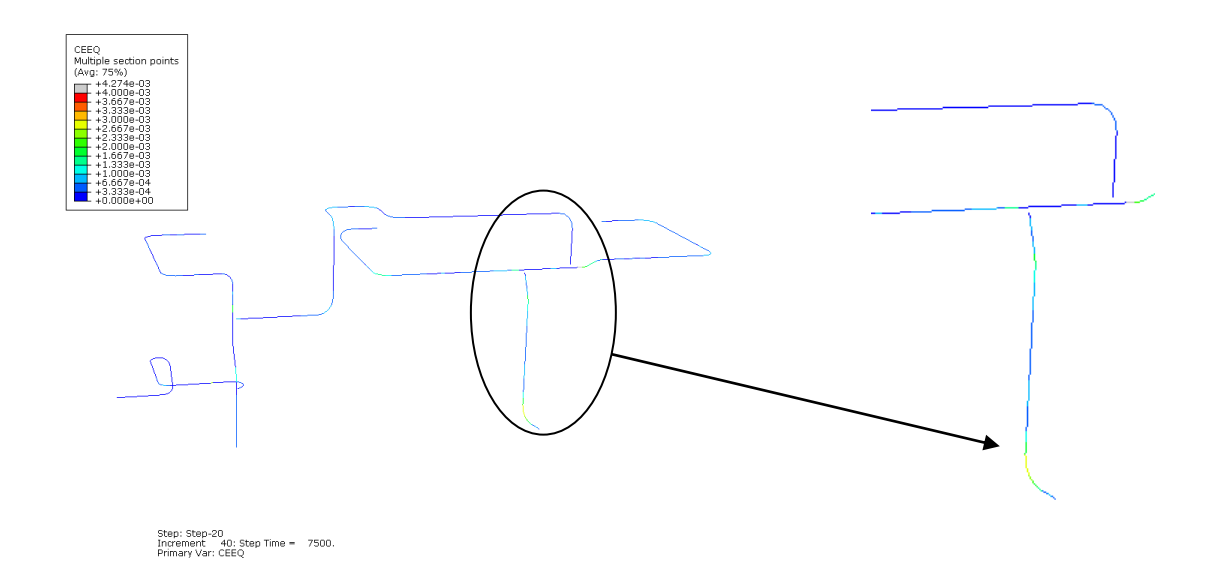
Figur 33. Ackumulerad kryptöjning i slutet av det andra året i drift. De högsta kryptöjningarna är i böjen nedtill i det inringade området.

Figure 33. Accumulated creep strain at the end of the second year. The highest creep stains are in the bends at the bottom.

After 5 years as well as after 14 years creep strain is still accumulating at the T-piece most to the right hand side and the lower bend where high stresses and relaxation reappeared as well as on the right hand side of the T-joint to the right, see Figure 34 and Figur 35. The analysis show strains up to $0.8\,\%$ after 14 years of service.

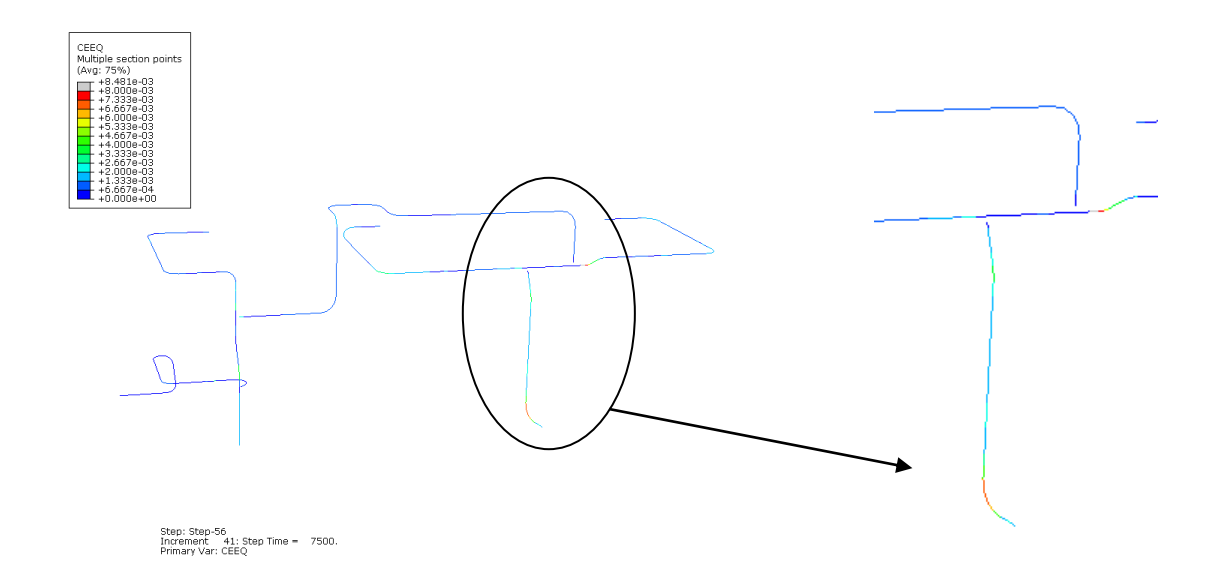
In the bends where high stresses were observed over the first year there is no continuous strain accumulation since starts and stops are not associated with reappearance of high stresses in these areas.





Figur 34. Ackumulerad kryptöjning i slutet av det femte året i drift. De högsta kryptöjningarna är i böjen nedtill i det inringade området.

Figure 34. Accumulated creep strain at the end of the fifth year. The highest creep stains are in the bends at the bottom.



Figur 35. Ackumulerad kryptöjning i slutet av år 14. De högsta kryptöjningarna är i böjen nedtill i det inringade området.

Figure 35. Accumulated creep strain at the end of year 14. The highest creep stains are in the bends at the bottom.



6.3 DISCUSSION

This pipe system was used in the first place in a Värmeforsk project [5] where it was modified to simplify the model. The simplifications and constrains on the model are applied from the Energi-forsk project, thereby we assume that the system is modelled in a realistic way and that we can rely on that information. In any case this model shows that the resulting kind of behavior is possible: a limited analysis of the system reaction cannot always represent the creep strain accumulation over a whole lifetime. At the first reaction after one year the results pinpoint a location that will not obtain the maximum creep strain after 14 years of operation. The present results indicate that a pipe system analyzed only with linear elastics could possibly not show the location of the most sensitive areas for creep damage.

The results also show that the stress level varies between different parts when the system is relaxed. The system stress distribution seems to be quite similar from one year to another in the relaxed condition, see Figur 30 and Figur 31. Thus, a variation in life time can be expected for different parts of the system according to the results of the analysis. For example, the orange and green areas in Figur 31 indicate stress levels of approximately 65 and 50 MPa, respectively. If a safety factor of 1.5 is applied on these stresses the resulting creep lives are 100.000 and 250.000 hours, respectively.

Welds are associated with reduced creep strength and occurrence of welds in areas with high stresses can involve significantly reduced life time. Replica testing of such welds is an obvious outcome of the analysis.

6.4 CONCLUSIONS OF THE EFFECT OF STARTS AND STOPS

After the first year of operation the system shows high stresses at the multiple bends in the middle of the system, see Figure 28. That is what a linear elastic pipe analysis would point out to be the most high risk areas for creep damage. After restarting the system every year the stresses increase at the single bend below, see Figur 29 and Figur 30. This bend continues to have increased stresses every time the system is restarted. While the multiple bends do not show as high stresses and seems to have relaxed at that area. This is clearer when the creep strain is considered. After the first year of operation the multiple bends show the highest creep strain, see Figur 32. Only a year later the situation is reversed, the creep strain accumulates in the single bend in question and continues to accumulate there after every restart, see Figur 33, 34 and Figur 35. This results in a maximum value for the creep strain that is much higher than in the multiple bends where the highest creep strain appeared after one year of operation. Thus, restarts of the pipe system may influence the locations of creep strain accumulation and thereby also the creep damage.

Furthermore, the results indicate that the linear elastic pipe analysis may not point out the most sensitive areas for creep damage, at least not in this case. The analyses showed a variation of stresses in different parts of the system in the relaxed condition. The resulting stress variations were demonstrated to correspond to essential differences in creep life.

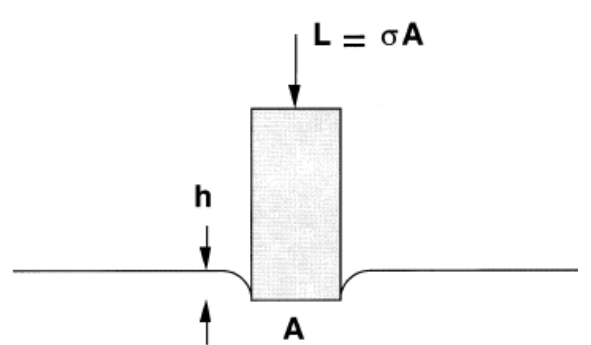


7 Impression creep testing

7.1 TEST METHOD

The impression creep (IC) test is well established and the validity of the technique has been supported by test data for a number of metallic materials at different temperatures and stresses. Over recent years, the test method has attracted increasing attention in power plant material and component assessment.

The IC test measures the displacement over time of an indenter set to push in to a specimen. The method was first presented in 1977 [14], the method have since then through extensive analyses showed to be a reliable test method [13][15]. Figure 36 shows the method schematically. An indenter, with the area A, is loaded with the load L, which creates an impression with the height h in the material.



Figur 36. En illustration av intryckskrypprovning.

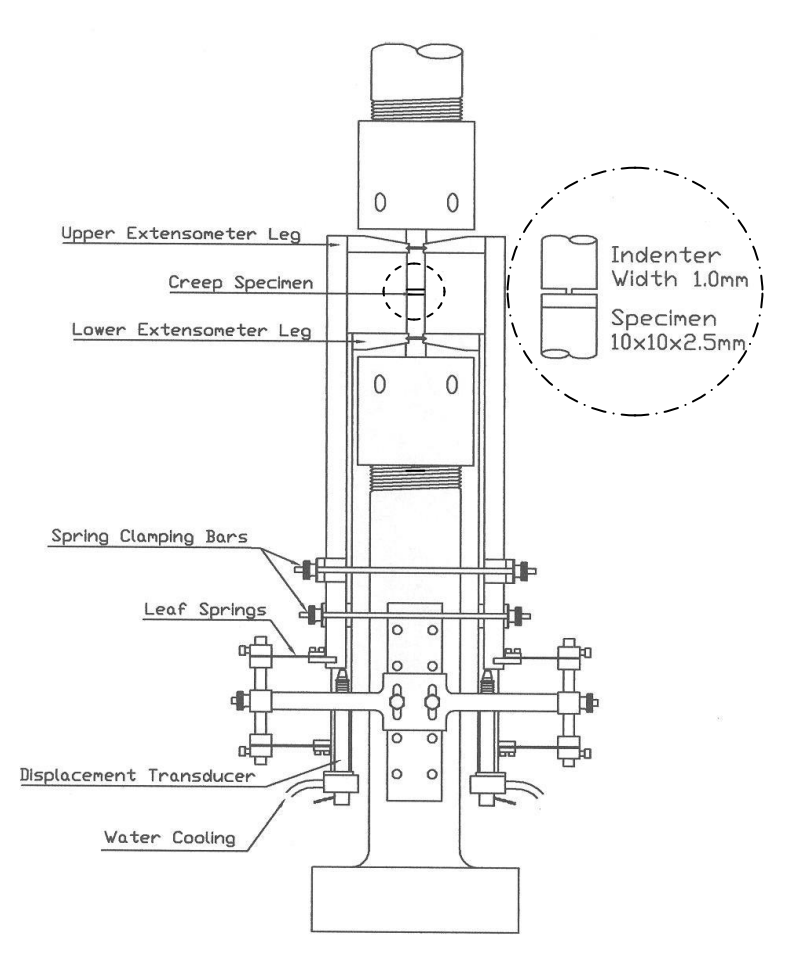
Figure 36. An illustration of the impression creep test.

The material during impression creep test exhibits the same stress and temperature dependence as the stress as a conventional tensile creep test [14]. IC tests can therefore be used to produce reliable creep strain rates, equivalent to those obtained from a normal creep test. Impression creep can also be used for localized in-situ testing measurements, where samples from various components in a system can be tested in order to determine the status of each component.

The impression creep test method, using a rectangular indenter, has been used extensively in the last 10 years, for a number of UK and EU projects and for industrial applications (e.g. TWI, British Energy, RWE npower, Structural Integrity Associates). Some industrial organizations have already built or are in the process of developing the test facilities for impression creep testing. EPRI has included impression creep testing into a collaborative (~ 25 partners) research programme in order to assess the practicality of the technique [15].

Both standard servo-electric machines and specially designed dead load rigs can be used for impression creep testing. The fundamental elements of the test machines should include the loading system, deformation measurement system, heating and temperature control system, inert gas environment (if necessary) and the data recording system etc. The loading fixtures and extensometers etc. are traditionally similar to a uniaxial creep test set up, can be seen in Figure 37 [15].





Figur 37. Lastfixtur och extensometersystem.

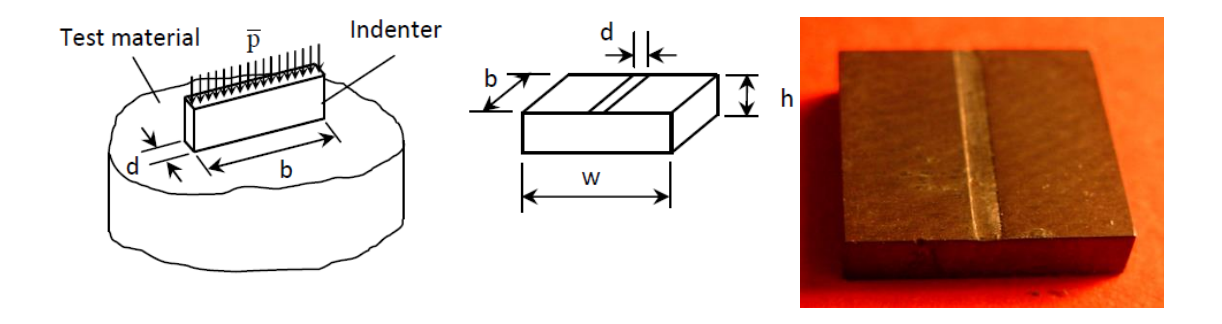
Figure 37. Loading fixture and extensometers systems.

The material of the indenter must be significantly stronger in creep than the test material. Nickel-based superalloys (Waspaloy and NIMONIC 105) have been used for the indenters. The minimum creep strain rates for these materials, at the same stress and temperature levels, are orders of magnitude lower than those of typical power plant steels, e.g. 10CrMo9-10 and P91, in the applicable stress and temperature ranges. The widths of the indenters which have been used are 1.0mm or 0.8mm. The length of the indenter should be slightly longer than the length of the specimen. The indenter must be carefully machined and should be checked after each test. Grinding of the contact surface of the indenter may be needed after a number of tests. Special care should be taken to ensure that the specimen surface is parallel to the flat surface of the indenter.

In most of the tests carried out so far, specimen dimensions of $w \times b \times h = 10 \times 10 \times 2.5$ mm with d = 1mm have been used. These specimen and indenter dimensions are recommended by the authors because the supporting FE analysis for the correlation parameters has been performed with these dimensions (Hyde, Sun, Brett, 2009). Such specimen sizes and dimension ratios ensure that full contact is maintained between the specimen and the supporting bar, and they prevent significant bending deformation



from occurring. In addition, specimens of this size can be produced, in most cases, from scoop samples, and from the HAZs from main steam pipe welds in power plants. Figure 38 shows the principle of the test and a typical test specimen after impression.



Figur 38. Principen för IC test och ett typiskt intrycksprov efter ett test.
Figure 38. The principle of the IC test and a typical impression specimen after test.

The obtained data result from an impression creep test will have the unit deformation in the specimen's thickness direction versus time. The data need to be converted in order to obtain the desired unit minimum creep strain rate (MCR) versus stress. Conversion parameters are used in order to transform the IC test data and obtain the minimum creep strain rates. The conversion equations are; equation 6 and 7:

$$\sigma = \eta \overline{p}$$

$$\dot{\varepsilon}_{ss}^{c} = \frac{\dot{\Delta}_{ss}}{\beta d}$$
(6)
$$(7)$$

, where \bar{p} is the uniaxial stress equivalent to the stress σ , $\dot{\Delta}_{ss}$ is the steady-state impression depth rate $\dot{\Delta}_{ss}$ equivalent to the uniaxial steady-steady state strain rate $\dot{\mathcal{E}}_{ss}$, d is the diameter of the intender and η and β are the conversion parameters. For a polycrystalline material in the range of n=2-15 in the Norton equation (5) where only a single deformation mechanism is dominating, the conversation parameters can be set to; equation 8 and 9:

$$\eta = 0.296$$
(8)
$$\beta = 0.755$$
(9)

The conversation parameters are affected by the dimension of the specimen and the diameter of the intender. The supporting FE analysis for the correlation parameters has been performed for the dimensions $10 \times 10 \times 2.5$ mm for the specimen and a diameter of 1 mm for the intender. Thus, these sizes are recommended. If there is insufficient specimen material available their the dimension $8 \times 8 \times 2$ mm and a intender diameter



of 0.8 mm can be recommended. A square-shaped specimen is recommended over any other shape (46). The derivation of the conversion parameters η and β can be seen in ref (47).

Some benefits with impression creep test over conventional creep test are [14]

- Shorter testing times, typically 300 hours for IC and about 7 000 hours for conventional creep test.
- The negative impact on the component can be reduced because i) less test material is needed, ii) more lenient sampling equipment can be used, e.g. electric discharge sampling equipment.
- The area reduction which occurs during conventional creep test does not have to be considered during IC testing.
- Localized sampling over individual zones in the material, e.g. a weld or a HAZ can be made.
- Can be used as a creep strength ranking test of components parent materials, in order to aid the selection of damaged components in need of testing in a system. This was successfully accomplished for an aged 1/2CrMoV pipework system in [15].

7.2 VTT DESIGN OF THE IMPRESSION CREEP EQUIPMENT

The starting point of the test rig design at VTT Finland was not to "replicate a uniaxial specimen" (see Hyde, Sun, Brett, 2009) as the impression creep test has very little in common with a uniaxial test. Consequently there was no need to replicate a uniaxial type of extensometer and the extensometer design could be based on a completely different principle. Also one problem with heating was addressed as in case of a normal resistance furnace the temperature of the relatively small specimen is sensitive to the temperature differences between the upper and lower loading bars as there is a very small contact area and thus little heat flow between the bars and the specimen. Therefore it was decided that the upper and lower bars can be heated by two Hotset WRP (Ø3.3mm) resistance cables and separate controllers (http://www.hotsetworldwide.com/fi/products/hotspring). When the load cell was placed below the furnace there was no more need for water cooling anywhere in the system.

The decision to mount two ceramic tube + rod type of extensometers inside the lower loading bar gave the possibility to measure the displacement as close to the indenter as possible as shown in Figures 39 and 40, and therefore the effect of the thermal fluctuation and thermal expansion is minimised. The extensometer system is also frictionless. The inner rod is supported from below only by the spring force of the displacement transducer. The effective gauge length is much smaller (<10mm) than in the traditional system (50mm) which helps in minimising the effect of thermal fluctuations. Two dis-placement transducers are mounted below the lower loading bar. In the initial design the ceramic rod is pushed by the displacement transducer spring against another piece of ceramic rod, which is fitted to the upper tool (made of GTD 111). In the current design the ceramic rod is pushed directly against the upper tool. Two Heidenhain's new Acanto transducers are used. The results have con-firmed that with this system the stability of the displacement signal is better than in the system developed at Nottingham University. The system is also very simple and inexpensive to build.



Heating is provided by resistance heating cables (250W each), see Figure 39. Heating cables are tightened by stainless steel sheets, see Figure 40. The heating of the upper and lower loading bars are controlled separately in order to minimise the temperature differences between the upper and lower tool. Two noble metal thermocouples are used for temperature control and two (also noble metal) for data logging. The measuring thermocouples are placed as close to the specimen as possible and the controlling thermocouples are embedded in the upper and lower tool a bit closer to the heating cables. A separate K-type thermocouple is integrated at the factory inside the heating cables to provide overheating protection (max. 750°C). Also a flat pressed cable is available for better heat transfer, but this is not critical. Continuous test temperatures of 600°C can be achieved with no difficulty.

Four steel bars ($d = \varnothing 20$ mm) on the top and at the bottom provide sufficient cooling, se Figure 40. The crosshead and the load cell remain at or close to room temperature. As there is no traditional furnace but just the resistance heating cables, what looks like a small furnace in Figure 41 is actually just a thermal insulation box.



Figur 39. Nedre del av rigg, delar av keramisk extensometer, resistansspole och undre laststång.

Figure 39. Lower tool, ceramic extensometer parts, resistance cable and loading bar.



Figur 40. Resistansspolarna är omslutna av höljen av rostfritt stål.

Figure 40. The heating cables tightened by stainless steel sheets.





Figur 41. Hela riggen med isolerande låda i mitten.

Figure 41. The complete assembly with insulation box in the middle.

7.3 APPLICATIONS OF IMPRESSION CREEP TECHNIQUE

From the impression creep test the outcome is a minimum creep rate at a given stress. Typically five stresses in increasing order can be tested on one specimen. Typically the minimum creep rate is achieved in 500 hours. The impression creep technique can be used as an alternative for uniaxial creep tests especially in cases when the amount of available test material is limited. With one standard specimen of 10*10*2.5mm up to five or six different stress levels can be used, which is normally sufficient for characterising the basic creep properties of the material. The volume of test material needed for conventional uniaxial testing would be more than 600 times bigger than for impression creep testing. The disadvantage of the IC method is that it only gives creep rates but not any information on ductility of the material. In this respect the uniaxial and SP methods have the advantage. One possibility to overcome this problem is to first do an IC test and then machine a SP test specimen from the opposite side and measure the fracture time and ductility from it.

One special benefit of the test method is that it can be used for testing of local material zones in inhomogeneous materials like HAZ of steel weldments. The specimen can be extracted in such an orientation from a weld that the specimen surface is parallel to the HAZ and the test surface can be placed for example on the coarse grained zone or the intercritical zone, which is normally the weakest zone in ferritic welds in creep regime. This feature is very valuable when material parameters are needed for a detailed FE analysis of a weld as with IC method the parameters of all the various zones of the weld can be characterized separately.



In testing the various zones of a HAZ the underlying zones will inevitably affect the results at least to some extent. The "effective depth" of material which determines the creep response in an IC test has not yet been defined, but this is an issue which the international IC test community lead by Nottingham University is looking at in the future.

7.4 UNIAXIAL AND IMPRESSION CREEP TESTING

The creep test programme consists of creep testing of a new welded pipe without service exposure and of the T-joint weld MR05 which was characterized with respect to creep damage, sees section 3.3. The new pipe was taken from the store at Heleneholmsverket and has the same dimensions as the main steam pipe. It was cut in two pieces weld joint prepared and welded in the same way and by the same welding company that has performed the welding at reconstructions of the Heleneholmsverket main steam piping over the last decade. The welding data is presented in Appendix 2.

In the new pipe uniaxial creep testing was performed on parent metal. The purpose of this testing is to verify the impression creep testing and the transformation parameters to uniaxial data by comparison with the impression creep test results of the same material. Then, a profile of impression creep tests from the parent metal across the HAZ and into the weld metal was performed. This is detailed below.

In the service exposed weld impression creep tests were conducted at material from weld metal and in two positions of the parent metal, one adjacent to the weld and another remote from the weld, where the adjacent position corresponds to the saddle position of the T-piece.

The results from the creep testing are then used for analyses of the pipe system and the T-joint. Up to date tabled data is used for such analyses. Thus, it will now be possible to compare analyses with tabled data to analysis with data from new material and from service exposed material. In addition, data from weld metals and the HAZ can be included in the analyses. Finally, the resulting creep strain distributions can be compared, and thereby verified, with the actual amount of creep damage that has been found in the studied components.

7.4.1 Uniaxial creep test results in new material

Three uniaxial base material creep test specimens with diameter 10 mm and gauge length 50 mm were machined from the 10CrMo9-10 pipe shown in Figure 42. The tests were carried out at 530°C at different stresses. The test results are shown in Table 7.

The individual strain curves are shown in Figures 43-44. The data was then reduced to about 100 data points for the calculation of strain rates by the ASTM E1457 incremental polynomial ("seven point") method. The strain rates versus time are shown in Figure 45 and the corresponding rates versus strain are shown in Figure 46. The strain rate curves in Figures 45-46 show that the behaviour of the test material was systematic without any anomalies.





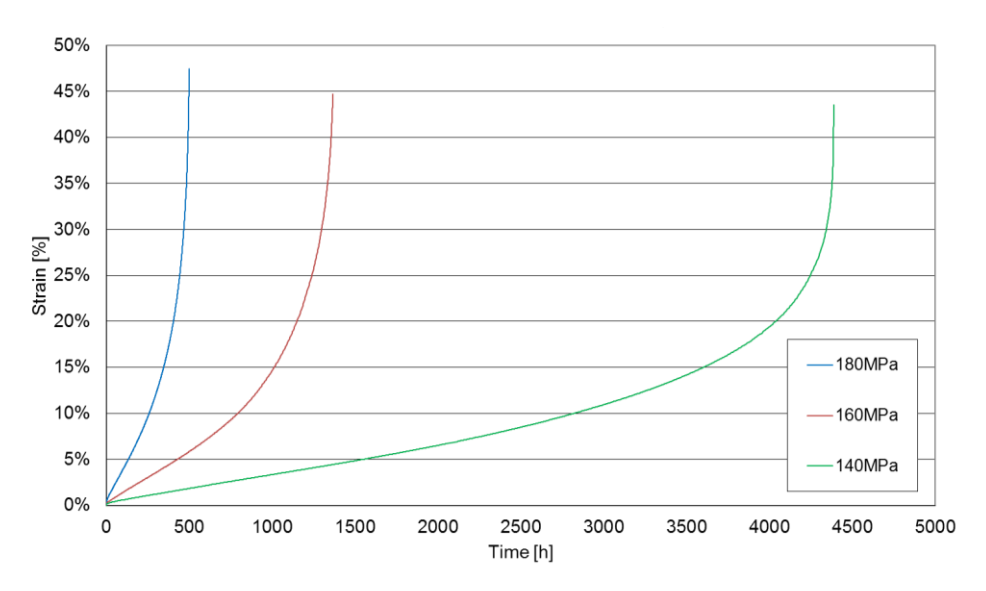
Figur 42. Svetsat rör av 10CrMo9-10 utan driftpåkänning efter att provmaterialet har sågats ut.

Figure 42. Welded 10CrMo910 pipe without service exposure after removal of test specimens.

Tabell 7. Resultat av krypprovning med enaxliga provstavar hos 10CrMo9-10 grundmaterial.

Table 7. Uniaxial creep test results for 10CrMo9-10 base material.

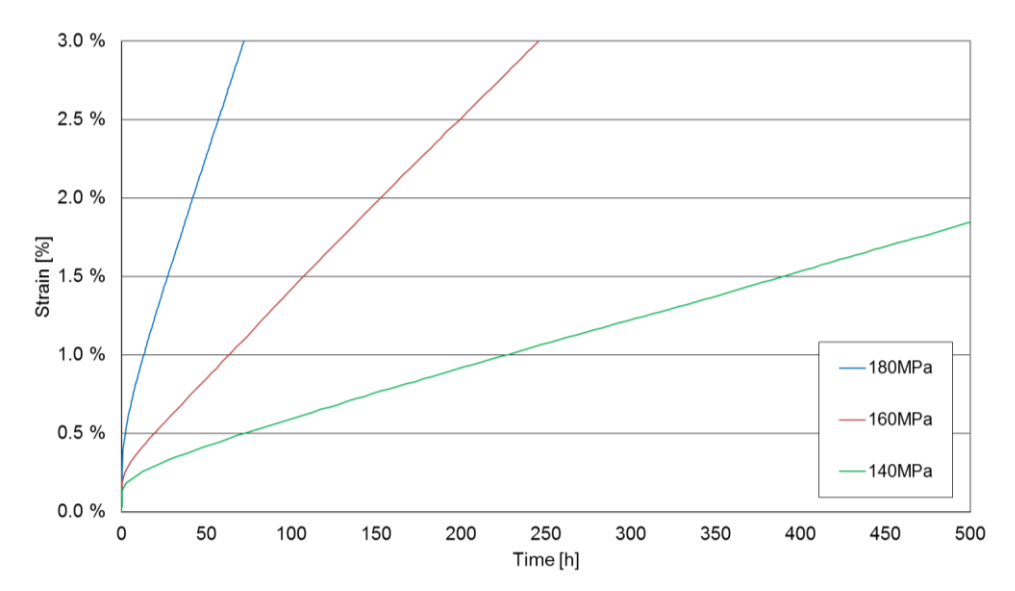
| | Stress | Temp | elongation | • | tr | min.rate |
|-------------|--------|------|------------|--------|--------|----------|
| Specimen | [MPa] | [°C] | ef [%] | RA [%] | [h] | [abs] |
| VF-A y433M9 | 180 | 530 | 62.4 | 87.7 | 500.2 | 3.32E-04 |
| VF-B y439M9 | 160 | 530 | 59.7 | 82.6 | 1371.5 | 1.07E-04 |
| VF-C y432M8 | 140 | 530 | 47.8 | 96.3 | 4386.6 | 2.95E-05 |



Figur 43. Kryptöjningskurvor för 10CrMo9-10 grundmaterial vid 530°C.

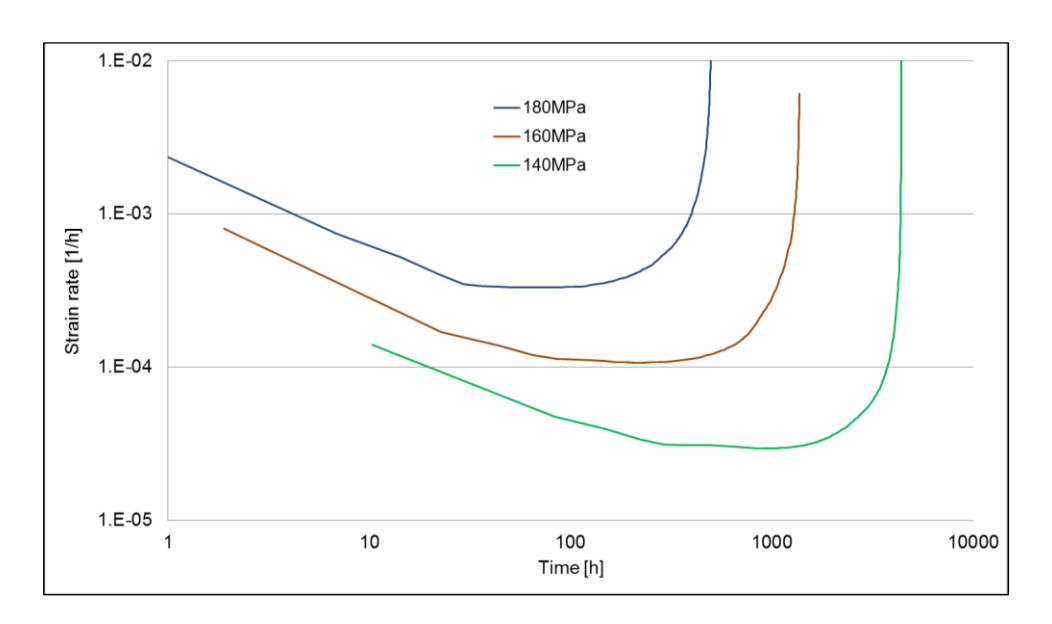
Figure 43. Strain curves for 10CrMo910 base material at 530°C.





Figur 44. Initial del av kryptöjningskurvorna för 10CrMo9-10 grundmaterial vid 530°C.

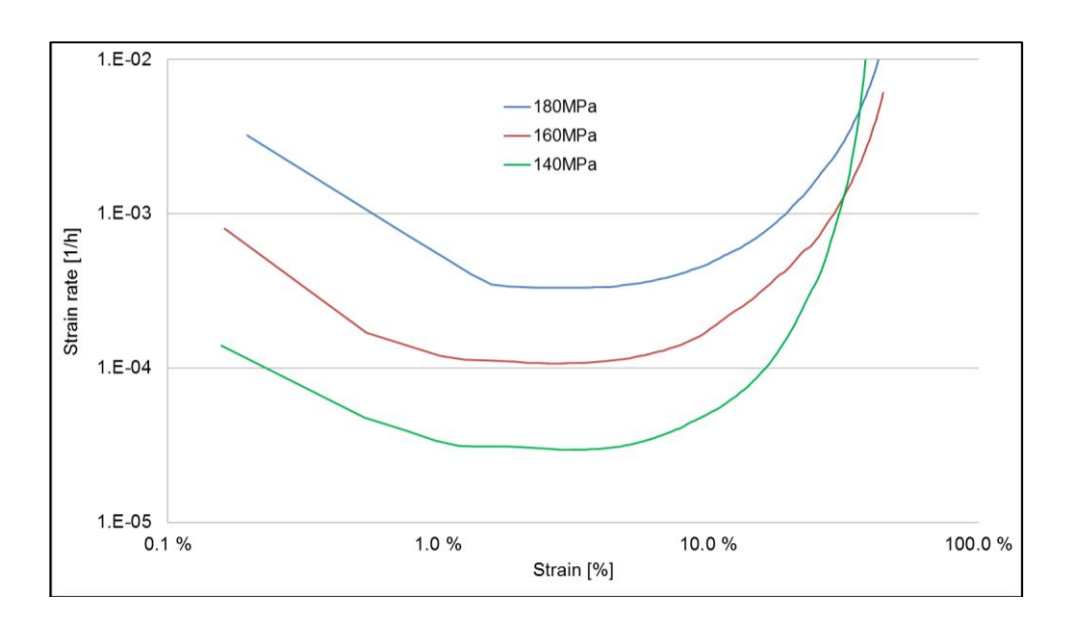
Figure 44. Initial part of the strain curves for 10CrMo910 base material at 530°C.



Figur 45. Tid som funktion av kryptöjningshastighet hos 10CrMo9-10 grundmaterial vid 530°C.

Figure 45. Strain rate curves versus time for 10CrMo910 base material at 530°C.





Figur 46. Töjning som funktion av töjningshastighet hos 10CrMo9-10 grundmaterial vid 530°C.

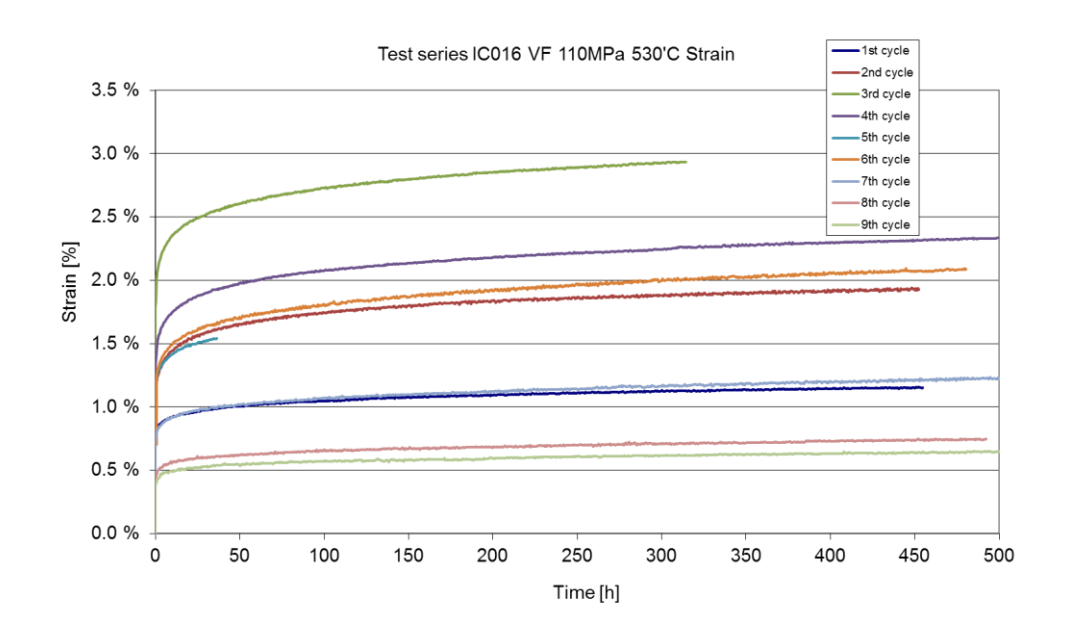
Figure 46. Strain rate curves versus strain for 10CrMo910 base material at 530°C.

7.4.2 Impression Creep test results of the new weld

For impression creep (IC) testing a non-standard test procedure was chosen. Because the purpose of the IC testing was to provide material parameters – strain rates particularly - for the HAZ of the T-piece for the FE analysis by Inspecta, it was decided to deviate from the practice in terms of the specimen thickness. While the standard specimen is 10*10*2.5 mm in size, an "oversize" specimen was made with thickness of 10 mm in such a way that the HAZ was parallel with the surface to be indented. After each 500 h test cycle a 0.5 mm layer was ground off from the indented surface, rotated by 90° in order to reduce the effect of the deformation from the previous test, and then the testing was continued with the same specimen until all layers of the sample were tested, starting from the base material (BM), across the HAZ, and finally ending up in the weld metal (WM). The corresponding uniaxial stress in these tests is 110 MPa.

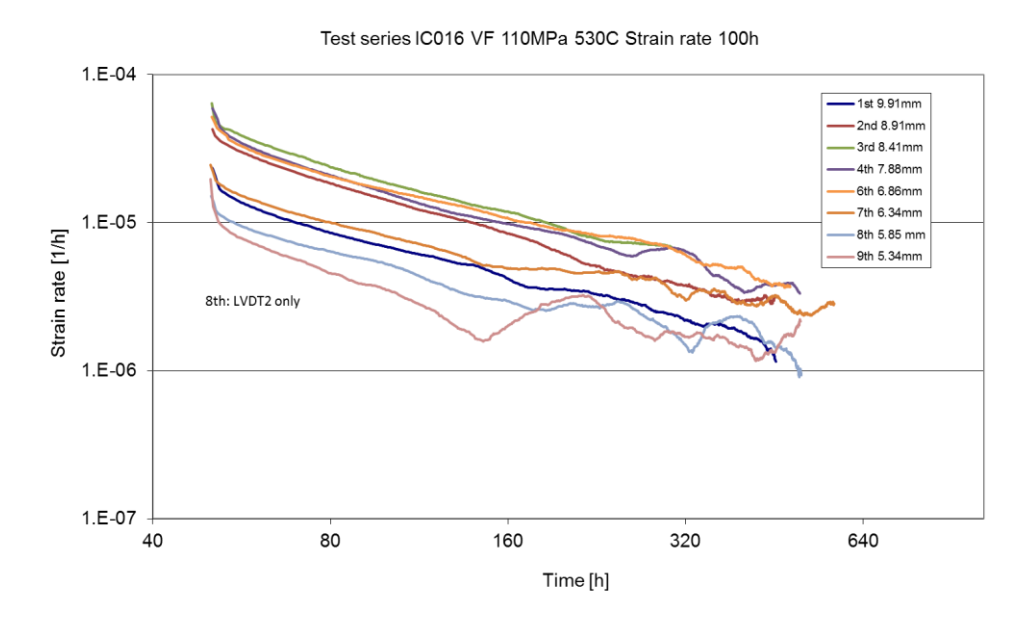
After each 500 h test cycle the minimum displacement rate was calculated and this was converted to a corresponding uniaxial strain rate by using a simple analytical equation established by Nottingham University for impression creep to uniaxial conversion. Also the displacement curves (indentation depth) were converted to uniaxial strain curves as shown in Figure 47 where the curves of only the nine first tests are shown. The continuous strain rate curves were calculated by moving a 100 h "calculation window" from the beginning of the test to the end as shown in Figure 48. It is seen that towards the end of each test the scatter increases when the strain rates become very small. In another project it was defined that below a strain rate of about 3*10-6 the accuracy will reduce. This is also partly due to the fact that towards the end of the test the number of data points in the 100 h calculation window reduces and in fact the last rate is calculated by a window of only 50 h. A linear trend line was fitted through the data of the last 100 h of each test in order to calculate the corresponding uniaxial minimum creep rate of each test. These creep rates are shown in Table 8.





Figur 47. Resultat av intryckskrypprovning omräknat till motsvarande enaxliga kryptöjningskurvor vid 110 MPa och 530°C.

Figure 47. Corresponding uniaxial strain curves calculated from the impression creep test series at 110 MPa and 530°C.



Figur 48. Kontinuerliga töjningshastighetskurvor från intryckskrypprovningsserierna vid 110 MPa och 530°C.

Figure 48. Continuous strain rate curves from the impression creep test series at 110 MPa and 530°C.



Tabell 8. Minsta linjära kryptöjningshastighet för varje tjocklek av provet.

Table 8. Minimum linear strain rates at each specimen thickness.

| Specimen | min. strain |
|-----------|------------------|
| thickness | rate (corrected) |
| [mm] | [1/h] |
| 9.91 | 1.75E-06 |
| 8.91 | 3.26E-06 |
| 8.41 | 3.90E-06 |
| 7.88 | 3.70E-06 |
| 6.86 | 4.58E-06 |
| 6.34 | 2.74E-06 |
| 5.85 | 1.65E-06 |
| 5.34 | 1.44E-06 |
| 4.85 | 1.79E-06 |
| 3.88 | 1.22E-06 |
| 3.09 | 9.47E-07 |
| 2.5 | 5.291E-07 |

The creep rate varied when moving from BM across the HAZ to the WM. The useful illustration of this behaviour is shown in Figure 49 where the brown curve shows the corresponding uniaxial strain at a constant time value of 300 h, being a rough relative measure of the amount of primary creep at each material layer. However, the quality of the initial contact between the specimen and the indenter is not necessarily perfect in each test, so there is some uncertainly associated with this strain parameter. However, the strain value (brown curve) and the calculated minimum creep rate (blue curve) for each test seem to go roughly hand in hand. Standard deviation values were added on the strain rate curve as calculated at the same time period as the minimum strain rate.

The test series was started with the specimen thickness of 10 mm and then the tested surface was in base material. After the first test 1 mm was ground off and in the second test the measured minimum strain rate had increased. After the following tests only 0.5 mm was ground off. In the third test the highest minimum strain rate achieved as shown in Figure 49, which initially indicated that this layer would be the inter-critical zone, which has the weakest creep strength and the highest creep rate. However, in this particular test with the highest creep rate and in another test (at thicknesses 8.41mm and 4.85mm) were run to only about 300 h instead of intended 500 h test duration. Based on the general trend in Figure 48 it was estimated that the creep rate at 500 h would be 0.544 times the rate at 300h. When these two test results are corrected the figure changes especially at the location which was thought to be the inter-critical zone, see Figure 50. The brown curve does not change as all the strain values have been measured at 300 h.

Based on the measurements from the cross-section of the new weld in Figure 52 it can be estimated that on top of the 10*10mm hole the location of the fusion line is at 3.72 mm and at the bottom at 5.12 mm. The location of the IC-HAZ/BM transition is more difficult to define but is located roughly at 6.28 mm on top of the hole and at 6.98 mm at the bottom. From these measurements it can be estimated that the width of the HAZ is 2.56 mm on top of the hole and 1.86 mm at the bottom, which seems like a rather

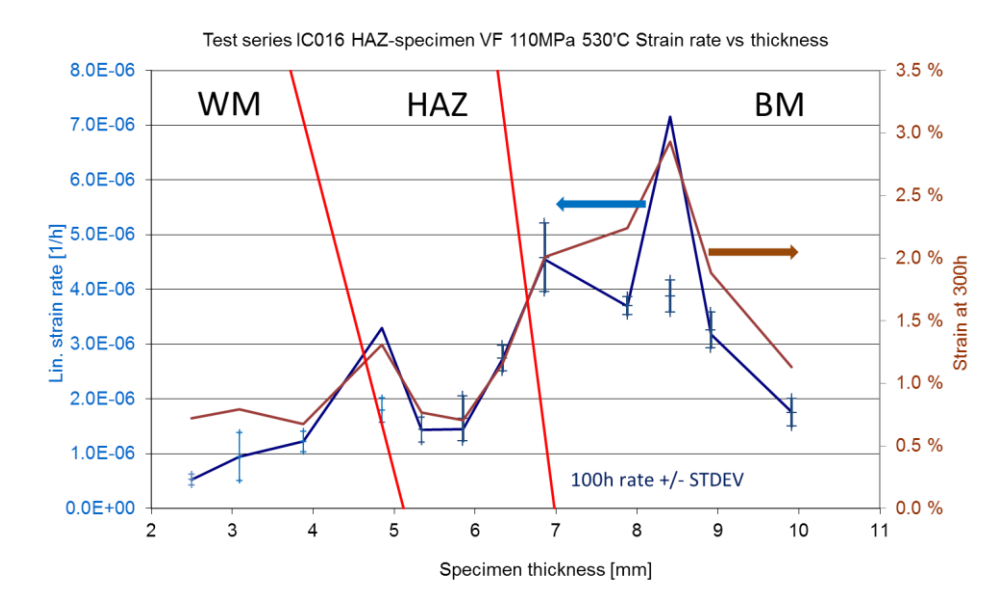


small value. The HAZ location has been sketched into Figs. 49, 50 and 55. The CG-HAZ is the strongest zone and has the lowest creep rate. The minimum creep rate results in Table 8 and in Figure 50 show that the highest strain rate of 4.58*10-6 in the HAZ is only 2.6 times higher than that in the base material (1.75*10-6). However, it was expected that the strain rate in the coarse grained zone would have been considerably lower than in the base material, but this is not the case. The low creep rates measured from the WM as shown in Figure 50 indicate that the creep strength of the WM is slightly higher than of the BM. The weld is therefore overmatching.

The reported minimum strain rate values did not necessarily hit the lowest and the highest values in the test specimen as the selected grinding thickness of 0.5 mm was a compromise between two factors. First, the smaller the grinding thickness, the smoother the curve in Figures 49-50 would have been (but would have increased the number of test cycles needed to scan through the specimen). Secondly, the smaller the grinding thickness, the more the deformation from the previous cycle would have influenced the following test. The FE analysis of the IC test specimen had shown that the deformation below the indenter does not progress deeper than 0.5 mm. However, this is of course dependent on the stress level.

When testing a HAZ specimen as described above one has to recognise also the fact that the sample is a sandwich structure in terms of material properties. At this point it is not known how the underlying different microstructures will affect the testing of the microstructure on the surface. This would require FE analysis which is not foreseen in the current project.

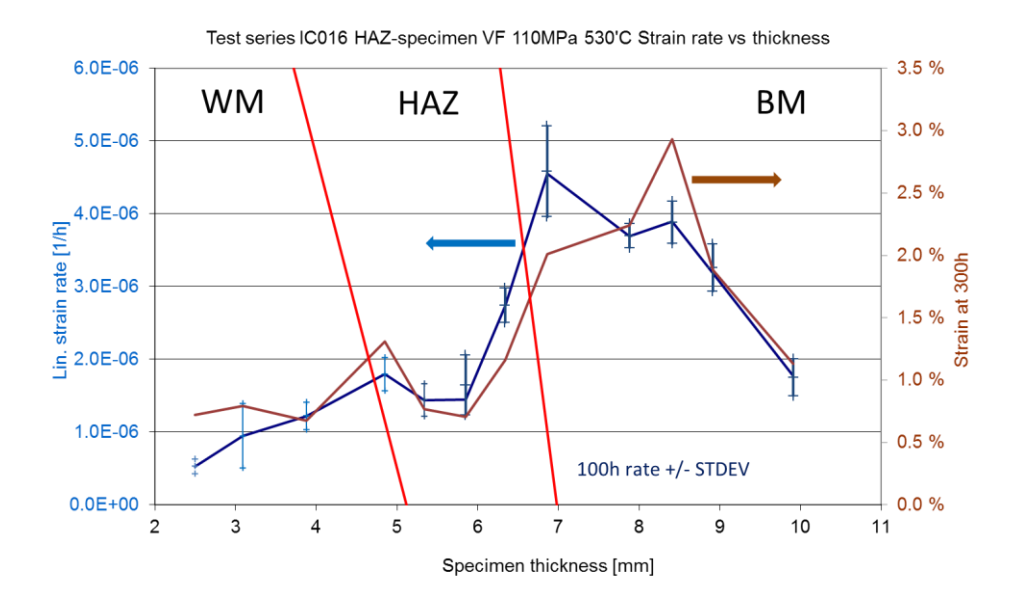
During a planned electricity maintenance brake a modification of the IC extensometer was done, which improved the gripping of the ceramic tube and this has greatly improved the stability of the displacement signal.



Figur 49. Beräknad minimum linjär kryptöjningshastighet och motsvarande enaxlig töjning vid 300 timmar för varje intryckskryptest vid 110 MPa och 530°C.

Figure 49. Calculated minimum linear strain rate and the corresponding uniaxial strain at 300 h for each impression creep test at 110 MPa and 530°C.





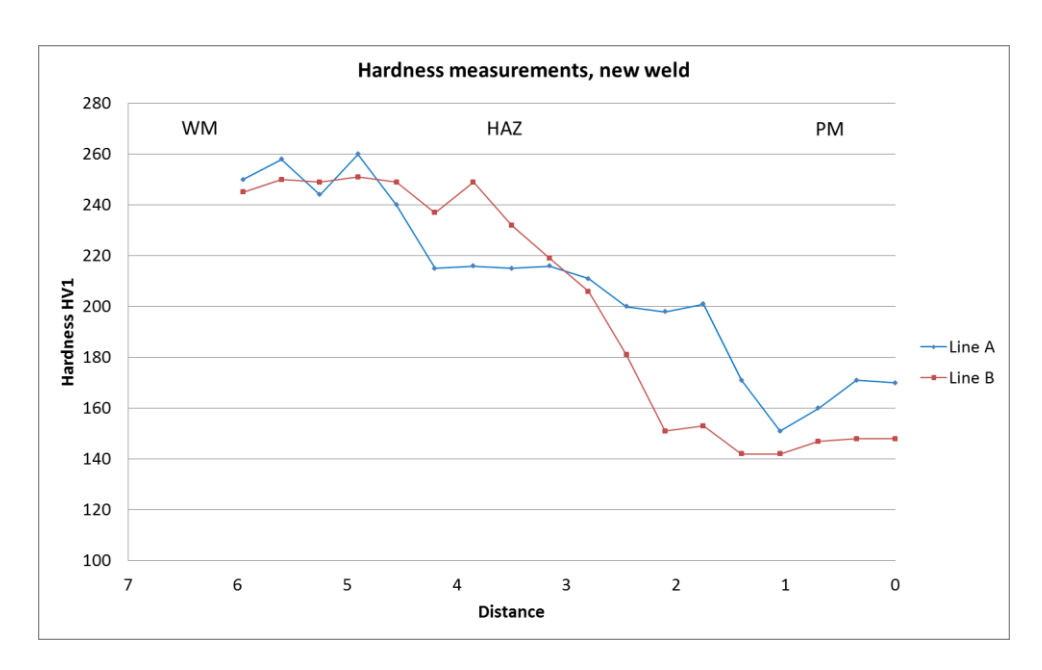
Figur 50. Korrigerade minsta linjära töjningar jämfört med figur 49.

Figure 50. The minimum strains corrected as compared to Figure 49.

Hardness was measured from the new weld and the results are shown in Figure 51. The locations of the hardness measurements are indicated on the left hand side picture in Figure 52. The hardness measurements in Figure 51 indicate that the width of the HAZ is about 4 mm, which does completely coincide with the measurements taken from Figure 52. The WM has a much higher hardness (250 HV1) than the BM (160 HV1), which means that the WM is overmatching. The high hardness of the WM is in line with the finding that the creep rate of the WM in Figure 50 is lower than the creep rate of the BM although the correlation between hardness and creep strength is not universal. It is well known, however, that a good correlation exists between hardness and tensile strength of steels.

In the left hand side picture in Figure 52 also the position where the impression creep specimen was extracted can be seen. The right hand side shows the microstructure in the HAZ area in the specimen. Weld metal can be seen to the left and towards the right hand side follows the fusions line, the HAZ and the parent metal. Close to the fusion line it can be observed that the HAZ microstructure is coarse grained.





Figur 51. Hårdhetsmätningar tvärs HAZ hos den nya svetsen.

Figure 51. Hardness measurements across the HAZ of the new weld.



Figur 52. Tvärsnitt av svetsen och positioner för intryckskrypproverna samt hårdhetsmätningen, markerade med svarta streck tvärs HAZ t.v. Mikrostruktur från provet t. h. med svetsgods åt vänster, smältgräns och HAZ åt höger.

Figure 52. Cross-section and the locations of the impression creep specimens and the hardness measurements across the HAZ, marked with black lines across the HAZ on the left hand side.

Microstructure from the specimen on the right hand side with WM to the left, fusion line and HAZ to the right.

7.4.3 Impression Creep test results of the service exposed T-piece

The 10CrMo9-10 T-piece from Heleneholmsverket (Figure 53) with significant creep damage in the saddle position was sectioned at VTT for determination of the exact dimensions and weld geometry by Inspecta Technology. One slice was removed for machining of IC test specimens, see Figure 54. Two specimens were removed from the base material of the main body, one near the saddle point (marked BM1 in Figure 55) and another further away from the saddle point (marked BM2). One specimen was removed from the WM. All these specimens were "oversize" specimens with regard to the thickness of the specimen in order to facilitate multiple tests from one sample with

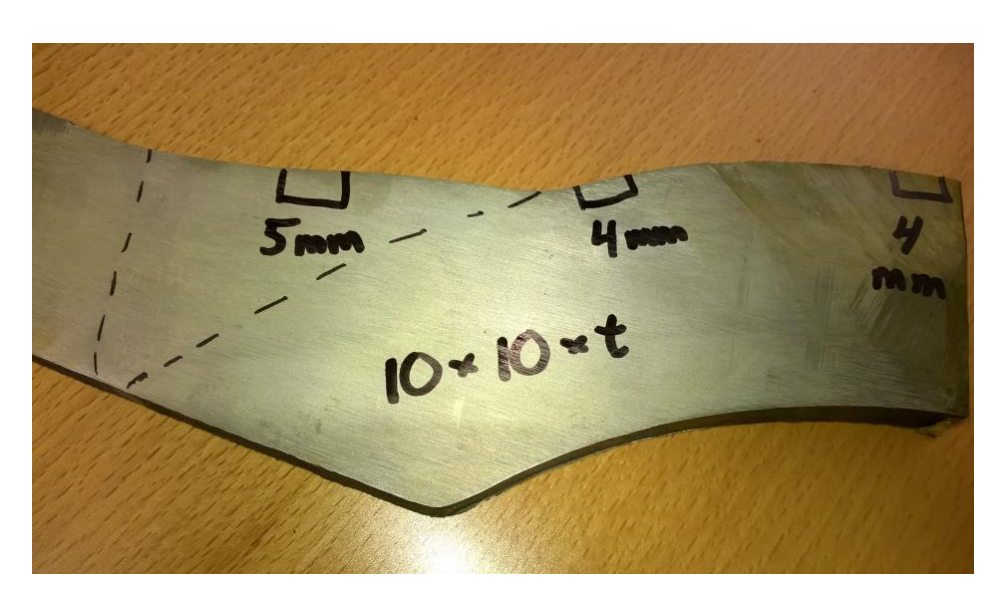


grinding of 0.5 mm between the tests in order to have a grip of the scatter in the minimum creep rate for BM and especially for WM which has a complicated non-uniform microstructure.



Figur 53. T-stycke av 10CrMo9-10 från Heleneholmsverket med krypskador.

Figure 53. 10CrMo9-10 T-piece from Heleneholmsverket with creep damage.



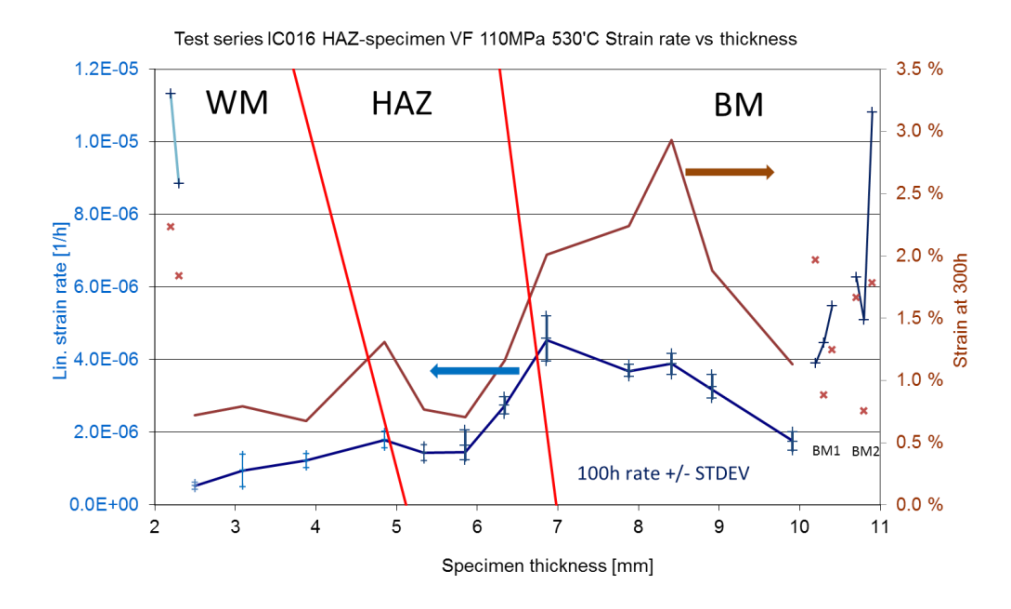
Figur 54. Positioner för intryckskrypprovbitar från T-stycket. Provet från svetsgods (WM) är till vänster, position grundmaterial 1 (BM1) i mitten och grundmaterial 2 (BM2) till höger.

Figure 54. Locations of the impression creep specimens from the T-piece. The WM sample location on the left, the BM1 location in the middle and BM2 on the right.



The impression creep data points from these WM and BM samples are shown in Figure 55. The WM data points have been added to the left hand side of the HAZ sample data set and the BM1 and BM2 data points on the right. It can be seen that the WM creep rate of 1.13*10⁻⁵ is much higher than the WM creep rate of the HAZ sample taken from the new weld. This can be due to either under matching of the T-piece weld or the fact that the T-piece has been service exposed and had already developed a crack in the saddle position. Therefore it is likely that the T-piece WM has suffered some creep damage and this has resulted in much higher creep rate in the impression creep test. Unfortunately only two tests were done for the T-piece WM because the oversize sample was damaged at the end of the second test as a result of a computer crash which resulted in the test machine pushing against the sample at 10 kN force. The specimen had plasticized and the indenter had fully penetrated into the specimen.

It can be seen in Figure 55 that also the T-piece BM strain rates are higher than those of the new weld. This is also due to the same fact that the T-piece has experienced some creep damage. However it is a bit illogical that the creep rate of the BM1 sample increase when going deeper from the outer surface. It was expected that due to maximum creep damage on the outer surface and additional decarburisation the creep rate at the outer surface would have been the highest.

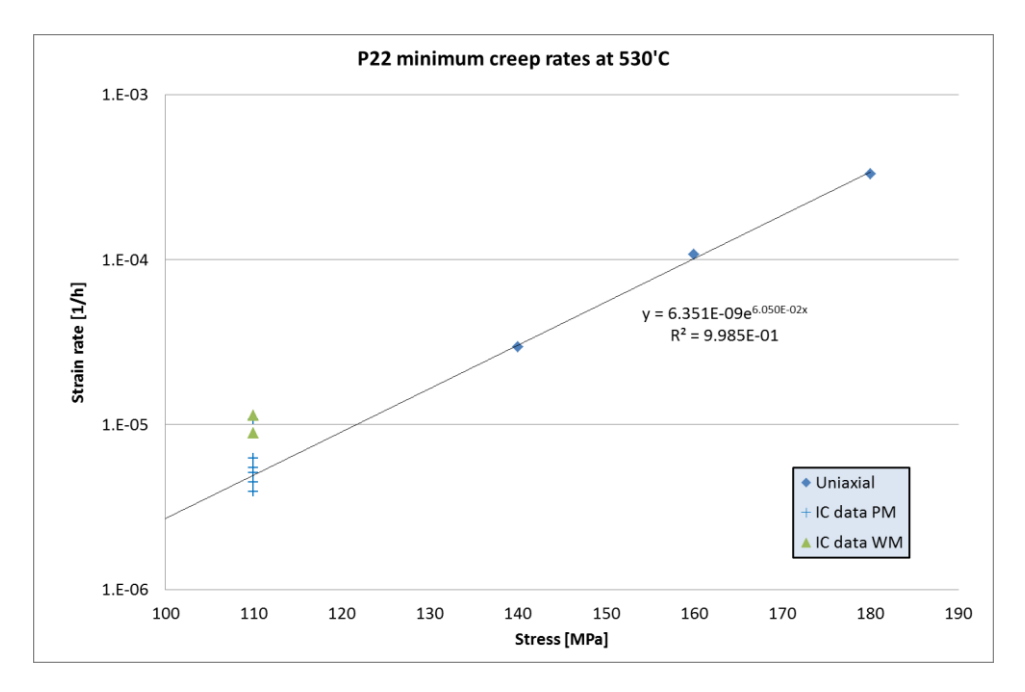


Figur 55. Resultaten från T-styckets svetsgods (WM, till vänster) och grundmaterial (BM, till höger) har adderats till de som finns i figur 50.

Figure 55. The data points on T-piece WM (left) and BM (right) samples added as compared to Figur 50.

The impression creep rates of the BM from the T-piece can finally be compared with strain rates measured in the uniaxial creep test for the new weld. The results are shown in Figure 56. The uniaxial creep tests had been performed at stresses of 140, 160 and 180 MPa and when an exponent function is fitted through those three points, the impression creep strain rates from the T-piece fall nicely on the extrapolated curve. The two impression creep data points measured for the WM from the new weld indicates a much higher creep rate. The impression creep rates for the BM measured from the new weld (the PM/HAZ/WM sample) would roughly overlap the rates from the BM1 and BM2 samples. The total testing of the impression creep tests was 9524h.





Figur 56. Minimum kryptöjningshastigheter hos 10CrMo9-10 uppmätta från den nya svetsen och de motsvarande töjningshastigheterna från svets (WM) och grundmaterial (BM) tagna från T-stycket.

Figure 56. 10CrMo9-10 minimum creep rates measured from the new weld at 530°C and the corresponding strain rates of the impression creep tests for the WM and BM taken from the T-piece.

7.4.4 Conclusions

An innovative way of applying impression creep testing was used by manufacturing a "sandwich" type of specimen of the new weld which allowed the creep rates to be scanned from the base material across the HAZ to the weld metal. The highest creep rate in the inter-critical zone of the new weld was, however, not as high as was expected: only 2.6 times higher than in the base material. However, this is in accordance with results in [20] where impression creep on HAZs was performed with another approach, namely by testing across the HAZ instead of perpendicular to it. The weld metal of the new weld is slightly overmatching as compared to the base material. The measured creep rates from the impression creep tests correlate very well with the minimum creep rates measured in the uniaxial creep tests of the base material of the new weld.

The creep rates measured from the service-exposed T-piece indicate elevated creep rates which are most likely due to the creep damage.



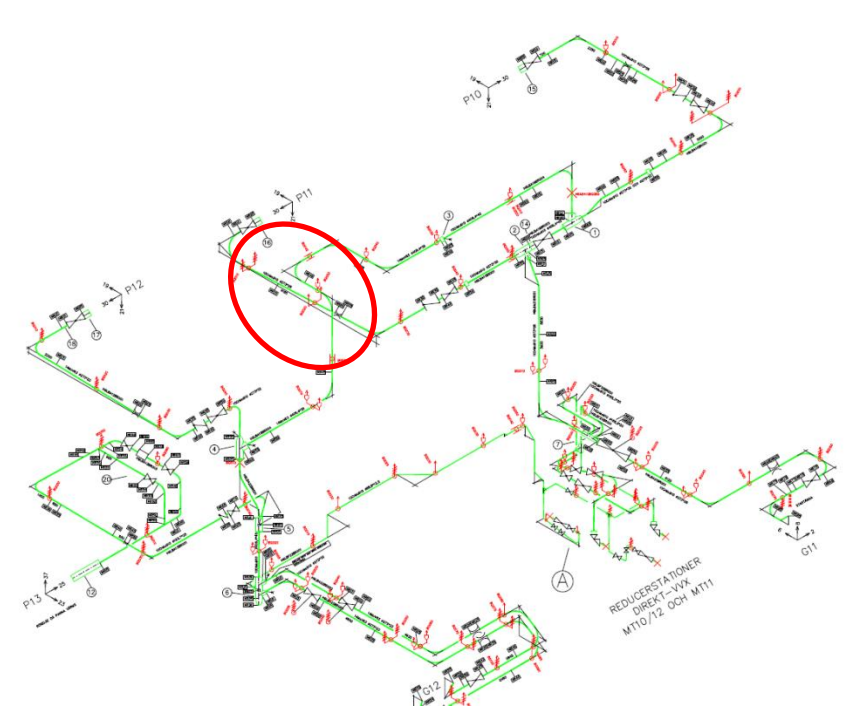
8 Evaluation of remaining lifetime of the main steam pipe system in Heleneholmsverket

8.1 PIPE SYSTEM ANALYSIS

The piping system that was translated with the script has been used for analyses with actual operational data from Heleneholmsverket. In addition, the effects of starts and stops according to the service data were studied. Five different parameter combination of the Norton creep material models have been tested for the piping system and will be evaluated against creep damages in a straight part of the piping shown in the red circle in figure 57, which shows the Caepipe model from PA Ingenjörssupport. Creep damages have been found in welds MR15 and MR20 and are shown in Table 3. The five models have different material parameters according to Norton's law, presented previously, see Eq. 10 below and the representing parameters B and n that vary between the models are shown in Table 9. Model number 1 in Table 9 is evaluated from creep data for 10CrMo9-10 in EN10028-2 and is the first choice for material constants if there is no specific creep data available. The second model is the 20 % lower bound of the average creep strength which is used in model no. 1. The constants in model 3 are given from an evaluation with the LCSP method [18]. Models 4 and 5 are from IC testing of new and service exposed material from Heleneholmsverket, respectively. A graphical presentation of the material models is shown in Figure 58, where all material models are shown with minimum linear strain rate vs. stresses amongst with the results of uniaxial creep of new material in section 4.2.1 and data points for base material BM1 and BM2 for the testing of the T-joint base metal.

$$\frac{d\varepsilon}{dt} = B\sigma^n \tag{10}$$





Figur 57. Caepipemodell av ångnätet hos Heleneholmsverket. Den röda cirkeln markerar positionen för svets MR15 och MR20.

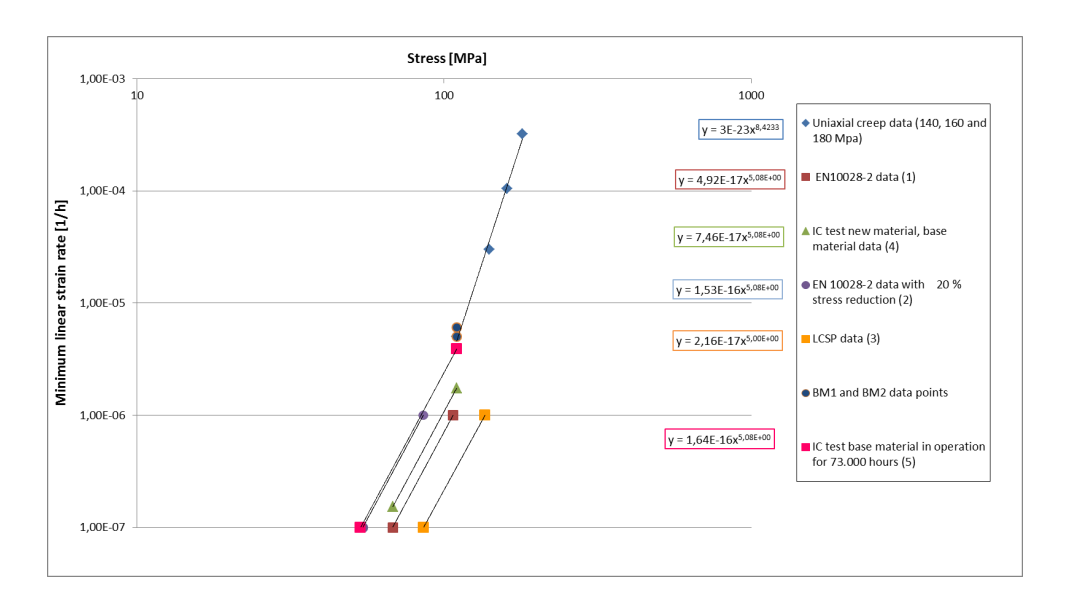
Figure 57. Caepipe model of the Heleneholmsverket steam pipe system. The red circle marks the location of the welds MR15 and MR20.

Tabell 9. Parametrar för Nortons krypmodell som användes vid röranalysen.

Table 9. Parameters for Norton's creep material model used for the piping analysis.

| Model | Description | В | n |
|-------|--|----------|------|
| No. | | | |
| 1 | EN 10028-2 | 4.92E-17 | 5.08 |
| 2 | EN 10028-2 – lower bound, 20 % lower rupture stresses at same creep strain rate. | 1.53E-16 | 5.08 |
| 3 | LCSP data (logistic creep strain prediction [18]. | 2.16E-17 | 5 |
| 4 | IC testing- new unused material, base material data. Modell is assumed to have the same <i>n</i> value as evaluated from EN 10028-2. | 7.46E-17 | 5.08 |
| 5 | IC testing for a base material that has been in operation in Heleneholmsverket for 73 000 hours of operation. | 1.64E-16 | 5.08 |





Figur 58. Spänning som funktion av minimum linjära kryptöjningshastigheter hos grundmaterial för flera Norton materialmodeller (numrerade 1-5) samt för producerade data från enaxlig krypprovning på nytt material och intryckskrypprovning av driftpåkänt material (BM1 och BM2).

Figure 58. Minimum linear creep rates versus stress of parent metal for several Norton material models (numbered 1-5) as well as for produced data of uniaxial creep on new material and of impression creep on service exposed material (BM1 and BM2).

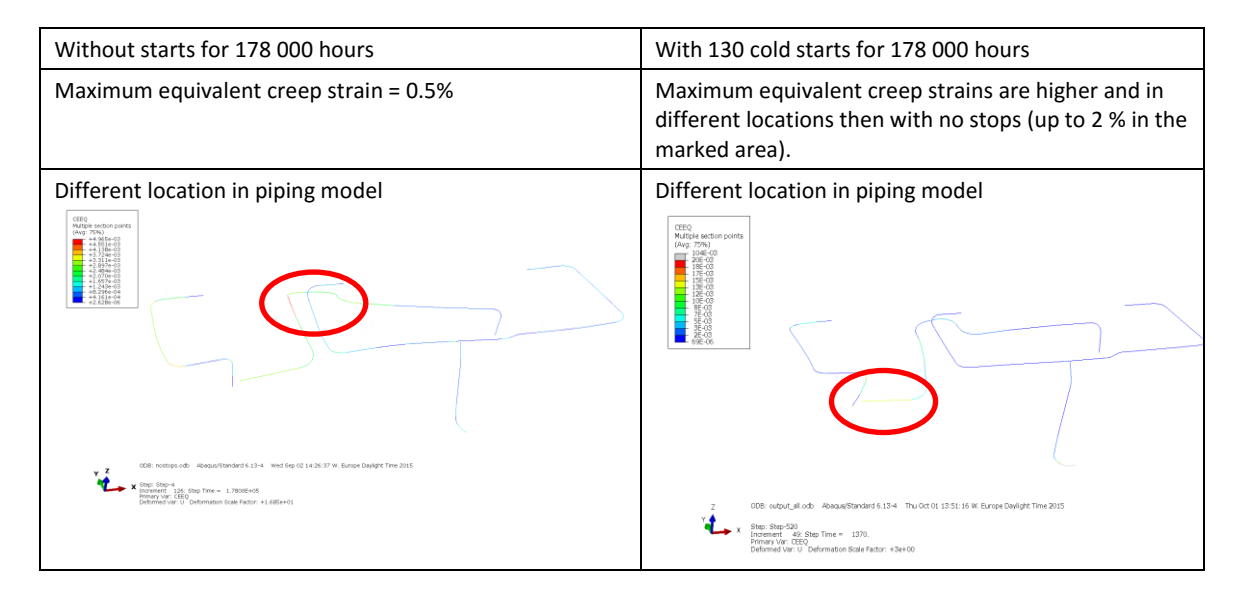
Operational time according to documentation from Heleneholmsverket states that operational time for P11 (Boiler11) of the piping circled red in Figure 57 is 178 000 hours and has undergone 130 cold starts during its lifetime. In the simulation of the starts and stops the average service period between each stop has been assumed, i.e. 1370 hours. This is a simplification since there is a variation in service time from one year to another. The internal pressure is 105 bars and temperature is 530°C at operation conditions. A short test of the effects of starts and stops has been done similar to the one performed in chapter 6.

8.1.1 The effects of start and stops with operational data, material model 1

The influence of starts and stops has been shown previously in this report by showing how the maximum creep deformation changes location in the piping model. The piping system has been stopped 130 times and started again, compared to if the whole lifetime is run for 178 000 hours with respect to creep.

In this example the material model 1 has been used to show the same effect for the operation conditions of the piping system. In Figure 59 it is obvious that the influence of starts and stops has large impact of the creep strain in the model and the location of the creep strain. Therefore, it would be necessary to include the cold starts and stops into the pipe system analysis also in many other cases to get proper results. However, the effect on the bend at the bottom of the system with this number of starts is unrealistically high (grey color at the point where model is cut, indicating up to 10 % creep strain). In this case it is obviously necessary to add the remaining part of the system that continues at this point to the model to dissolve the constraint effects there.





Figur 59. Demonstration av effekterna av starter och stopp där modellen har körts i 178 000 timmar utan stopp på den vänstra sidan medan den på den högra sidan har haft 130 kallstarter under 178 000 timmar.

Figure 59. Demonstration of the effects of starts and stop where on the left hand side the model is run for 178 000 hours without stops, whereas the model on the right hand side has been stoped 130 times during 178 000 hours.

8.1.2 Results of the evaluation of material parameters and comparson with creep damage in the service exposed main steam pipe system in Heleneholmsverket

At the end of operation after 178 000 hours the creep strains in element 5 (MR15) and 6/7(MR20) are compared for the different material models and is shown in Table 10 and 11. The creep damages in the welds MR15 and MR20 are presented in Table 3. In a large part of the welds there were creep damages with index around 2a or 2b. Locally both higher and lower values were, but an average of 2a is estimated for the welds, with MR20 giving slightly higher creep damage on the average than MR15. Creep damage index 2a is estimated to correspond to a creep strain in the range 0.5-1 %.

Tabell 10. Resultat av ekvivalent kryptöjning genom modellen.

Table 10. Equivalent creep strain results from the model.

| Model No. Part in system | 1 | 2 | 3 | 4 | 5 |
|--------------------------|---------|--------|---------|--------|--------|
| Element 5 (MR15) | 0.085 % | 0.26 % | 0.029 % | 0.13 % | 0.27 % |
| Element 6/7 (MR20) | 0.1 % | 0.29 % | 0.042 % | 0.15 % | 0.31 % |

Tabell 11. Samband mellan faktorn B i Nortons kryplag och storleken på ekvivalenta kryptöjningar.

Table 11. Correlation between the factor B in the Norton creep law and the amount of equivalent creep strain.

| B factor in Norton creep law | 2,16E-17 | 4,92E-17 | 7,46E-17 | 1,53E-16 | 1,64E-16 |
|--|----------|----------|----------|----------|----------|
| Model | 3 | 1 | 4 | 2 | 5 |
| Equivalent creep strain from table 10 for MR20 | 0.042 % | 0.1 % | 0.15 % | 0.29 % | 0.31 % |



8.1.3 Discussion and conclusions of pipe system analysis

The influence of the *B* factor in Norton creep law on the equivalent creep strain is obvious in table 11, since the *n* factor is always around 5. When comparing the models to the creep damage in welds MR15 and MR20, the material models 2 and 5 give the highest creep strains, around 0.26 % - 0.31 % creep strain. It is noted that these values do not precisely coincide to the creep damage in the parent metal close to the welds MR15 and MR20, damage rating 2a (see Table 3). The observed creep cavitation would typically correspond to creep strains in the range 0.5-1% [19]. However, the weld is not modelled in Abaqus at these positions and in the literature it can be found that the local strain in parent metal close to the HAZ can be at least twice the remote parent metal and several times higher in the HAZ after longer times. This has been measured with speckle techniques [20]. Usually welds are associated with reduced creep strength and occurrence of welds in areas with high stresses can involve significantly reduced life time. Therefore, it can be considered that if the welds were modeled in these locations the resulting creep strains would correspond very well to creep damages as observed in the welds MR15 and MR20. There were clearly somewhat higher amounts of creep cavitation in the parent metal close to the weld in MR 20 than in MR 15. Thus, the model verifies that the creep strain at the location for MR 20 is slightly higher than for MR15. The IC testing for a service exposed material (model 5) and EN10028-2 minimum data (model 2) gives a very good estimate of the creep strain in the piping when we consider that the calculated strain, 0.3 %, is a least two times higher in the parent metal close to the HAZ (2x0.3=0.6 %) and that the observed creep damage approximately correspond to this creep strain. Other material models do not show as good correlation to the creep damages in the welds MR15 and MR20, and are therefore not considered as good for evaluating creep damages in this piping system. This points out that the impression creep testing has an important role to rank the creep properties of the materials in a system in relation to tabled data.

When comparing the material models with the VTT data in figure 58, it is considered there is a good correlation between the VTT data for uniaxial creep for 140, 160 and 180 MPa tests and the BM1 and BM2 data points and the material model 2 and 5. The creep properties have a tendency to give a knee in the linear strain rate and stress graph. It is considered that here the BM1 and BM2 points are located in this knee where the material parameters change to give another incline on the model for higher stresses than 110 MPa.

8.2 COMPONENT ANALYSIS

To evaluate stress and strain distributions during creep in a component it is not only necessary to model the component with respect to internal pressure. It is also necessary to super impose the effects of system stresses from the pipe system that may occur from the thermal expansion, cold starts and dead weight. The displacements that act on the component will be determined by the pipe system analysis, demonstrated above. The boundaries for the component modeling to allow for correct super position of the stresses from the system are described in section 5.

8.2.1 Model of the chosen T-piece for the sensitivity analysis

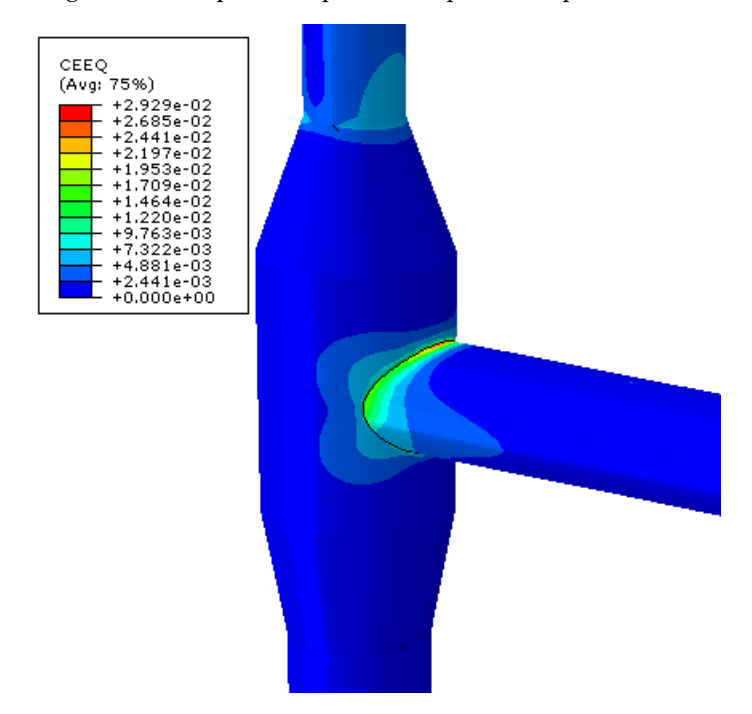
The T-piece that was studied in the sensitivity analysis in section 5, see Figure 21, was modelled by FEM with appropriate extension, se extension 2 in Figure 26. In this case the Abaqus model of the system that was performed by Segle and Algotsson [5] was



used for the determination of the resulting displacements due to system stresses that act on the component. Boundary conditions and loading for the component model consist of displacements on the boundary obtained from the pipe system model in section 6; internal pressure of 130 bar applied to the inner surface of the component models and temperature of 530°C applied on the entire model to get correct displacements due to thermal expansions. The pipe system analysis simulated the system life of 14 years with a stop every year. Because of this the component analysis also needed to take in account the yearly stops. Due to the lengthy calculation times for a full 3D model to simulate creep behavior only the first 6 years were analyzed for the component. Two analyses were performed, one were the load was applied in the same way as for the piping system simulating a shutdown once every year and the other one without simulating the shutdowns.

8.2.2 Results

In Figure 60 the equivalent plastic creep strain is plotted for the T-piece.

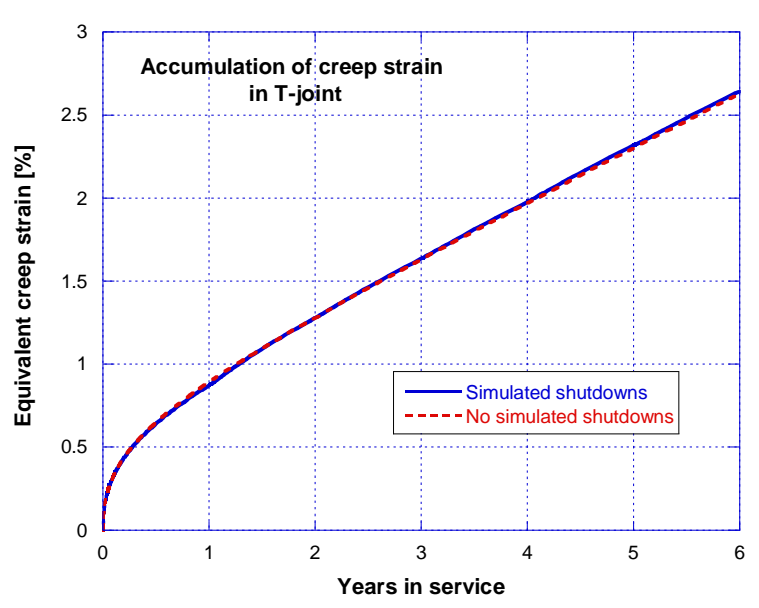


Figur 60. Ekvivalenta plastiska kryptöjningar hos T-stycket efter sex års drift.

Figure 60. Equivalent plastic creep strains for the T-piece after six years of service.

Below, in Figure 61, the equivalent plastic creep strain for the two models, with and without starts/stops is plotted against time. As can be seen there is no effect of starts/stops on strain accumulation in this component.

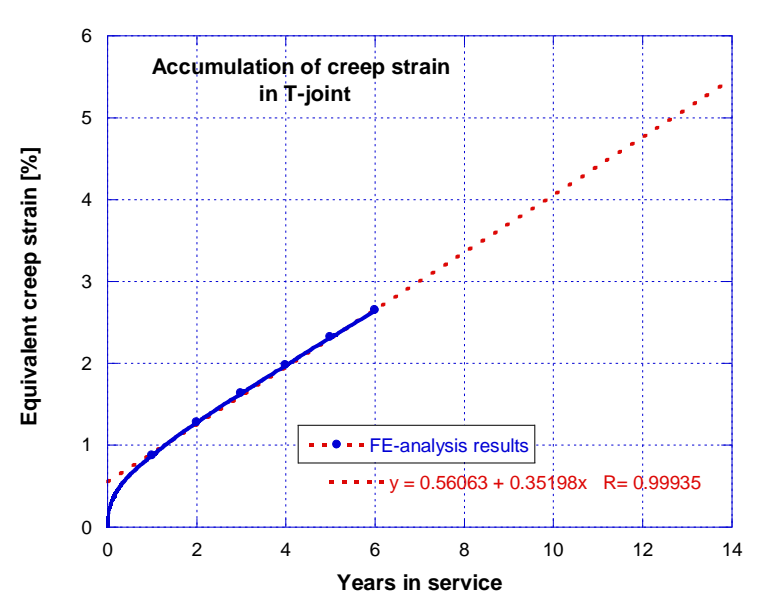




Figur 61. Ackumulerad kryptöjning i T-stycket efter sex år vid kritisk position.

Figure 61. Accumulation of creep strain in T-piece after six years at the critical position.

In Figure 62 the results are shown with a linear fit up to 14 years for the results after the initial year.



Figur 62. Ackumulerad kryptöjning med linjär extrapolation av data efter det första året.

Figure 62. Accumulated creep strain with a linear fit for data points after the first year.

From the results presented in Figure 60 it can be seen that the highest creep strains are not found at the saddle point but rather at the straight angle point. This is due to the thermal strains and dead weight. If the pressure would have been the governing load the highest strains would have been seen at the saddle point. It is also seen that the



weld between the upmost pipe and the cone show some higher creep strains compared to the lowermost pipe connection. The results in Figure 61 show a good correlation between the two performed analyses.

As can be seen from the results in Figure 62, the creep strain increases rapidly the first year. After the first year primary creep has moved into the secondary stage where a linear increase in creep strain can be seen. If this linear trend is valid the accumulated creep strain can be calculated for 14 years without performing a lengthy analysis. It is unknown at which strain the tertiary creep with accelerating strain rate would start but according to long term creep tests of 10CrMo9-10 this may be expected at 3-5 % creep strain [21][21]. The behavior over time for the component is dependent on how the pipe system changes over time. A reanalysis of the system at a certain time of service after the first analysis may result in modified input data to the component analysis and possibly also a deviation from the linear trend.

It should also be mentioned that the creep strain seen in the component analysis is far greater than the creep strains seen in the pipe analysis in section 5. The pipe system analysis performed earlier with Abaqus do not give any results for the T-joints in the pipe system. Therefore it is necessary to look at the T-joints separately with a component model to be able to obtain the entire picture of the system. In the present case over 5 % creep strain was predicted after 14 years (and 105 000 hours of operation) indicating that the creep life is about to be fully consumed after that time. There are no welds modelled in the T-piece. Since the critical strains are in the position where a weld typically is situated it is likely that the predicted creep life would be shorter if a weld was included in the analysis. No recordings of replica test results could be found for this T-piece. It was replaced after 110 000 hours in service.

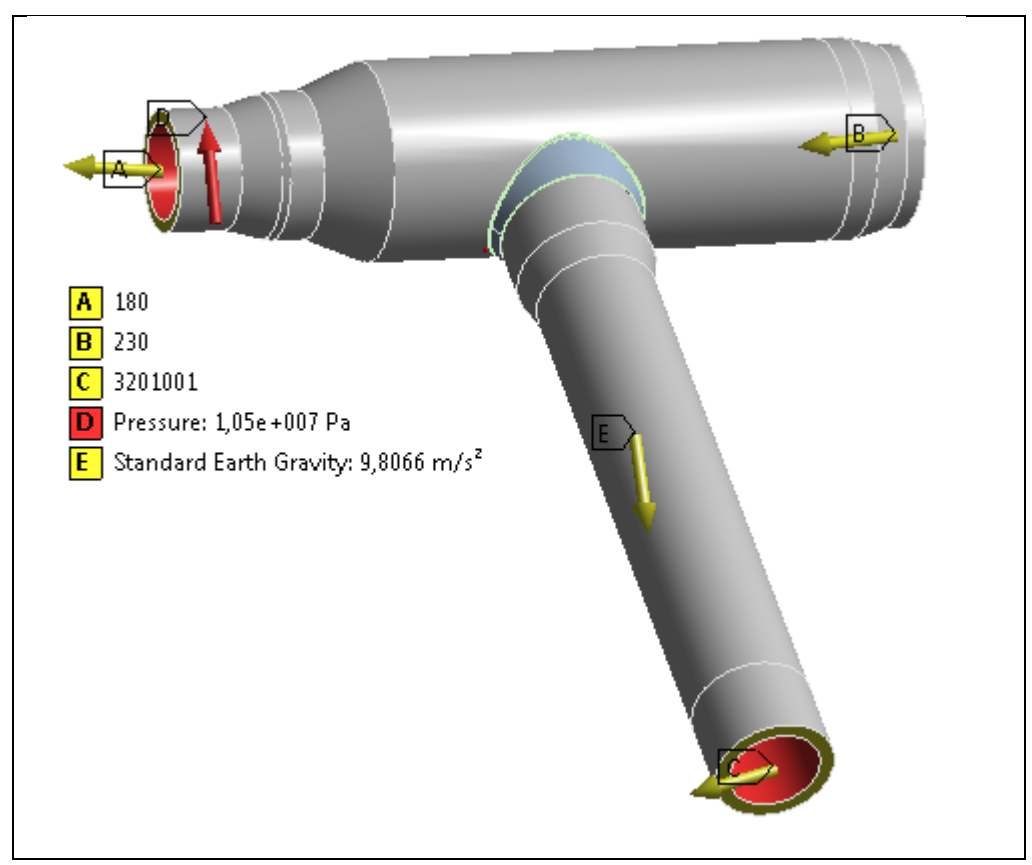
8.2.3 Model of the service exposed T-piece that was investigated in the present study

The T-piece that was cut out for examination and impression creep testing was modelled by FEM. The geometries were taken from the drawing of the T-piece. Also the T-piece branch weld geometry was included in the drawing. The HAZ was measured and modelled to 3.0 mm (Table 4) at the saddle point side of the weld, which is of particular interest since significant creep damage was observed there.

The analysis was first performed with materials data that correspond to tabled creep data. The creep properties in the weld metal and the heat affected zone were in analogy with the present test results of the new material, where the weld metal and the HAZ had approximately 2 and 3 times higher creep rate than the parent metal, respectively. The same factors were then used in relation to the parent metal properties evaluated from tabled creep data.

Since there was a significant effect of starts and stops on strain distributions in the system analysis, starts and stops were evaluated in the same way also for the T-piece, i.e. each start/stop sequence is 1370 hours. Figure 63 shows the model and the loads from internal pressure, dead weight and thermal expansion. The numbers on the right hand side of boxes A, B and C in the legends are the node numbers at these positions.



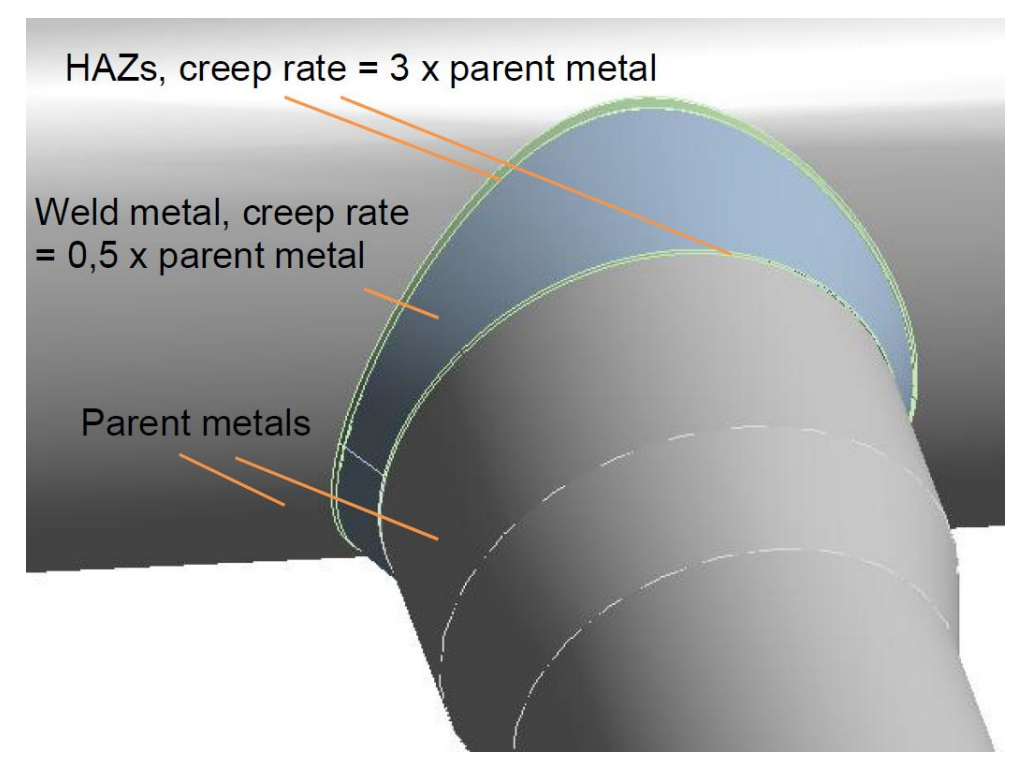


Figur 63. Modell av T-stycket med laster i form av inre övertryck, egenvikt samt förskjutningar pga. termisk expansion vid modellens ändar.

Figure 63. Model of the t-piece with loads of internal pressure, dead weighet and displecements at the boundaries due to thermal expansion.

In Figure 64 the modelled weld is shown in detail. Creep rates in weld metal and HAZ with the factors 0.5 and 3 times the parent metal creep rate, respectively, were used in the analysis. These factors are rounded numbers of the relative creep rates of the impression creep results of the new weld.





Figur 64. Detalj av T-styckemodellen med svetsgods och värmepåverkade zoner. Kryphastigheter i svetsgods och HAZ relativt grundmaterial finns markerade.

Figure 64. Detail of the T-piece model with weld metal and HAZs. The creep rates in the weld metal and the HAZ relative the parent metal is marked.

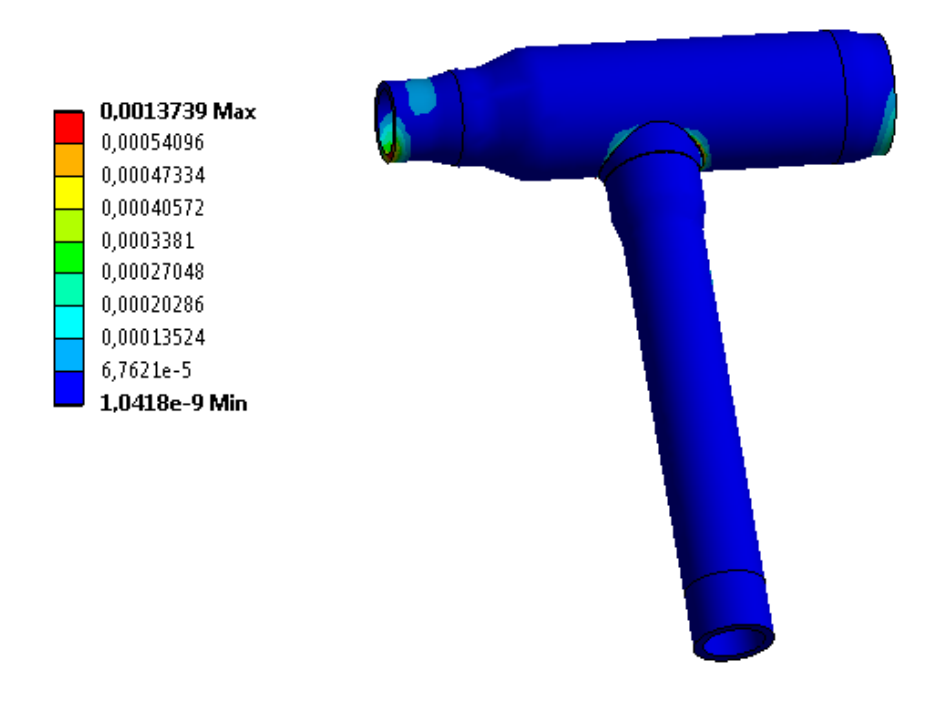
8.2.4 Results of initial service

Figure 65 shows the creep strain distribution in the T-piece after the first 1370 hours in operation of the system (the average service period between two start/stop cycles at Heleneholmsverket). Although the T-joint that was received for creep testing and metallographical examination was the third T-joint at the same place it is interesting to study the first period where the effect of creep relaxation is largest.

The highest strains are present in the branch weld. Figure 66 shows the branch weld in detail and it can be seen that the highest strains are in the HAZs at both sides of the weld. The highest strains (red areas) started at the right angle positions at the T-connection and expanded along the HAZs and at 1370 hours the relatively high strains have spread half way to the saddle point, as can be seen in the figure. The maximum strain is 0.14 % already after 1370 hours. Although the system layout for the first 20 years of the service was not exactly the same as the modelled system, which correspond to the following 20 years, it can be noted that the highest damage in the corresponding component was at the right angel positions as well, see component 32, positions k and l in Figure 1.

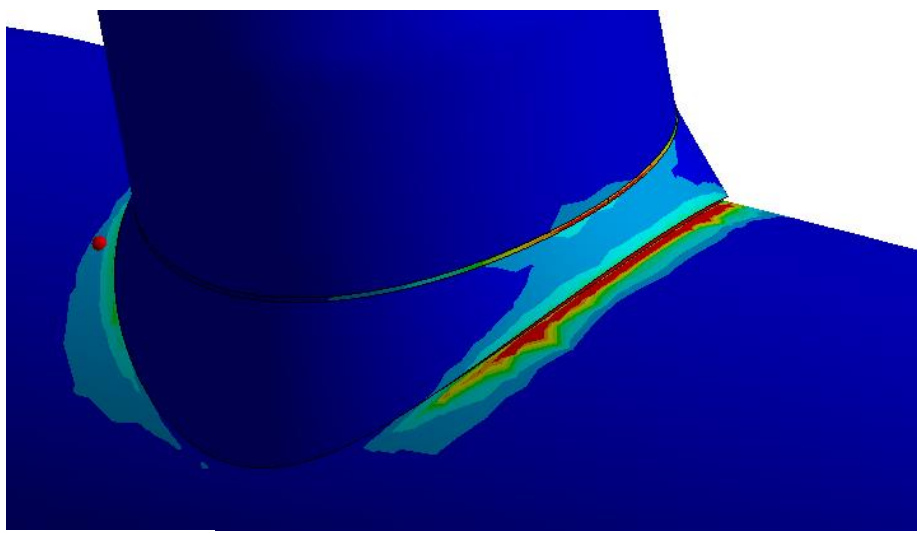


Expression: EPCR1

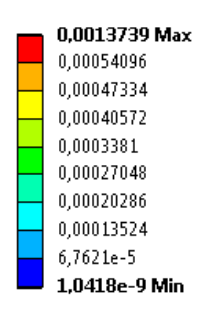


Figur 65. Töjningsfördelning i T-stycket efter 1370 timmar.

Figure 65. Strain distribution in the T-piece after 1370 hours.



Expression: EPCR1



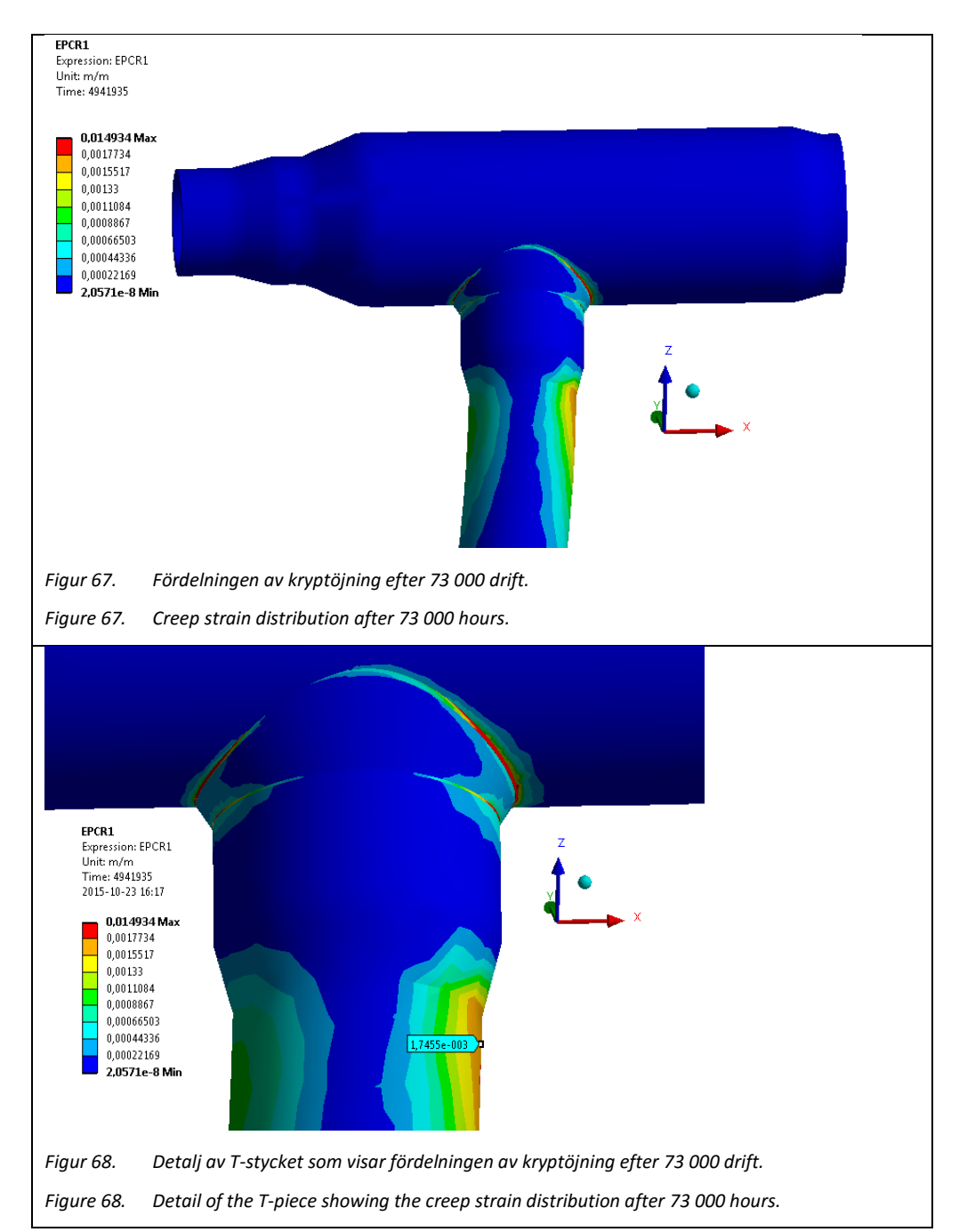
Figur 66. Detalj av T-stycket som visar fördelningen av kryptöjning efter 1370 drift.

Figure 66. Detail of the T-piece showing the creep strain distribution after 1370 hours.

8.2.5 Results of simulation of service that corresponds to the studied T-piece

In this section simulations are performed that covers the actual life of the studied T-piece. This is in 1990 when the system has an accumulated service time of about 105 000 hours. Thus, the analysis starts with actual system stresses at that time and continues for another 73 000 hours when it is taken out from operation. First, two service periods of 1370 hours were simulated to see if there were any effects of starts and stops on the stress- and strain distributions in the T-piece. This was not the case and since such effects would be largest within the first cycles it was concluded that a continuous simulation for 73 000 hours should give an equal result as a simulation with 53 stops, which would have been enormously time consuming. Figure 67 shows the results and a close-up of the results at the modelled weld can be seen in Figure 68.





It can be seen that there is a bending force on the vertical pipes that results in enhanced strains on the right hand side of the weld and in an area close to the increase of thickness of T-piece at the same side. The more diffuse colors at the opposite side indicate strains in compression. The level of the strains is up to 1.5 % in the HAZ to the horizontal pipe and 0.18 % in the area close to the T-piece wall thickness increase.

A comparison between the simulated strain distribution and the observed creep damage distribution in the T-piece shows that damage rating 2b with up to 2 000 creep cavities/mm² appears in the area with highest strain concentration. However, in the saddle point areas the correlation is not that good. The simulated creep strain level is significantly lower than that that should correspond to the observed creep damage (damage rating 3b and up to 3 000 creep cavities/mm²).



9 Result analysis

9.1 IMPRESSION CREEP

The impression creep test results of different parts of the HAZ show relatively small differences in creep rates compared to parent metal. Results with significantly higher HAZ/parent metal creep rate ratio can be found in the literature [22] where HAZ/parent metal creep rates ratios of 10 and higher is reported. These results are based on tests of heat treated material. However, it is impossible to heat treat material in quantities enough for uniaxial creep testing in the same way as the thermal cycle of a HAZ. Although the heat treated materials may have about the same grain sizes and hardnesses as different HAZ microstructures the creep properties necessarily are not similar. The present results show that there is a significant difference between simulated HAZs by heat treatment and the ones.

The impression creep test results are overall consistent except one result of the service exposed parent metal at the test position BM2 where one data point that has about two times higher creep rate than the other five tests of the same material. Unfortunately, it has not been possible to find an explanation to this deviation.

Finite element analysis of impression creep tests by use of the LCSP method gave similar creep curve shapes but much lower creep rates than experimental results. The magnitude of the strain and strain rate reduction is similar to the system analysis when experimental data and Norton data evaluated from the LSCP method are compared, see Table 9-11. Since the LCSP method has been shown to work very well for 10CrMo9-10 material elsewhere [2][18], further analyses are required to sort this out.

9.2 SYSTEM ANALYSIS

Elastic pipe analyses are frequently used for steam piping operating in the creep range to check that the stress levels due to thermal expansion are not higher than allowable. The results are often also used to indicate critical positions in the system for non-destructive testing such as magnetic particle testing (MT) and replica testing. Present work pinpoints that:

- It is necessary to consider creep relaxations in the system with respect to allowable stresses.
- It is necessary to consider effect of starts and stops on the distribution of accumulated creep strain after long term operation.

Thus, elastic analysis on systems that operate in the creep range may overestimate the actual stresses as soon they have creep relaxed. It is also evident that the results of elastic analysis not always can indicate all critical positions for non-destructive testing.

Although the present analyses have been performed with very well documented background data the system has been reconstructed a few times before the present model of the system. Thus, the effects of thermal expansion for the first 90 000 hours of operation are different to what is shown in the model. However, it is considered that strains in the part of the pipe that include welds MR15 and MR20 should not have been affected by thermal expansions from previously reconstructed parts of the system.



The results of the analyses with different creep data in Table 10 show that lower bound data, i.e. 20 % creep strength reduction, gives about three times higher creep strains than average data (EN 10028-2) at the analysed positions. The analysis with creep data from the new material gives somewhat higher creep strains than average data whereas the corresponding analysis with data from the service exposed material gives slightly lower creep strains than the lower bound data. Thus, it is clear that use of standard average data may overestimate the real creep behavior and that lower bound data can be considered as conservative enough.

The use of different data in the analyses is also a sensitivity analysis of the model. The 20 % strength reduction and the corresponding 3 times higher creep strain can be compared to creep data in EN13704:2008 [23][23][23] which is represented as Larson-Miller parameter (i.e. a commonly used time-temperature parameter for) versus stress. The results is a life time reduction with a factor of 3.2 for the 20 % strength reduction at service data, 105 bar and 530°C. Thus, the agreement with the present results is very good.

The bend at the lower right hand side in figure 59 shows 10 % strain which likely is higher than in reality. This strain appears at the very end of the model. The model was simplified to be able to be verified with [5]. I reality, as can be seen in Figure 8, the system continues and there is less constraint. This shows that it is necessary to model the entire system to ensure that the results are fully accurate.

9.3 COMPONENT ANALYSIS

Simulations have been performed on T-pieces without and with a weld. Since the HAZ is associated with lower creep strength than the parent metal it is not surprising that creep strains preferably accumulate in these zones. The results show that:

- HAZs are particularly sensitive to creep strain accumulation in case of system stresses. Thus, it is a great advantage to include critical welds in a component model. However, since superimposing system stresses require modelling of the entire component such analyses can be quite time consuming.
- Areas where stress concentrations occur because of the geometrical shape of the Tpiece are also sensitive to system stresses. Such areas often coincide with the
 location of welds, resulting in significant life time reductions.

The simulation of service life of the T-piece in section 8.2.5 resulted in strain distributions that did not fully conform with the observed distribution of creep cavitation. A possible explanation for this is that there is an extension of the real system that was not modelled, see above. Instead there is a fix point at the stop of the model which affects the boundary conditions and, unfortunately also seems to affect the displacements at the vertical pipe into the T-piece. Again, modelling of the entire system is crucial also for a component creep life assessment when system stresses are considered.



10 Discussion

Creep data from standards are based on long term testing. Conventional creep testing that is performed on material from power plant components to assess the condition typically involves rather relatively short testing times. It may be possible to compare such results roughly with each other by use of the Larson-Miller Parameter but it is likely that the specific test data is performed at so much higher stresses than those at service that the deformation mechanisms are not the same.

Instead, iso-stress creep testing at a representative stress is frequently used. The testing is performed at a series of temperatures that are higher than the service temperature. The results are then extrapolated the service temperature and a remaining lifetime is obtained. The disadvantage is that constitutive equations, such as the Norton creep law, cannot be used with this method and the results can therefore not be used for creep analysis.

Impression creep testing allows significant lower stresses and the present results indicate that they can be fully comparable with standard data. Thus, such data is very useful for creep analyses of pipe systems as well as for components where even welds can be included in the models.

The idea of creep testing of service exposed material can be discussed. First, the results are a measure of the future creep behavior. Thus, semi-destructive creep testing methods, such as impression creep testing, can be used for determination of remaining life. However, creep testing of service exposed material typically results in higher reductions of creep life at higher stresses than at lower. Thus, extrapolations will give the longest creep lives for the service exposed material at service stresses since the stress rupture versus time or stress versus linear creep rate curves will cross each other. In the present project tests on service exposed material was performed at only one stress level. Then, the same slope of the curve as for the new material was anticipated. This is, paradoxically enough, likely a better approach than linear extrapolation of test results at enhanced stresses, in cases where more than one test result exist.

It is has been demonstrated that it is possible to model a T-piece in a pipe system including its welds and simulate the development of the creep strain distribution over time. System stresses according to a pipe system analysis are superimposed as well and the creep properties of the weld metal and the HAZ are implemented by use of the results of the impression creep testing. This is a novel and an innovative approach. Only a few and less advanced studies in this area can be found in the literature. One example is [24], where creep simulations were performed on a straight pipe with a weld under the loading conditions internal pressure with and without an extra axial load. Simulations with this approach have been performed in previous Värmeforsk projects as well, e.g. [25].



11 Conclusions

The following conclusions can be drawn from the present study:

- Significant creep cavitation was observed in two butt welds and in a T-piece from the main steam pipe from a power plant that had been in operation for 170 000 hours and 73 000 hours, respectively. The damage in the T-piece can be considered as pre-mature.
- Impression creep testing was performed with a new approach on welds of new and service exposed material from the power plant. The HAZ was scanned by testing each 0.5 mm from the parent metal, through the HAZ and into the weld metal. The maximum creep rate in the HAZ was in the intercritical part and was 2.6 times higher than in the parent metal.
- Impression creep testing of parent and weld metals with 73 000 hours service exposure showed 3 and 6 times higher creep rates, respectively, than for corresponding materials in a virgin weld.
- The impression creep test results of virgin parent metal showed very good correlation with uniaxial creep testing of the same material.
- The behavior of the impression creep test was analysed by FEM and strain
 distributions were calculated. The displacement versus time behavior was also
 analysed, but when this curve was transferred into equivalent uniaxial strain and
 finally to strain rate, the comparison against the experimental data was not very
 convincing. This requires further study.
- Creep analysis of a main steam pipe system showed that significant stress relaxation occurs after a relatively short service period. These effects cannot be covered by an elastic analysis, such as a Caepipe analysis.
- Creep analyses of a main steam pipe system including starts and stops resulted in
 higher levels of creep strain than without the starts and stops. In addition, the
 positions where the highest strains occurred were not the same. Thus, it is shown
 that a creep analysis that includes the effects of starts and stops can be needed to
 show actual creep strains as well as critical positions for non-destructive testing.
 Identification of critical positions with critical positions by elastic pipe system
 analysis, which is quite common today, should therefore be carried out with
 caution
- Creep analysis of the main steam piping was carried out with creep data from standards and from the impression creep test results. Creep test results of new material and standard data gives similar creep strains in the system, approximately 0.1 % after 178 000 hours. The same analysis but with use of creep tests results of service exposed material and with lower bound standard data resulted in 0.3 % creep strain.
- A component model of a T-piece where system stress can be superimposed to internal pressure was developed successfully.
- A branch weld was then included in the model of the T-piece. The relative
 differences of creep rates between parent metal, HAZ and weld metal that was
 obtained by the impression creep testing was used in the model for simulations of
 service exposure.
- A quite good agreement between simulated creep strain distribution after 73 000
 hours in service and observed creep damage in the real T-piece after the same time
 in service.



12 Recommendations

- Elastic stress analyses of pipe systems that operate in the creep range should be supplemented by a creep analysis for determination of critical positions for nondestructive testing as well as for assessments of creep exhaustion.
- The entire steam pipe system should be modelled to ensure a correct creep analysis. Starts and stops should be included in the analysis as well.
- System and component analyses based on tabled creep data should include both
 average and lower bound data (20 % stress reduction of average creep strength) for
 comparison. Lower bound data is preferable for lifetime assessments since average
 data may be non-conservative.
- Lower bound data may, according to general experience, be too conservative. More realistic data for the creep analysis can then be obtained by impression creep testing.
- In creep analyses of components such as T-pieces welds should preferably be included in the model. Adequate creep rate for the HAZ would be 3 times the one used for parent metal. The weld metal may have both higher and lower creep rates than, as well as quite equal to, the parent metal. If impression creep is not an option, hardness measurements may give some indications of the relative creep rates. Otherwise, simulations with both 2 times higher and lower creep rates than parent metal could be evaluated.
- Creep analyses of high temperature pipe systems should be seen as a complement
 to non-destructive testing such as magnetic particle testing, ultrasonic testing and
 replica testing. Verification of the analysis by replica test results would qualify for
 life time assessments.



13 Proposals for future research

By use of the developed script for translation of an elastic model in Caepipe to Abaqus in the present project creep analysis of pipe systems is now an option in effect. In the creep modelling the Norton creep law was used. This has great advantages from an engineering point of view because it is very well established and enables analysis of complex geometries including welds. Introduction of more advanced creep models that considers the entire creep curve would be the next step for a more precise analysis. At least in the later parts of the lifetime of welded components this can be expected to better describe the real behavior since stress redistributions occur when the weakest part of the weld enters tertiary creep with accelerated creep rates [26][26].

Creep analyses with different creep data such as tabled and impression creep test data gave significant differences in creep exhaustion. Since a steam pipe system likely contains components from a number of batches it would be interesting to study the effects of somewhat different creep properties in different sections of the pipe system in the analysis. Such results would further increase the knowledge on strategies for representative sampling from a pipe system for impression creep tests.

It can also be proposed to develop of a method for direct creep analysis of the remaining creep lifetime of steam pipe components in service by use of miniature creep test results on service exposed material.

More studies of HAZs and weld metals as well as parent metals, new and service exposed, by miniature creep tests such as impression creep and small punch testing is needed. A data base of such results would be very useful. Systematic analyses with different sets of creep data is also needed to increase the knowledge of the possible variation of the creep behavior.



14 References

- [1] Vilhelmsen T et. al.; "Utveckling av krypskador hos svetsade komponenter av P91 och X20", Värmeforskrapport 1197, Stockholm mars 2011.
- [2] Holmström S; "Engineering tools for robust creep modeling", VTT 728, Espoo, 2010.
- [3] Payten W; Large scale multi-zone creep finite element modelling of a main steam line branch intersection. International Journal of Pressure Vessels and Piping 83, 2006
- [4] Yee R K, Cohn M; "Creep relaxation behavior of high energy Piping", Journal of Pressure Vessel Technology, Vol. 122, November 2000.
- [5] Segle P, Algotsson P, Samuelsson Å; "Inverkan på ingrepp i ångledningssystem på dess återstående livslängd", Värmeforskrapport 672, Augusti 1999.
- [6] Cohn M, "Main steam pipe girth weldment stresses and life consumption considering malfunctioning supports. Journal of Pressure Vessel Technology", Vol. 132, October 2010.
- [7] Hahn B et. Al.; "In-service Condition Monitoring of piping systems in power plant requirements and advanced techniques", OMMI, Vol. 1, Issue 1, April 2002.
- [8] Storesund J, Rönnholm, M; Utvärdering av krypskadeutveckling genom replikmetoden, Värmeforskrapport 779M9-844, Stockholm, maj, 2002.
- [9] Nordtest Method NT NDT 010, NORDTEST, Esbo Maj 1991.
- [10] Auerkari P, Borggreen K, Salonen J; Guidelines for evaluating in-service creep damage, Nordtest report NT TR 302, VTT Manufacturing Technology, Esbo Augusti 1995.
- [11] EN10028-2:2009.
- [12] ABAQUS, version 6.10 6.13. Simulia.
- [13] Chu S N G and Li J C M; Impression creep; a new creep test, 12, s.l.: JOURNAL OF MATERIALS SCIENCE, 1977. pp. 2200-2208.
- [14] Sastry DH; Impression creep technique-An overview. 2005, Materials Science and Engineering A409, pp. 67-75.
- [15] Hyde T H, Sun W, Brett S; Recommendations on the standardisation of impressions creep testing, Conference, Creep and Fracture in High Temperature Components; 2009; Zurich, Switzerland, pp 1079-1087.
- [16] Brett S; Small Scale Sampling and Impression Creep Testing of Aged 1/2 CrMoV Steam Pipework Systems, Conference, Creep and Fracture in High Temperature Components; 2009; Zurich, Switzerland, pp 1088-1096.
- [17] Wang S H, Impression creep behaviour in weldments, J. Marine Sci. and Tech, Vol 2, No 1, pp 17-24, 1994.
- [18] Holmström S, Auerkari P; Robust prediction of full creep curves from minimal data and time to rupture model, Energy materials, Materials Science & Engineering for Energy Systems Vol. 1 (2006), 4, pp 249-255.
- [19] Bollerup J, Hertzman S, Ludvigsen P B, Sandström R, von Walden E; Cavitation in new and service exosed 1Cr-0,5Mo steel, High Temperature Technology Vol. 4 No 1 February 1986.



- [20] Van Vulpen R; Creep Monitoring of Repair Welds in High Temperature Components, OMMI (Vol. 2, Issue 2) Aug. 2003.
- [21] Wu R, Storesund J, Steingrimsdottir K; Long term and pilot study of HAZ creep behavior and simulation of weld repaired low alloy heat resistant steels, Värmeforsk report 1204, Stockholm, January 2012.
- [22] Middleton, C. J and Metcalfe, E.; A rewiev of laboratory Type IV cracking data in high chromium ferritic steels, Paper C386/027, Published in IMechE Proceedings, London, 1990.
- [23] EN13704:2008
- [24] Vakili-Tahami F, Hayhurst D R, Wong M T; High-temperature creep rupture of low alloy ferritic steel butt-welded pipes subjected to combined internal pressure and end loadings, Phil. Trans. R. Soc. A (2005) 363, 2629–2661.
- [25] Storesund J, Borggreen K, Zang W, Nilsson H, Samuelson Å; Krypskador i svetsar av X20CrMoV12-1 stål, Etapp 2 Studier av långtidspåverkat material och skadedatabas samt beräkning av skadefördelning och skadetålighet, Värmeforskrapport 874, Stockholm, september 2004.
- [26] Storesund J, Andersson P, Samuelsson L Å, Segle P; prediction of creep cracks in low alloy steel pipe welds by use of the continuum damage mechanics approach. Ageing of materials and methods for the assessment of life times of engineering plant, Penny (ed.), Balkema, Rotterdam, (1997), pp. 129-144.



Appendices

A Script for automatic translation of a Caepipe model to a Abaqus model for creep analysis

```
TRANSLATION SCRIPT.m
                                                                                                                                                                                                                                                    2015-09-01
TRANSLATION_SCRIPT.m
                                                                                                                           one page = strfind(GEO,'---');
end_page = [find(~cellfun('isempty',one_page))];
%----- TRANSLATION FROM CAEPIPE TO ABAQUS
                                                                                                                           last_page_start=Coor_nr(end)+4;
last_page_end=end_page(end)-1;
% TO RUN HAVE TWO .txt FILES FROM CAEPIPE. FIRST ONE ONLY COORDINATES IS INSERTED FOR "ins", THE SECOND % ONE IS "E-open" IN LINE 98.
                                                                                                                           %If there is only one page of coordinates, this loops is used
% INSERT TXT FILE IN "ins" that contains only the coordinates of the input
file in CAEPIPE
Withe txt file contains all the information about the coordinates of the
                                                                                                                           if How_many_pages==0
    begin=Coor_nr(1,1)+4;
    ends=end_page(end)-1;
    for i=begin:ends
    GEO_ny = [GEO_ny; GEO{i,1}(1,:)];
    ord
The in Caprice

With cat file contains all the information about the coordinates of the piping in CAPPIPE
lines=size(GEO_ny);
lg=lines(1,1);
%
Whis loop reads in the coordinates
ins = fopen('coor_segle.txt','s');
if ins =--1, error ('cannot open file'), end
GEOtxt = textscan(ins,'%s','delimiter', '\n', 'whitespace', '');
GEO - GEOtxt(1);
fclose(ins);
                                                                                                                           for i=1:1g $\tt GEO\_separate\_strings(i,1:4)=strsplit(strtrim(GEO\_ny(i,:)),' ',1); end
%Generate nodes from the keypoints in Caepipe
Coor = strfind(GEO,'Coordinates');
%Cell array that saves the positions of the Coordinates in the file
Coor_nr = [find(-cellfun('isempty',Coor))];
                                                                                                                           %Find all the nodes that the bends start at and end, and add the number 1001 and 1002 to the node number \$\$----
                                                                                                                           **If the node numbers are larger than allowed in ABAQUS, change '1001'/'1002' to something else
Caepipe_jump_out = strfind(GEO,'Caepipe');
jump_out_lines = [find(~cellfun('isempty',Caepipe_jump_out))];
%A matrix that has the starting number too read coordinates in first column %and end number in the second column Block_all=[];
How many pages=(length(jump_out_lines)-1);
for i=1:How_many_pages
Block=[Coor_nr(i,1)+4,(jump_out_lines(i+1,1)-1)];
Block_all=[Block_all;Block];
end
                                                                                                                           modGEO_A=strrep(GEO_separate_strings,'A','1001');
modGEO=strrep(modGEO_A,'B','1002');
                                                                                                                            %-----Line up nodes in the order that Caepipe sets
k=1; GEO_ny=[];
for i=1:How many_pages
    st=Block_all(i,1); en=Block_all(i,2);
                                                                                                                           **This text sets the node order, that is from which node to another node the piping is set up.
          for j=st:en
    GEO_ny = [GEO_ny ; GEO{j,1}(1,:)];
    k=k+1;
% Find the dotted lines in the code that represents the page ends and the end of the code in this case
                                                                                                                           E_open = fopen('all_segle.txt','r');
if E_open ==-1, error ('Cannot open file'), end
EL = textscan(E_open,'%s','delimiter', '\n', 'whitespace', '');
ele_read = EL(1);
fclose(E_open);
                                                                                                                           %Find the lines that begins a pipeline, that is starts with FROM from = strfind(ele read, 'From'); from find = [find(-cellfun('isempty',from))]; start_layout=from_find(1,1);
```

```
TRANSLATION_SCRIPT.m
                                                                                                                                                                                                                                                                                                                                                                                                                                                         2015-09-01
   TRANSLATION SCRIPT.m
                                                                                                                                                                                                                                                       for i=1:length(elem)
    if (isempty(elem(i,2))==0)
        no_empty=[no_empty; elem(i,:)];
    end
   %Can be adjusted in the txt file
to = strfind(ele read, 'Anchors');
to find = [find("cellfun('isempty',to))];
end_layout=to_find(1,1)-2;
                                                                                                                                                                                                                                                       % Take away all comments that are written in the code
% The second column in "elem" is the start of the node number. If there is
a "alpha" betic letter there
% then the code will not include it in the elements.
   end
                                                                                                                                                                                                                                                       inbetween = strfind(read,'Caepipe');
inbetween_find = [find(~cellfun('isempty',inbetween))];
   end_inbtw = strfind(read,'#');
end_inbtw_find = [find(~cellfun('isempty',end_inbtw))];
  if isempty(inbetween_find)==1
%If the code is only one page, this loop will only read the first page
ALL=read;
    else
    %First page
    read l=cell();
    for j=1:inbetween_find(1,1)=1
        read_1 = [read_1 ; read{j,1}];%(1,:)];
    end
                                                                                                                                                                                                                                                                              end
                                                                                                                                                                                                                                                       end
                         end
                          BENDS-----
                                                                                                                                                                                                                                                       %Find bends in the code
st_bend = strfind(loc_nod(:,3),'Bend');
st_bend_find = [find(~cellfun('isempty',st_bend))];
                           %ALL nodes set up in the correct order
ALL=[read_1; read_2; read_3];
   end
                                                                                                                                                                                                                                                       %Eliminate the multiple bends in the loc_nod matrix
matr=cell();
for i=1:length(st_bend)-1;
   %Divide the nodes into separate strings/cell
div=size(ALL);
length ALL-div(1,1);
ALL separate_strings=cell();
a hII=[1.
if (isempty(st_bend(i,1))==0) && (isempty(st_bend(i+1,1))==0)
                                                                                                                                                                                                                                                                             relation for the matrix of the
                                                                                                                                                                                                                                                                                                  matr=[matr; loc_nod{i,:}];
                                                                                                                                                                                                                                                        end
matr=[matr; loc_nod{end,:)];
                                                                                                                                                                                                                                                       straight_b=cell();
double_b=cell();
trippel_b=cell();
```

```
TRANSLATION SCRIPT.m
                                                                                                                                                                                                                                                                           2015-09-01
                                                                                                                                                                                                                                                                                                                       TRANSLATION_SCRIPT.m
                                                                                                                                                                                                                                                                                                                                                                                                                                                                                                                                                                                            2015-09-01
                                                                                                                                                                                                                                                                                                                                                        st_bend_find(i+1,1)==1)
four b=[four b; loc_nod{(b_nod-2),2} st_b_nod1];
four b=[four b; e b_nod1 st_b_nod2];
four b=[four b; e_b_nod2 st_b_nod3];
four b=[four b; e_b_nod3 st_b_nod4];
four b=[four b; e_b_nod4 loc_nod((b_nod+3),2)];
four_b=cell();
first_b=st_bend_find(1,1);
% For a single bend this code applies
single_bend=strfind(matr(:,3),'Bend');
single_bend_find=[find(~cellfun('isempty',single_bend))];
for i= 1:length(single_bend_find)-1
    b_nod=single_bend_find(i,1);
    st_b_nodl=strjoin({matr{b_nod,2},'1001'},'');
    e_b_nodl=strjoin({matr{b_nod,2},'1002'},'');
    st_b_nod2=strjoin({matr{b_nod+1,2},'1001'},'');
    e_b_nod2=strjoin({matr{b_nod+1,2},'1001'},'');
                                                                                                                                                                                                                                                                                                                                                        %end
                                                                                                                                                                                                                                                                                                                                                        straight_b=[straight_b; matr{(b_nod-1),2} st_b_nod1];
straight_b=[straight_b; e_b_nod1 matr{(b_nod+1),2}];
end
%Last bend added to cell straight_b
last_b=single_bend_find(end,l);
st_last_b nod=strjoin((matr(last_b,2),'1001'),'');
end_last_b_nod=strjoin((matr(last_b,2),'1002'),'');
                                                                                                                                                                                                                                                                                                                         %If there is a trippel bend in the end of the code
last_trippel=st_bend_find(end,1);
st_last_trippel1=strjoin({loc_nod(last_trippel-2,2),'1001'),'');
end_last_trippel1=strjoin({loc_nod(last_trippel-2,2),'1002'),'');
st_last_trippel2=strjoin({loc_nod(last_trippel-1,2),'1001'),'');
end_last_trippel2=strjoin({loc_nod(last_trippel-1,2),'1001'),'');
end_last_trippel3=strjoin({loc_nod(last_trippel,2),'1001'),'');
end_last_trippel3=strjoin({loc_nod(last_trippel,2),'1002'),'');
straight_b=[straight_b; matr(last_b-1,2) st_last_b_nod]; straight_b=[straight_b; end_last_b_nod_matr[(last_b+1),2)];
%This code applies for the double and trippel bends, that is when two or
three bends are written
%one after another in the caepipe code
                                                                                                                                                                                                                                                                                                                          if there is a double bend in the beginning of the code
f st_bend_find(2,1)-st_bend_find(1,1)=-1
    first_bnod=st_bend_find(1,1);
    st_first_double1-strjoin({loc_nod{first_bnod,2},'1001'},'');
    end_first_double1-strjoin({loc_nod{first_bnod,2},'1002'},'');
    st_first_double2-strjoin({loc_nod{first_bnod+1,2},'1001'},'');
    end_first_double2-strjoin({loc_nod{first_bnod+1,2},'1001'},'')
                                 double_b=[double_b; loc_nod{first_bnod-1,2} st_first_double1];
double_b=[double_b; end_first_double1 st_first_double2];
double_b=[double_b; end_first_double2 loc_nod{first_bnod+2,2}];
                                                                                                                                                                                                                                                                                                                          %------Divide the bends in four parts-------
end
% if there are three bends besides each other then go into this loop
for i=3:length(st_bend_find)-2;
    b_nod=st_bend_find(i,1);
    st_b_nod=strjoin((loc_nod(b_nod-1,2),'1001'),'');
    e_b_nod!=strjoin((loc_nod(b_nod-1,2),'1002'),'');
    st_b_nod2=strjoin((loc_nod(b_nod,2),'1001'),'');
    e_b_nod3=strjoin((loc_nod(b_nod,2),'1002'),'');
    st_b_nod3=strjoin((loc_nod(b_nod+1,2),'1002'),'');
    e_b_nod3=strjoin((loc_nod(b_nod+2,2),'1001'),'');
    e_b_nod3=strjoin((loc_nod(b_nod+2,2),'1001'),'');
    e_b_nod4=strjoin((loc_nod(b_nod+2,2),'1002'),'');
                                                                                                                                                                                                                                                                                                                          AKK=cell();
BKK=cell();
CKK=cell();
for i=1:length(GEO_separate_strings)
                                                                                                                                                                                                                                                                                                                                                          start_bend=strfind(GEO_separate_strings(i,1),'A');
start_bend_find=[find(~cellfun("isempty',start_bend))];
                                                                                                                                                                                                                                                                                                                                                        if (isempty(start_bend_find)!=1)
    AKK=[AKK; modGEO(i,2) modGEO(i,3) modGEO(i,4)];
    BKK=[BKK; modGEO(i+1,2) modGEO(i+1,3) modGEO(i+1,4)];
                                 if (st_bend_find(i,1)-st_bend_find(i-1,1)==1) && (st_bend_find(i+1,1)-st_bend_find(i,1)==1) && (st_bend_find(i+2,1)-st_bend_find(i,2)=1) && (st_bend_find(i,2)-st_bend_find(i,2)-st_bend_find(i,2)-st_bend_find(i,2)-st_bend_find(i,2)-st_bend_find(i,2)-st_bend_find(i,2)-st_bend_find(i,2)-st_bend_find(i,2)-st_bend_find(i,2)-st_bend_find(i,2)-st_bend_find(i,2)-st_bend_find(i,2)-st_bend_find(i,2)-st_bend_find(i,2)-st_bend_find(i,2)-st_bend_find(i,2)-st_bend_find(i,2)-st_bend_find(i,2)-st_bend_find(i,2)-st_bend_find(i,2)-st_bend_find(i,2)-st_bend_find(i,2)-st_bend_find(i,2)-st_bend_find(i,2)-st_bend_find(i,2)-st_bend_find(i,2)-st_bend_find(i,2)-st_bend_find(i,2)-st_bend_find(i,2)-st_bend_find(i,2)-st_bend_find(i,2)-st_bend_find(i,2)-st_bend_find(i,2)-st_bend_find(i,2)-st_bend_find(i,2)-st_bend_find(i,2)-st_bend_find(i,2)-st_bend_find(i,2)-st_bend_find(i,2)-st_bend_find(i,2)-st_bend_find(i,2)-st_bend_find(i,2)-st_bend_find(i,2)-st_bend_find(i,2)-st_bend_find(i,2)-st_bend_find(i,2)-st_bend_find(i,2)-st_bend_find(i,2)-st_bend_find(i,2)-st_bend_find(i,2)-st_bend_find(i,2)-st_bend_find(i,2)-st_bend_find(i,2)-st_bend_find(i,2)-st_bend_find(i,2)-st_bend_find(i,2)-st_bend_find(i,2)-st_bend_find(i,2)-st_bend_find(i,2)-st_bend_find(i,2)-st_bend_find(i,2)-st_bend_find(i,2)-st_bend_find(i,2)-st_bend_find(i,2)-st_bend_find(i,2)-st_bend_find(i,2)-st_bend_find(i,2)-st_bend_find(i,2)-st_bend_find(i,2)-st_bend_find(i,2)-st_bend_find(i,2)-st_bend_find(i,2)-st_bend_find(i,2)-st_bend_find(i,2)-st_bend_find(i,2)-st_bend_find(i,2)-st_bend_find(i,2)-st_bend_find(i,2)-st_bend_find(i,2)-st_bend_find(i,2)-st_bend_find(i,2)-st_bend_find(i,2)-st_bend_find(i,2)-st_bend_find(i,2)-st_bend_find(i,2)-st_bend_find(i,2)-st_bend_find(i,2)-st_bend_find(i,2)-st_bend_find(i,2)-st_bend_find(i,2)-st_bend_find(i,2)-st_bend_find(i,2)-st_bend_find(i,2)-st_bend_find(i,2)-st_bend_find(i,2)-st_bend_find(i,2)-st_bend_find(i,2)-st_bend_find(i,2)-st_bend_find(i,2)-st_bend_find(i,2)-st_bend_find(i,2)-st_bend_find(i,2)-st_bend_find(i,2)-st_bend_find(i,2)-st_bend_find(i
```

```
TRANSLATION SCRIPT.m
                                                                                     2015-09-01
                                                                                                     TRANSLATION SCRIPT.m
                                                                                                                for i=1:(1_elem(1,1)-1)
nod = [nod; loc_nod(i,2) loc_nod(i+1,2) loc_nod(i+1,3)];
end
                     CKK=[CKK; modGEO(i+2,2) modGEO(i+2,3) modGEO(i+2,4)];
 end
else
                                                                                                                for j=from_elem_find(1):(from_elem_find(2)-2)
    nod = [nod; loc_nod{j,2} loc_nod{j+1,2} loc_nod{j+1,3}];
                                                                                                               end
          %number of elements
%main_pipe bend is a separate script that can divide the number of
elements in the bend, here only
% four elements is used for each bend section. Cannot change
without large consequences.
                                                                                                               nels = 4;
[x,y,z] = main_pipe_bend(A,B,C,nels);
           %extranodes_b=[extranodes_b; x(2:end-1); y(2:end-1); z(2:end-1)]; for i=2:nels
                     extranodes_b=[extranodes_b; x(i) y(i) z(i)];
           end
                                                                                                               end
 end
                                                                                                                loc_end=size(loc_nod);
for i=from_elem_find(end):(loc_end(1,1)-1)
nod = [nod ; loc_nod{i,2} loc_nod{i+1,2} loc_nod{i+1,3}];
%Find the maximum node number to add to the coordinate matrix
modGEO_tot=[];
for i=1:length(modGEO)
    modGEO_num=str2num(modGEO{i,1});
         modGEO_tot=[modGEO_tot; modGEO_num];

                                                                                                     % Find the lines with a bend in the matrix nod that lists the elements
sb_find=strfind(nod(:,3),'Bend');
wo_bend=cell();
wo_bend=[wo_bend; nod(1,:)];
for i=2:length(sb_find)-1
    if (isempty(sb_find(i,1))=-1) && (isempty(sb_find(i-1,1)=-1));
        wo_bend=[wo_bend; nod(i,:)];
         -----MAXIMUM node
 bend_coordinates=cell();
for i=1:(length(extranodes b))
   bend_coordinates=[bend_coordinates; modGEO_MAX+i extranodes_b{i,1}
   extranodes_b{i,2} extranodes_b{i,3} ];
                                                                                                                         wo_bend=wo_bend;
                                                                                                     end
 end %
                                                                                                     pr_wo_bend=wo_bend(:,1:2);
                                                                                                     elements1=[pr_wo_bend; straight_b; double_b; trippel_b; four_b];
 elements-----
                                                                                                      $*************************
 %----
                                                                                                     \$ If the in between elements from a straight pipe to a bend have no length, take away the element
                                                                                                      from_elem = strfind(loc_nod(:,3),'From');
from_elem_find = [find(~cellfun('isempty',from_elem))];
 new_elements1=cell();
for i=1:length(elements1)
                                                                                                               loc_N1 = strfind(modGEO(:,1),N1);
find_loc_N1 = [find(~cellfun('isempty',loc_N1))];
loc_N2 = strfind(modGEO(:,1),N2);
find_loc_N2 = [find(~cellfun('isempty',loc_N2))];
count=1;
nod=cell();
if from elem find=1
    s elem=size(loc nod);
    l_elem=s_elem(1,1);
                                                                                                                coor_N1=[modGEO(find_loc_N1(1,1),2) modGEO(find_loc_N1(1,1),3)
                                                                                                                                                    8
```

```
TRANSLATION SCRIPT.m
                                                                                                                                                      TRANSLATION_SCRIPT.m
                                                                                                                                                                                                                                                                               2015-09-01
               \label{eq:modGEO} $$ \mbox{modGEO}(\mbox{find loc_N1}(1,1),4)];$ $$ \mbox{coor_N2=[modGEO}(\mbox{find loc_N2}(1,1),2) $$ $$ \mbox{modGEO}(\mbox{find_loc_N2}(1,1),3) $$ \mbox{modGEO}(\mbox{find_loc_N2}(1,1),4)];$
                                                                                                                                                                     pr elements1_num=[pr_elements1_num; star_element(i,:);
elements1_num(i,:)];
                                                                                                                                                      end
               C X1=class(coor_N1{1,1});

C X2=class(coor_N2{1,1});

C Y1=class(coor_N1{1,2});

C Y2=class(coor_N2{1,2});

C Z1=class(coor_N1{1,3});

C Z2=class(coor_N2{1,3});
                                                                                                                                                      bend_ele=cel1();
star_element_bend={'*ELEMENT', 'TYPE=ELBOW31', 'ELSET=EB1'};
               if C_X1=='char'
                              X1=str2num(coor N1{1,1});
                                                                                                                                                      count=1;
calc=1;
for i=1:length(GEO_separate_strings)
               else
                              X1=coor_N1{1,1};
               end
                                                                                                                                                                    start_bend=strfind(GEO_separate_strings(i,1),'A');
start_bend_find=[find(~cellfun("isempty",start_bend))];
               if C_X2=='char'
                               X2=str2num(coor_N2{1,1});
                                                                                                                                                                   if (isempty(start_bend_find)!=1)
    bend_ele=[bend_ele; modGEO(i,1) bend_coordinates(calc,1)];
    bend_ele=[bend_ele; bend_coordinates(calc,1)];
    bend_cle=[bend_ele; bend_coordinates(calc,1)];
    bend_coordinates(calc+1,1)];
    bend_coordinates(calc+2,1)];
    bend_coordinates(calc+2,1)];
    bend_ele=[bend_ele; bend_coordinates(calc+2,1)];
    modGEO(i+2,1)];
    calc=calc+3;
    count=count+1;
    belset number=num2str(count);
    star_element_bend=[star_element_bend; '*ELEMENT' 'TYPE=ELBOW31' strcat('ELSET=EB',belset_number)];
end
                               X2=coor_N2{1,1};
               else
                              Y1=coor_N1{1,2};
               end
               if C_Y2=='char'
                               Y2=str2num(coor_N2{1,2});
               else
                              Y2=coor_N2{1,2};
               end
                                                                                                                                                      end
                              if C_Z1=='char'
Z1=str2num(coor_N1{1,3});
                                                                                                                                                     % Find the maximum element number already defined, and then add to it
MAX_ele so_far=length(pr elements1_num)/2+1;
belements={MAX_ele so_far, num2str(bend ele{1,1}), num2str(bend ele{1,2})};
% Find the maximum element number defined so far and then add the number
bnumber=MAX_ele so_far+1;
for i =2:length(bend ele)
    belements={belements; bnumber num2str(bend_ele{i,1})}
    num2str(bend_ele{i,2})};
    bnumber=bnumber+1;
                               Z1=coor_N1{1,3};
               else
                              Z2=coor_N2{1,3};
                                                                                                                                                      end
               length_P1_P2=sqrt((X2-X1)^2+(Y2-Y1)^2+(Z2-Z1)^2);
                                                                                                                                                      end
                                                                                                                                                     pr_belements2_num=cell();
ji=1;
for i=1:length(star_element_bend)-1
    pr_belements2_num=[pr_belements2_num; star_element_bend(i,:);
    str_belements(ji,:); str_belements(ji+1,:); str_belements(ji+2,:);
    str_belements(ji+3,:)];
}
count-fri,
elset number=num2str(count);
star element=[star element; **ELEMENT' 'TYPE=ELBOW31' strcat('ELSET=
E', elset number)];
```

B Welding data for the new pipe weld

| | 2014 | 7-5-01 | AT | Sve | etsdata EN ISO 156 | blad WPS | WPS NR.: PH 141/111-Gr5 WPQR NR.: | 5.2-01 | |
|--|--|---|----------------------------------|--|---|--|---|---------------------------------|--|
| Li | OW | ER HE | AI | V | Velding F | Procedure | 371KAB698 | | |
| | | | | | Specifi | cation | Rev: | Övrigt: | |
| | -1 / 0 | -1-1 A /D | | | | | A ISO 15 COR 2005 | PED | |
| Basmaterial / Basematerial A/B | | | | | | Material grupp / Material group | 5 ISO 15608:2005 | Giltighet / Valid WPQR 5.2 | |
| 10CrMo910 / 10CrMo910 Sätt för droppöverföring / Mode of metal transfer | | | | | Grupp 5.2/5.2 5.2 Materialtjocklek / Material thickness (mm) | | | | |
| Satt for droppoverforing / Mode of metal transfer | | | | | BW 14-56 / FW 14-33,6 | | | | |
| Svetsmetod och förbandstyp/ Joint type and welding method | | | | | | Ytterdiameter / Outer diameter (mm) | | | |
| | | FW i/see SS-EN ISC | | | | ≥109,5 och plåt/and plate | | | |
| | | och rengöring / Method of | preparation and | cleaning | | Svetsläge / Welding position | | | |
| - | g/Grindin | | elding sequence: | s 1 | | Alla lägen utom PG Fogutformning och svetsföljd 2 | / Joint design and welding seg | uences 2 | |
| Fogutformning och svetsföljd 1 / Joint design and welding sequences 1 | | | | | Övrig Fogform se/Other joint design: SS-EN ISO-9692 | | | | |
| Svetsda | ta / Weldin | g details | | | | | | | |
| Sträng/ Run | Metod / Process | Tillsatsmaterial / Filler material (øD mm) | Ström / Current (A) | Spänning / Voltage (V) | Strömtyp / type of current (polaritet) | Trådmatningshastighet / Wire feed speed (mm) | Svetshastighet / Travelspeed (mm/min.) | Värmetillförsel / Ho (KJ/mm) | |
| 1 | 141 | 2,4 | 85-90 | 12-14 | DC- | | 45-55 | 0,67-1,01 | |
| 2-3 | 111 | 2,5 | 65-80 | 22-23 | DC+ | | 75-85 | 0,81-1,18 | |
| 4-5 | 111 | 3,2 | 95-110 | 22-23 | DC+ | 4 | 65-85 | 1,18-1,87 | |
| 6-n | 111 | 3,2 | 95-110 | 22-23 | DC+ | | 75-95 | 1,06-1,62 | |
| Beteckning tillsatsmaterial inkl. fabrikat / Filler material designation and make OK 13.22, 76.28/ AWS A5.28 ER90S-G, A5.5: E9018-B3 Särskild värmning eller torkning / Any special baking or drying - | | | | Oscillering: Amp. frekv. hålltid / Oscillation: amp. freq. dwell time - Pulssvetsning detaljer / Pulse welding details - | | | | | |
| Designation | ng skyddsgas, p ongas, flux shi / EN439: | | Betäckning sky Designationgas | ddsgas, pulver r , flux backing | rotsida / | Avstånd kontaktrör/arbetsstyc | ke / Distance contact tube/wo | rkpiece | |
| _ | toppsida (I/mi | | Gasflöde rotsid | da (I/min.) / | | Plasmasvetsning, detaljer / Plas | smawelding, details | | |
| | ate shielding | | Gasflow rate ba | acking | | | | | |
| 8-12 I/ | (1977/02/14 | dimension / Tungsten electro | - nde tyne/size | | | Brännarvinkel / Torch angel | | | |
| WT20 | | intension, rongsten electric | ode type/size | | | brainer vinkery roter onger | | | |
| Rotmejsli SS-Nb | ng / rotstöd d | etaljer / Details of back goug | zing/backing | | | Efterföljande värmebehand. och PWHT-Gr5.2-002 | ch / eller âldring / Post-weld he | at treatment and/or ag | |
| | | tur (°C) / Preheat temperatu | ır | | | Tid, temperatur och metod / Time, temperature and method | | | |
| | 150 - 200 | | | | | 1tim/1h, 680-720 °C, Elmatta / Electric Uppvärmnings- och svalningshastigheter för värmebehand. / Heating and cooling rat | | | |
| Mellansträngstemperatur (°C) / Interpass temperature Max. +350 °C | | | | | | PWHT-Gr5.2-002 | | | |
| Verkni | ingsgrad lj | endling (maximal strängbre usbåge/arc efficier max bredd)/Weavi | ncy 141=0,6 | 111=0,8 | | | | | |
| Tillverkar | e / Manufactu | rer | | | | Ganskare eller granskande orga | n / Examiner or axamining bod | у | |
| Power | Heat Pip | ing Sweden AB | | | | | | | |
| Ort, datu | m och signatu | r / Name, date and signatur | | | | Ort, datum och signatur / Name | , date and signatur | | |
| | | -04 Per Magnussoi | Peul | (na | | | | | |
| E2000 | = 2012 17 | -04 Per Magnusson | reul | no | | | | | |

C Finite element analysis of impression creep

The impression creep test was analysed by the FE method with Abaqus CAE software (version 6.14). A quarter model of the impression creep test for the 2.5mm thick standard specimen was used, see Figure C1. For the 10mm thick specimen a different mesh was used, see Figure C2. Specimens were meshed with 62500 and 48000 quadratic elements (C3D20R), respectively.

The LCSP creep model for 10CrMo910 was used at 525°C with a contact pressure of 255.8 MPa, which corresponds to a uniaxial stress of 110 MPa, which was used in the IC test programme. The temperature of 525°C was used in the analysis instead of the real test temperature of 530°C, because the parametric LCSP model did not converge properly, but the LCSP model trimmed for 525°C was available and worked nicely. This difference in temperature leads to an error of less than 10% in strain rate.

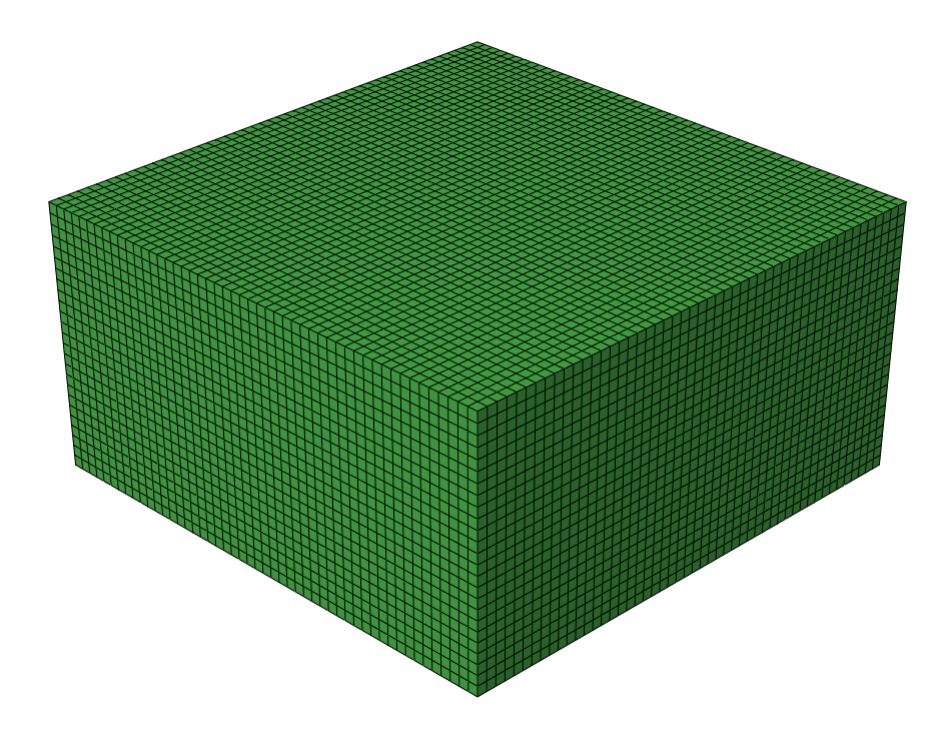


Fig. C1. The FE mesh for the 2.5mm thick specimen.

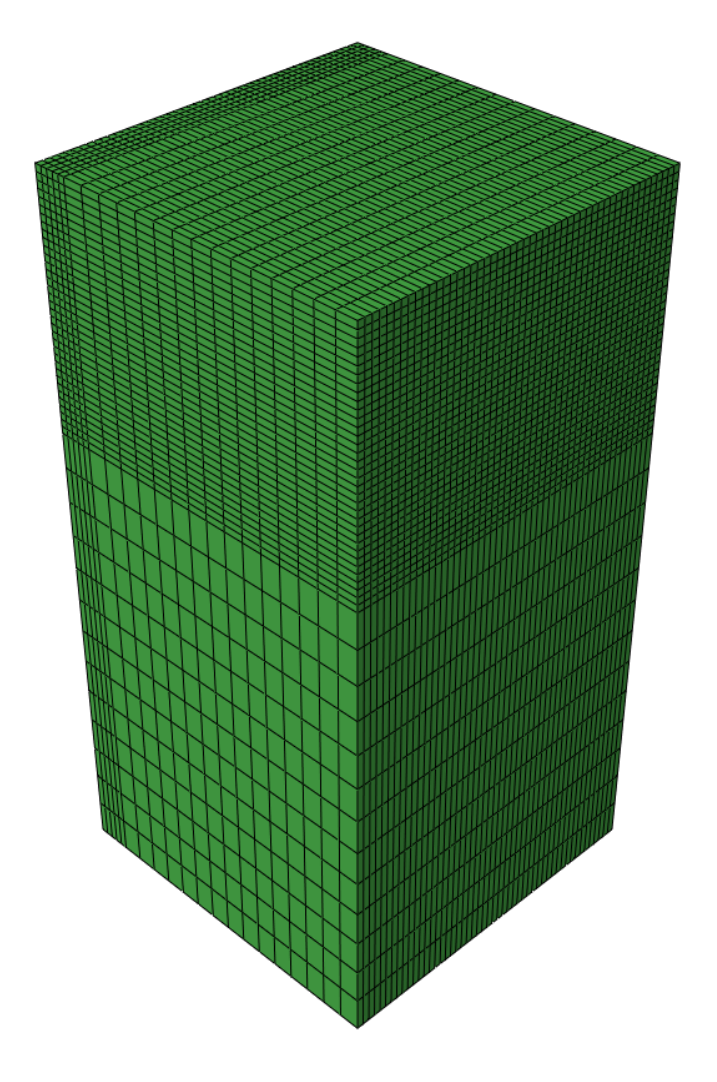


Fig. C2. The FE mesh for the 10mm thick specimen.

The plots of the equivalent strain in Figures C3 and C4 show that the maximum strain is located a short distance below the indenter edge and about 0.5mm below the indenter in the middle. This means that when 0.5mm of the 10mm thick specimen was ground after each test cycle, some strain (less than 0.08%) from the previous test was left on the surface of the ground specimen in the area directly under the indenter. The effect of this was however minimised by turning the specimen 90° along the vertical axis. After turning the specimen about 90 % of the surface under the indenter is practically unstrained. The strain at the underside of the 2.5mm specimen is rather small.

The strain distribution in the 10mm thick specimen in Figure C5 is rather similar to the 2.5mm thick specimen in Figure C3 and C4, but the strain in the thick specimen seems to spread deeper than in the standard specimen.

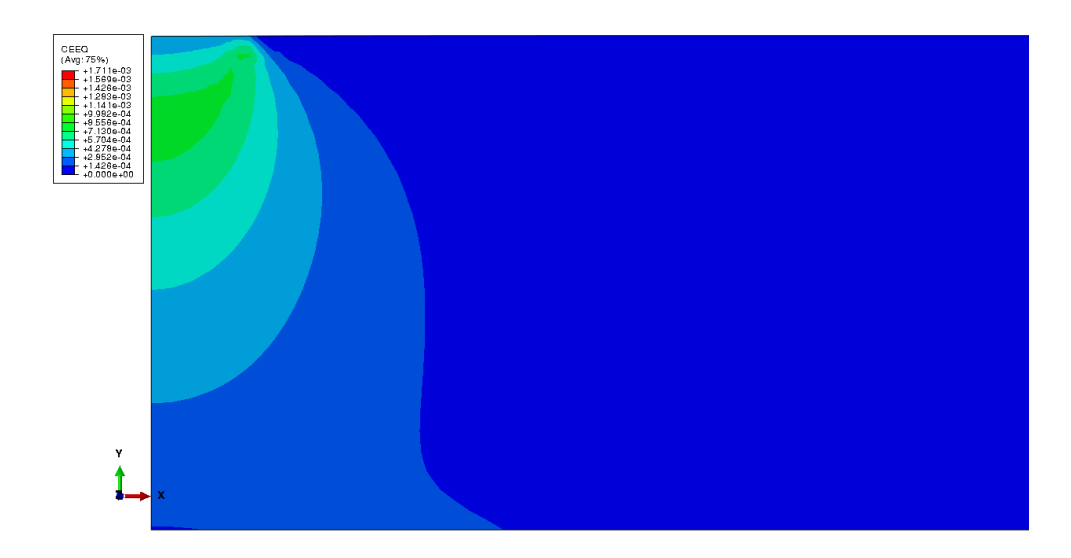


Fig. C3. The equivalent strain distribution in the 2.5mm thick specimen.

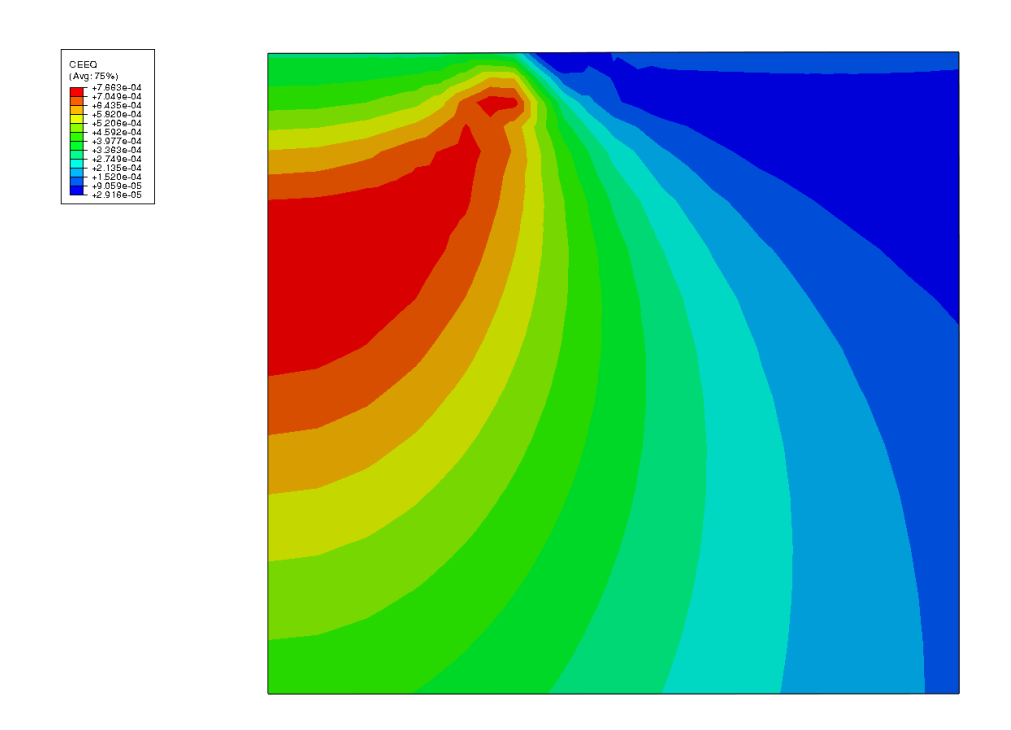
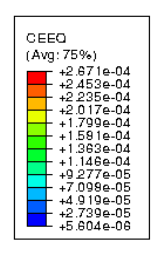


Fig. C4. Close-up of Fig. 18 (1.4*1.3mm).



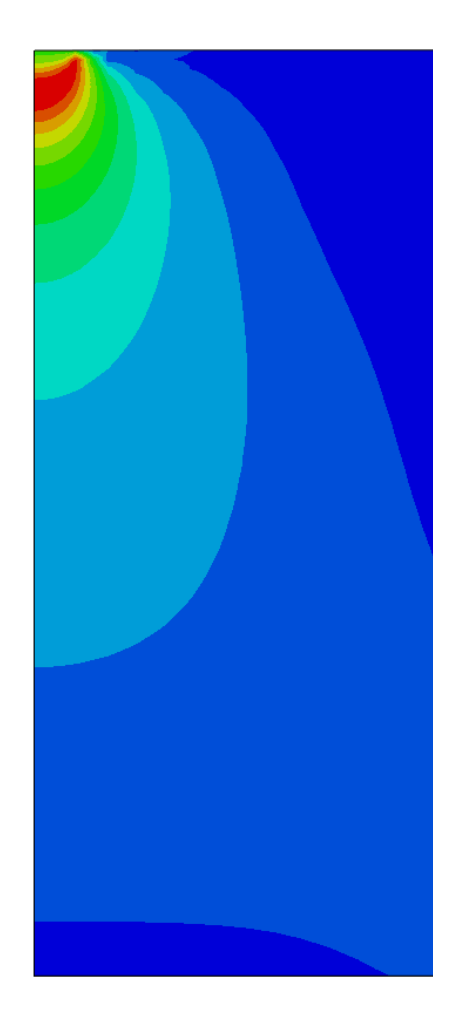


Fig. C5. The equivalent strain distribution in the 10mm thick specimen.

The displacement versus time was also predicted by the FE analysis and the curves for the standard and for the thick specimen are shown in Figure C6. It was a bit surprising that the displacement in the thick specimen is so much bigger than in the standard specimen as the expectation was that making the specimen thicker would not make much difference in the displacement curve, because most of the strain should be concentrated just below the indenter.

The comparison of the predicted and measured strains and strain rates in Figures C7 and C8 shows that the FE analysis underestimates both the strain and strain rate levels by a factor of five. The shapes of the predicted curves are roughly correct, but the absolute levels are not right. The reason for this discrepancy is not clear at this moment and needs further investigation. The 5°C difference in temperature does not account for this discrepancy.

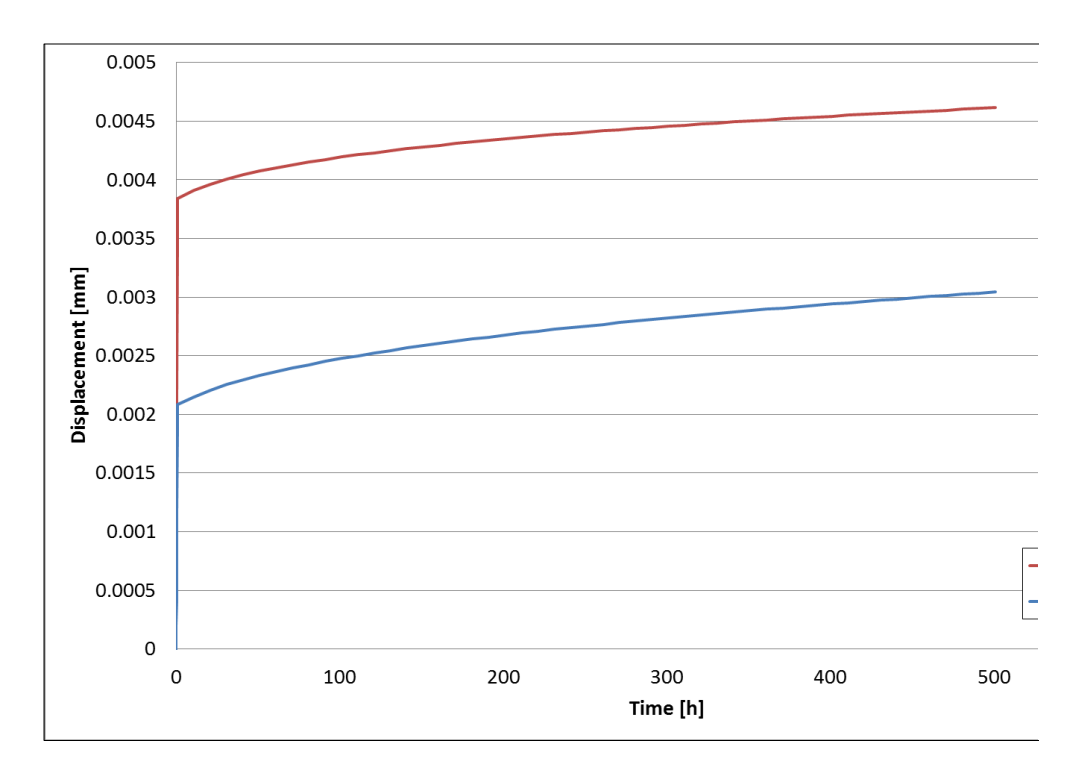


Fig. C6. The FE prediction of indenter displacement.

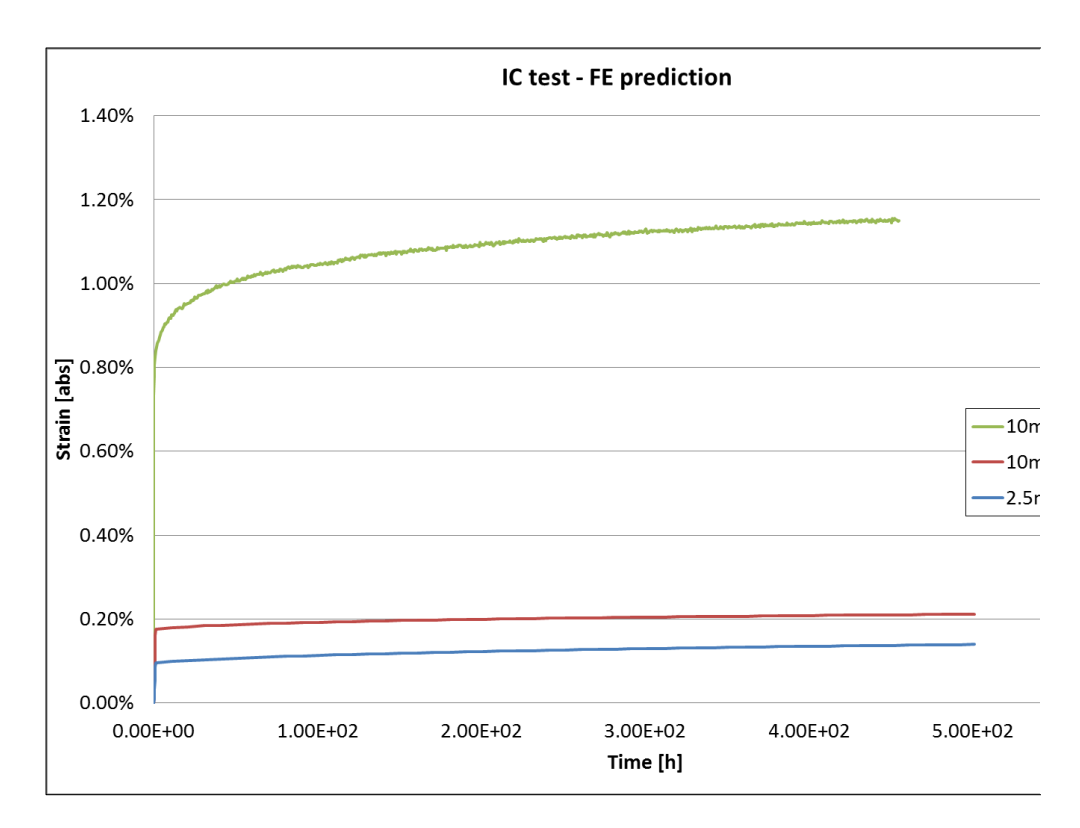


Fig. C7. Comparison of the equivalent uniaxial strain between the first IC test for the 10mm thick specimen and the FE prediction.

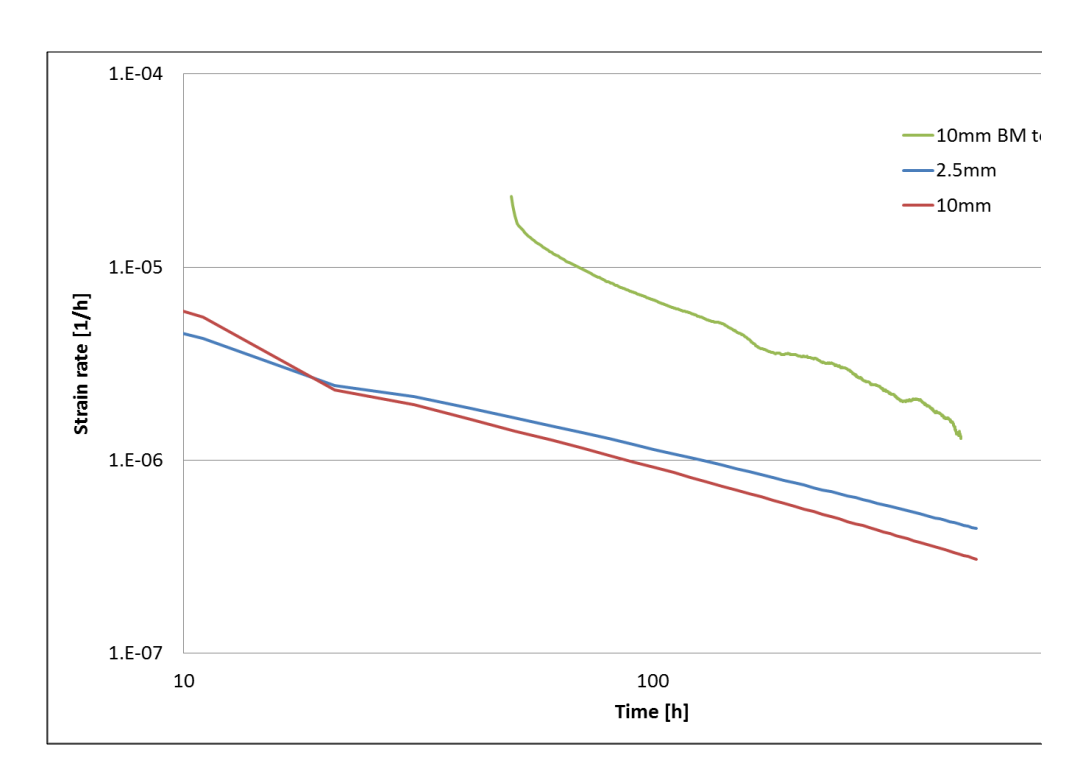


Fig. C8. Comparison of the strain rates between the first IC test for the 10mm thick specimen and the FE prediction.

Conclusions

An innovative way of applying impression creep testing was used by manufacturing a "sandwich" type of specimen of the new weld which allowed the creep rates to be scanned from the base material across the HAZ to the weld metal. The highest creep rate in the inter-critical zone of the new weld was, however, not as high as was expected: only 2.6 times higher than in the base material. The weld metal of the new weld is slightly overmatching as compared to the base material. The measured creep rates from the impression creep tests correlate very well with the minimum creep rates measured in the uniaxial creep tests of the base material of the new weld.

The creep rates measured from the service-exposed T-piece indicate elevated creep rates which are most likely due to the creep damage.

The behavior of the impression creep test was analysed by FEM and strain distributions were calculated. The displacement versus time behavior was also analysed, but when this curve was transferred into equivalent uniaxial strain and finally to strain rate, the comparison against the experimental data was not very convincing. This requires further study.

LIFETIME ASSESSMENT OF HIGH TEMPERATURE PIPING

Livslängdsbedömning av ångledningssystem med hjälp av spänningsanalys och provning.

Högtrycksångledningar hos kraftvärmeanläggningar har i regel drifttemperaturer som medför att livslängden begränsas av krypning. Projektet har, genom krypanalys och intryckskrypprovning, resulterat i ett genombrott för bedömning av kryplivslängd hos ångledningssystem.

Another step forward in Swedish energy research

Energiforsk – Swedish Energy Research Centre is a research and knowledge based organization that brings together large parts of Swedish research and development on energy. The goal is to increase the efficiency and implementation of scientific results to meet future challenges in the energy sector. We work in a number of research areas such as hydropower, energy gases and liquid automotive fuels, fuel based combined heat and power generation, and energy management in the forest industry. Our mission also includes the generation of knowledge about resource-efficient sourcing of energy in an overall perspective, via its transformation and transmission to its end-use. Read more: www.energiforsk.se

